

# **Blocking the Hemagglutinin of Influenza A Virus by Multivalent Inhibitors**

**Wenjing Lu**

**鲁文静**

**2019**

ISBN: 978-90-393-7128-2

Printed by: ProefschriftMaken || [www.proefschriftmaken.nl](http://www.proefschriftmaken.nl)

© Wenjing Lu, 2019.

All rights reserved.

# **Blocking the Hemagglutinin of Influenza A Virus by Multivalent Inhibitors**

**Blokkering van de hemagglutinine van influenza A  
virus door multivalente remmers**

(met een samenvatting in het Nederlands)

**Proefschrift**

ter verkrijging van de graad van doctor aan de Universiteit Utrecht  
op gezag van de rector magnificus, prof.dr. H.R.B.M. Kummeling,  
ingevolge het besluit van het college voor promoties  
in het openbaar te verdedigen op maandag 6 mei 2019 des middags te 2.30 uur

door

**Wenjing Lu**

geboren op 14 juni 1988  
te Shaanxi, China

**Promotor:**

Prof. dr. R. J. Pieters

The reseach described in this thesis was financially supported by a scholarship (No.201306300064) to Wenjing Lu from the China Scholarship Council (CSC).

# Table of contents

<b>Chapter 1</b>	Introduction and thesis outline	<b>7</b>
<b>Chapter 2</b>	Synthesis of building blocks for hemagglutinin inhibitors of Influenza A virus	<b>29</b>
<b>Chapter 3</b>	Synthesis of the di- & trivalent hemagglutinin inhibitors of Influenza A virus	<b>59</b>
<b>Chapter 4</b>	Evaluation of the di- & trivalent hemagglutinin inhibitors of Influenza A virus	<b>91</b>
<b>Chapter 5</b>	Summary and future perspective	<b>111</b>
<b>Appendices</b>	Nederlandse Samenvatting	<b>122</b>
	List of Abbreviations	<b>126</b>
	List of Publications and Presentations	<b>129</b>
	Acknowledgements	<b>130</b>
	Curriculum Vitae	<b>133</b>



# *Chapter 1*

## *Introduction and thesis outline*

*Carbohydrate-protein interactions and multivalency:  
implications for the inhibition of  
Influenza A virus infections*

## 1.1 Introduction

Carbohydrate-protein interactions are at the heart of many important biological processes.<sup>1-3</sup> These interactions play a key role in the binding of bacteria, viruses and toxins to cell surfaces. The numerous glycan-binding proteins on the surface of these microbes enable the binding or adherence to glycosylated cell surfaces as the first step of the infection process, and constitute a major threat to human health. One of the infectious diseases that is transmitted using carbohydrate-protein interactions is the influenza infection (known as the flu), where an initial sialic acid dependent binding to the host cell surface is a necessary requirement to trigger the infection.<sup>4</sup>

A single interaction between a protein and a carbohydrate is usually weak, but multivalent ligands can compensate for this deficiency by binding two or more binding sites simultaneously. Over the past few years, advanced by numerous biochemical studies, we obtained a better understanding of multivalent interactions which are of importance to the modulation of many critical biological systems.<sup>5</sup> In this review, we will discuss the importance of the multivalency effect in carbohydrate-protein interactions and how this could help to discover new drugs to treat or prevent the influenza infection.

## 1.2 Multivalency effect in carbohydrate-protein interactions

### 1.2.1 Mechanisms of multivalent binding

There are several possible mechanisms that can contribute to the potency of multivalent interactions: the chelate effect, subsite binding, statistical rebinding and also aggregation (Figure 1).<sup>6,7</sup>

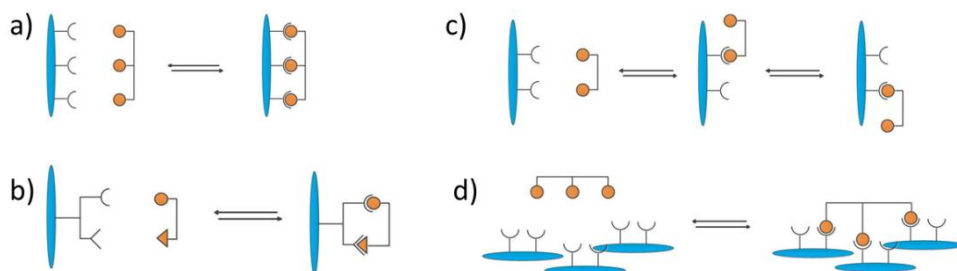


**Figure 1.** Mechanisms of multivalent binding. a) chelate effect; b) subsite binding; c) statistical rebinding; d) aggregation (cross-linking).



In a multivalent system, lowered entropic barriers may favor binding between the ligand and the protein and thus lead to higher affinity or inhibitory potency.<sup>8</sup> In the binding of a multivalent ligand, the translational entropic cost is paid by the first binding event and all the subsequent binding interactions can proceed with smaller entropic penalties. As a result, due to the lower entropic cost in total, stronger binding may occur. This mechanism involving simultaneous binding of two or more (sub)ligands is commonly named as the chelate effect.<sup>9</sup> Subsite binding is another type of chelation that involves secondary binding interactions with a receptor other than the primary binding site. With the additional binding event, the multivalent ligands also become more effective.<sup>10</sup> When only one binding sites is involved in an interaction, multivalent ligands can still show increased inhibitory potencies due to high local concentration of subligands around that binding site, which is referred to as the mechanism of statistical rebinding. This effect is caused by the slower off-rate of the multivalent ligand, due to the non-bound subligands rapidly replacing the bound subligand after it releases. This may result in a higher binding affinity. Instead of intramolecular association, large aggregation (cross-linking) of intermolecular binding is often observed. This effect is dependent on factors like concentrations, valencies, binding affinities, different kinds of interactions, etc. Together, these different modes of binding give us unique information of multivalent carbohydrate-protein interactions.

### **1.2.2 Carbohydrate-based multivalent inhibitors**

Carbohydrates play a central role in living organisms as recognition markers to enable biological processes like cell adhesion, fertilization, differentiation, and tumor-cell metastasis through carbohydrate-protein interactions.<sup>11-13</sup> Pathogens take advantage of the carbohydrates for cell adhesion and the subsequent infection or invasion of the host. Furthermore, certain microbes mimic the host cell glycans which facilitates their evasion from the immune response.

The discovery of the diverse biological roles of carbohydrate-protein interactions is increasingly of interest in the search for applications in drug discovery. By using ligands to mimic the carbohydrate binding sites and block the recognition or adhesion process, many infectious diseases might be prevented. However, the binding affinity between an individual carbohydrate and a target protein is relatively weak therefore inhibitor design is directed towards using the multivalency effect. As there are multiple copies of the glyco-ligands presented on the surface, an optimized multivalent ligands could bind to the target protein much stronger than the monovalent ligand. By taking advantage of this effect, recent

progress has been made in the design and synthesis of carbohydrate-based multivalent ligands thereby serving as powerful inhibitors.

This can be exemplified with the lectin LecA, one of the virulence factors of the problematic pathogen *Pseudomonas aeruginosa*. LecA is a tetrameric lectin specific for binding with oligo- and polysaccharides containing a terminal  $\alpha$ -D-galactose and an interesting target for the design of multivalent carbohydrate-based inhibitors. The shortest distance between two neighboring binding sites of LecA is *ca.* 26 Å.<sup>14</sup> Guided with the structural information, several multivalent inhibitors like glycopeptide dendrimers,<sup>15</sup> calixarenes,<sup>16</sup> resorcinarenes,<sup>17</sup> fullerenes<sup>18</sup> and cyclooligosaccharides<sup>19</sup> were designed and tested which resulted in potent inhibitors. A series of divalent ligands was reported by our group, presenting galactose residues with variations in the spacer length between them to fit the divalent binding mode (Figure 2).<sup>20–22</sup> Linear and relatively rigid spacers based on glucose-1,2,3-triazole alternating units linked via ‘click’ chemistry were developed. Divalent galactoside **1** exhibited an IC<sub>50</sub> value of 0.12 μM for LecA, which was 484-fold stronger in relative potency per sugar compared to a monovalent reference compound. A slightly shorter and more rigid version (compound **2**) exhibited a much more potent inhibition, which was over 7500-fold (IC<sub>50</sub>=2.7 nM) stronger than that of the monovalent galactose derivative (IC<sub>50</sub> 22 μM). This finding could be explained by the design of compound **2** which contains the perfect spacing between the two galactosides to match to the dimeric geometry of LecA.

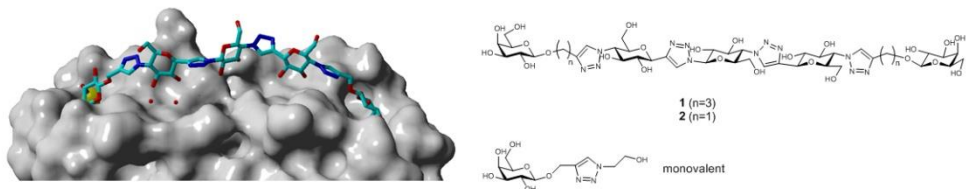


**Figure 2.** Divalent inhibitors based on the structure of lectin LecA (PDB ID: 4YWA).

Cholera Toxin, an AB<sub>5</sub>-subunit toxin, consists of a single disease-initiating A-subunit and five lectin-like B-subunits.<sup>23</sup> The ring-shaped pentameric B-subunits play an important role to trigger the attachment of the toxin to the cell surfaces of the intestines by recognizing the exposed part of the GM1-ganglioside, i.e. the GM1os (GM1 oligosaccharide) moieties and then facilitate the endocytosis process.<sup>24</sup> Multivalent glycoconjugates based on different carrier platforms like pentacyclen,<sup>25</sup> calixarenes,<sup>26</sup> corannulenes,<sup>27</sup> even CTB (cholera toxin B-subunit) itself<sup>28</sup> have successfully shown effective inhibition of the CTB binding (Figure 3).

It was reported by our group that highly effective dendrimers targeting CTB were prepared, which combined three important parts in the design for improving binding affinity: multivalent dendritic scaffolds, the GM1os ligand, and elongated flexible linkers with optimal length. The building blocks were efficiently coupled via ‘click’ chemistry to give a variety of dendrimers which showed different effects. The best dendrimer which contained eight GM1os ligand exhibited an 47,500-fold enhancement per GM1 derivative compared to monovalent GM1os.<sup>29–31</sup>

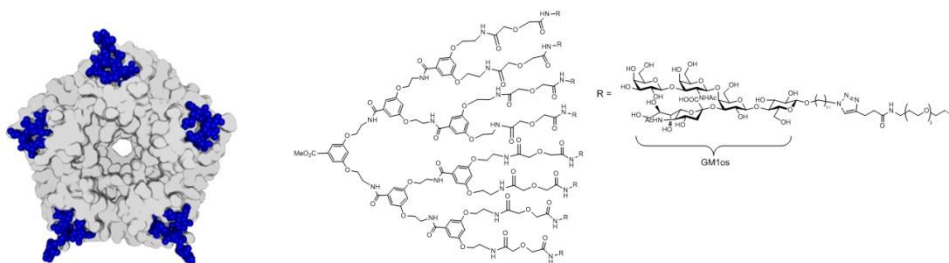


**Figure 3.** Glycodendrimer targeting the cholera toxin B-subunit (PDB ID: 3CHB, CTB with 5 bound GM1os molecules).

These results of multivalent inhibitor design strategy strongly encourage the use of multivalent glycoconjugates in other carbohydrate-related therapies such as viral and fungal infections. A water-soluble globular fullerene<sup>32</sup> was employed as a biocompatible scaffold and decorated with 120 peripheral carbohydrate subunits using ‘click’ chemistry to build a multivalent inhibitor for the Ebola virus. This giant molecule was produced in a minimum of synthetic steps and infection assays showed that the fullerene inhibited the cell infection in the subnanomolar range ( $IC_{50}=0.667$  nM). Multivalent carbohydrates have also been moved forward towards medical applications. The glycopeptide MK-2640 contains 4 fucoside moieties on an insulin molecule that modulate its availability by binding to the mannose receptor C-type 1 depending on blood glucose levels.<sup>33,34</sup> Furthermore, two studies involving multivalent versions of the Gb<sub>3</sub> carbohydrate were shown to be effective in mouse studies,<sup>35,36</sup> while related compounds showed promising effects against *Streptococcus suis* in mice.<sup>37</sup>

Meanwhile, as one of the most common diseases all over the world, flu is caused by an infection of the influenza virus, which draws more and more attention to researchers to investigate how to prevent the viral infection by using multivalent carbohydrate-based inhibitors. We are going to discuss these studies in detail.

## **1.3 Multivalent strategies for the inhibition of the influenza A virus**

### **1.3.1 Influenza A viruses**

Influenza A viruses (IAVs), which infect the epithelial cells of the respiratory tract, cause the highly contagious flu to humans. The regularly recurring seasonal influenza results in substantial morbidity and the deaths of 250,000-500,000 people each year, with children and the elderly representing the majority of the victims. Worldwide pandemics can cause even more severe mortality, such as in 1918 when approximately 50 million deaths were attributed to the Spanish flu.<sup>38</sup>

Different subtypes of IAVs are labeled according to the combinations of different virus surface proteins: 18 hemagglutinin (HA) subtypes and 11 neuraminidase (NA) subtypes. For example avian influenza 'bird flu' virus H5N1 and H7N9 or swine influenza "swine flu" virus H1N1 and H3N2. Occasionally, viruses are transmitted from wild aquatic birds to domestic poultry, and this may also cause an outbreak or give rise to a human influenza pandemic.

### **1.3.2 Infection process of IAVs**

Typically, to initiate an infection, the virus adheres to the target host cell by using its surface glycoprotein HA to recognize glycoconjugates that contain terminal  $\alpha$ -(2,3)- or  $\alpha$ -(2,6)- linked sialic acid residues. Following receptor binding, the viruses are endocytosed, leading to their residency in intracellular vesicles. Then the low pH-induced fusion of viruses occurs from the endosomal compartment, releasing the uncoated viral genome into the cytoplasm, followed by replication in the nucleus.<sup>39</sup> Budding of new virion takes place after the replication, where the membrane is generated from the host plasma membrane and contains the viral transmembrane proteins. Finally, The glycosidase enzyme (NA) removes the sialic acid group from the glycan which allows the newly produced viruses to release from the cell surface and help the viruses to spread.<sup>40,41</sup>

### **1.3.3 Current treatment for IAV infection**

Interference with the effects of IAV is of importance for both humans and animals. The current options to combat IAV infection include vaccination and two classes of antiviral compounds, the M2 ion channel blockers and the NA inhibitors. Vaccination is a valuable clinical approach for the seasonal IAV variants which are usually life threatening for children and the elderly. The more dangerous IAV variants are commonly seen in epidemics when we need other kinds of anti-viral agents to tackle these more severe cases. In those cases, oseltamivir (Tamiflu®) and

zanamivir (Relenza®) are successful carbohydrate-based drugs that block the function of NA and significantly inhibit the release of IAV.<sup>42</sup> The M2 ion channel has also been targeted by a class of drugs referred to as the adamantanes, which include amantadine (Symmetrel®) and rimantadine (Flumadine®) (Figure 4).

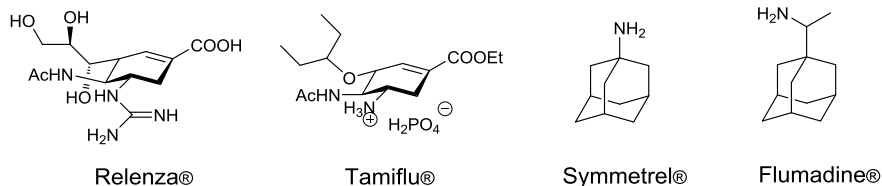


**Figure 4.** Current anti-viral drugs approved for clinical use.

Unfortunately, a major problem that has been observed with both classes of antiviral drugs is the rapid emergence of drug-resistant strains of IAVs. And the vaccines that were developed also can't prevent the flu epidemics effectively. Thus, novel IAV inhibitors with new mechanisms of action to combat the virus would be of great value.<sup>43,44</sup>

### 1.3.4 Multivalent interactions between HA and the host cell

As we have already gained the knowledge of the life cycle of IAV, several therapeutic targets should be paid more attention to. Among them, HA is one of the most appealing targets present with ca. 300-400 copies on the viral surface. This adhesion protein contains three symmetrical binding pockets (Figure 5). The spacing between HA trimers is ca. 100 Å from center to center, while the distance between binding pockets within a trimer is ca. 42 Å.<sup>45</sup> HA binds to sialylated glycans:  $\alpha$ -2,6 linked sialyl N-Acetyllactosamine ( $\alpha$ -2,6-SiaLacNAc) binds specifically to human-type-specific HA while  $\alpha$ -2,3-SiaLacNAc binds to avian-type-specific HA,<sup>40,45,46</sup> both with weak affinities in the millimolar range. In order to increase the overall strength of the interaction between the virus and the host cell surface, multiple HA molecules on the virion surface bind to various glycoproteins based on the multivalency effect.<sup>5</sup> In that sense it is a logical and attractive strategy to block the viral infection with a multivalent sialic-acid-based inhibitor to mimic the binding between the HA and the cell surface glycans, to prevent the virus infection.

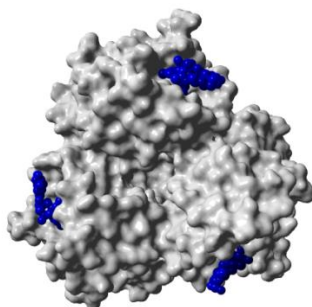


**Figure 5.** Top view of the binding between the trimeric HA and 3 bound  $\alpha$ -2,6-SiaLacNAc molecules (PDB ID: 3UBN).

### 1.3.5 Multivalent inhibitors targeting HA

#### 1.3.5.1 Polymeric inhibitors

To increase the potency of synthetic HA inhibitors, several approaches for polyvalent sialoside systems have been tested. Large molecular entities, e.g. functionalized polymers,<sup>47–53</sup> chitosan,<sup>54</sup> liposomes,<sup>55,56</sup> nanostructures,<sup>52</sup> and dendrimers,<sup>57</sup> showed their inhibitory advantages by interacting with multiple HA trimers simultaneously and/or binding to more than one binding site within an HA trimer.

Matrosovich and coworkers<sup>47</sup> synthesized a polyvalent inhibitor composed of anomeric aminobenzylglycosides of N-Acetylneuraminic acid (Neu5Ac) linked to a polyacrylate carrier, which is the first example of a totally synthetic and comparatively potent inhibitor of HA. The macromolecular carrier containing 10 mol% of Neu5Ac showed a 2040-fold potency increase per sugar compared to the corresponding monovalent benzylsialoside.

The group of Whitesides designed an  $\alpha$ -sialoside linked to acrylamide,<sup>48,50</sup> which formed high molecular weight copolymers. These polymeric inhibitors showed  $10^4$ - $10^6$  times enhanced potencies when compared to the reference  $\alpha$ -methyl sialoside. They concluded that for polymers containing a high density of sialic acid, the inhibition happened both by binding the HA binding pockets and the NA active sites.

The group of Wong reported a lysoganglioside GM3 (lyso-GM3) conjugated to the polymer poly-L-glutamic acid.<sup>58</sup> This polyvalent inhibitor contained a hydrophobic part, which could interfere with the fusion process and gave a picomolar inhibition ( $IC_{50}=1.9$  pM). They also designed a series of *p*-nitrophenyl  $\alpha$ -*O*-glycosides of *C*-3 modified sialic-acid liposomes which acted as inhibitors for both of HA and NA.<sup>56</sup>

A 1000-fold enhancement was observed in the binding affinity assay against A/Puerto Rico/8/1934 (H1N1) and A/Aichi/2/1968 (H3N2), indicating that liposomes are effective platforms for the development of multivalent IAV inhibitors.

Yeh and coworkers<sup>55</sup> also developed an efficient multivalent system based on the conjugation of phospholipids to the thio(S)-linked glycoligand (*S*- $\alpha$ -2,6-Sia-LacNAc). The self-assembled liposomes were found to have potent inhibitory activity. Effects were shown in both the virus neutralization assay ( $EC_{50} = 71 \pm 5.5 \mu\text{M}$ ) and the hemagglutination inhibition assay ( $K_i = 125 \mu\text{M}$ ) where sialic acid did not inhibit, and they could also effectively interfere with the entry of the H1N1 into MDCK cells.

The group of Rainer Haag used biocompatible nanoparticles as scaffolds for multivalent HA inhibitors. They first reported sialic-acid-coated glycerol dendrons immobilized on 2 nm and 14 nm gold nanoparticles.<sup>59</sup> The 14 nm particles exhibited inhibition in the nanomolar range in a hemagglutination assay while the 2 nm particles had no inhibitory effect. Later, they also described a series of sialic acid-conjugated, hyper-branched polyglycerol-based nanoparticles<sup>52</sup> with diameters in the 1-100 nm range. Their 50 nm particle were 7000-fold more effective than the 3 nm one which had similar sugar concentrations. The further increase of particle size did not lead to the corresponding increase of inhibition effect but to a reduced activity. Their work emphasized the importance of matching particle sizes and ligand densities to mimic the virus surfaces and achieve maximum efficiency.

Kwon and coworkers<sup>60</sup> designed multivalent 6'-sialyllactose (6'SL) moieties by linking them to polyamidoamine (PAMAM) dendrimers with a 1.2-3.1 nm distance between multiple sialic acid ligands. The conjugates with spacings of around 3 nm showed the strongest inhibition effect of HA trimer binding and H1N1 infection both *in vitro* ( $IC_{50} = 1.7 \mu\text{M}$ ) and *in vivo*. As the distance between 6'SL binding sites in the trimeric HA is around 4 nm, 3.1 nm distance within a flexible framework, seemed fit the binding sites of HA the best within this series and enhanced the binding affinity the most. Therefore, modulating the interligand spacing was shown to be an important aspect, more so than the valency of the HA inhibitors.

Li and coworkers<sup>54</sup> presented two novel 3'-sialyllactose (3'SL) modified chitosan-based materials: a water-soluble polymer and a functionalized fiber, targeting viral adhesion inhibition and decontamination. A surface plasmon resonance study revealed that the monovalent 3'SL had no visible binding with the HA at 1 mg/mL (1.57 mM) or less, while the 3'SL-chitosan conjugates showed higher avidity ( $K_d =$

0.59-1.93  $\mu\text{M}$ ). The result demonstrated that multivalent presentation of 3'SL ligands on a chitosan skeleton is effective in enhancing the binding of HA.

Dendrimers are alternative scaffolds of potential synthetic inhibitors to prevent IAV infection. Reuter and coworkers<sup>61</sup> evaluated a series of dendrimers such as linear, linear-dendron copolymers, comb-branched and dendrigraft polymers, for their ability to inhibit HA and to block virus infection *in vitro*. The dendrigraft inhibitors showed up to 50000-fold increased activity against the IAVs ( $\text{IC}_{50}$  = 0.1  $\mu\text{M}$ ) and do not exhibit cytotoxicity to MDCK cells at therapeutic concentrations. Roy and coworkers<sup>57</sup> synthesized water-soluble dendritic  $\alpha$ -thiosialosides using hyperbranched L-lysine scaffolds which achieved inhibition of HA at a concentration of 19  $\mu\text{M}$ . These dendritic macromolecules could mimic multi-antennary glycoproteins and showed inhibition properties of HA and NA. Bhatia and coworkers<sup>53</sup> compared the linear and dendritic polyglycerol sialosides (LPGSA and dPGSA) *in vitro* and *in vivo*, which differed with respect to molecular weight and number of sialic acid units. The linear LPGSA inhibited IAV infection with an  $\text{IC}_{50}$  in the lower nanomolar range, which was better than the dendritic dPGSA. LPGSA also exhibited potent activity against two avian influenza strains and showed low toxicity. This study revealed that high ligand densities are not necessary for designing effective IAV inhibitors. Similarly, a carbosilane dendrimers with valencies of 4 was shown to be 60-fold more potent than a monovalent reference compound.<sup>3</sup>

Xiao and coworkers<sup>62</sup> prepared several pentacyclic triterpene-cyclodextrin conjugates using the copper(I)-catalyzed azide-alkyne cycloaddition (CuAAC) reaction. The heptavalent cyclodextrin conjugate bound tightly to HA with a  $K_d$  of 2.08  $\mu\text{M}$ , which also showed a 125-fold potency enhancement of its  $\text{IC}_{50}$  value (1.60  $\mu\text{M}$ ) over the corresponding monomer. These multivalent inhibitors exhibited potent antiviral activity against H1N1 virus (A/WSN/33), even equivalent or superior to oseltamivir, with a lower cytotoxicity, and also exhibited broad spectrum inhibitory activity against the two other human influenza viruses A/JX/312 (H3N2) and A/HN/1222 (H3N2) with  $\text{IC}_{50}$  values of 2.47-14.90  $\mu\text{M}$ .

In many of the mentioned cases the sialic acid moieties have the natural O-linkages. These can in principle be cleaved by the neuraminidase also present on the virus. This is not reported in all studies, as e.g. only HA may have been used in the assay. There are however several studies in which S-linked sialic acids are used, and these are the most likely ones to become part of therapeutics, as they are stable to the neuraminidases,<sup>52,53,55,57,63-66</sup> however C-glycosides have also been used.<sup>49</sup>



### 1.3.5.2 'Small' molecule inhibitors

In the macromolecular approaches, structural information on the spatial arrangement of the trimeric binding sites of the HA protein is not usually taken into account for the design of the multivalent inhibitors. It was found that smaller molecules containing proper carbohydrate units can in some cases be effective IAV inhibitors depending on whether their topological design allows them to bind simultaneously to several binding sites of a single HA trimer,<sup>6,67</sup> or even to binding sites on nearby trimers.

Bridging binding sites within an HA trimer is a challenging task when using relatively small molecules, while their activity may also come from bridging HA trimers on the densely packed viral surface. The latter phenomenon was supposed to be the cause of enhanced inhibition in early experiments with divalent sialosides linked by spacers with varying lengths and flexibilities, since the enhancements (100-fold) would only be observed in the assay with whole viruses and not with just the HA trimer.<sup>68</sup> Similarly, a 10-fold enhancement was exhibited with a system containing two Neu5Ac $\alpha$ 2-6Gal $\beta$ 1-4GlcNAc (i.e.  $\alpha$ -2,6-SiaLacNAc) units linked to a single galactoside moiety,<sup>69</sup> the bivalent trisaccharide ligands would give the structures more rigidity when anchored to the sugar hydroxyls of a galactose residue. Marra and coworkers<sup>64</sup> synthesized tetra- and octavalent sialoside clusters via multiple 'click' reactions of a propargyl thiosialoside with calix[4]arene polyazides. The calix-sugars were shown to inhibit the hemagglutination and the viral infection at submillimolar concentrations.

Ohta and coworkers<sup>70</sup> reported a chemoenzymatic synthesis of mono-, bi-, and tri-substituted (schematically shown as **5**, Figure 6) involving cyclic peptides presenting three  $\alpha$ -2,3-SiaLac units. Only the bi- and tri-substituted derivatives showed significant affinity to HA with  $K_d$ 's of 1.6 mM and 0.63 mM respectively.

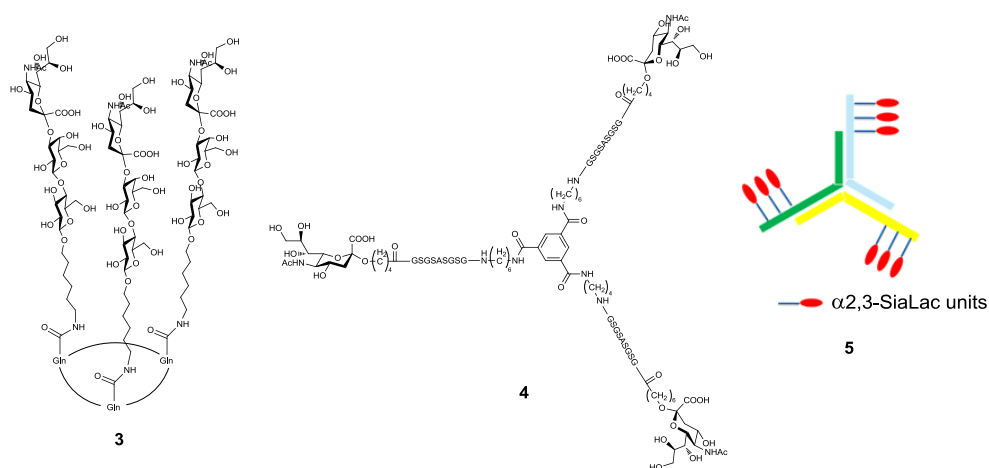


**Figure 6.** Trivalent inhibitors of HA protein.

Feng and coworkers<sup>71</sup> designed trivalent sialyllactoside inhibitors against IAV strain A/Puerto Rico/8/1934 (H1N1) based on trisphenol and trisaniline skeletons. The flexible hydrophilic spacer between 3'SL and the scaffold was made up of polyethylene-glycol units. Trisphenol-sialyllactoside showed a significant inhibitory effect at 400  $\mu\text{M}$  in a plaque reduction assay with MDCK cells while unexpectedly, both of the trisphenol and trisaniline sialyllactosides exhibited no hemagglutination inhibition activity.

Waldmann and coworkers<sup>72</sup> described the computer design, chemical synthesis and binding analysis of a trivalent glycopeptide inhibitor **4**, which has a scaffold of trisubstituted benzene ring linked to sialic acid residues via peptide-based spacers. This compound bound much stronger to avian influenza H5N1 (A/Vietnam/1203/2004) ( $K_d = 446 \text{ nM}$ ) comparing to 2-O-methyl- $\alpha$ -Neu5Ac, but only 4.9-fold better than the monovalent glycopeptide. Most of the effect was not due to multivalency but to a combination of sialic acid and peptide binding, the latter of which was shown to bind HA even stronger than the sialic acid derivative.

Yang and coworkers<sup>65</sup> prepared a series of multivalent conjugates based on thiosialoside ligands and human serum albumin or bovine serum albumin to enhance the binding affinity to HA and NA. The synthetic glycoproteins with a higher density of the S-sialoside on the protein surface had a higher affinity for HA ( $K_i = 3.13\text{-}50 \mu\text{M}$ ) than the di-, tri-, tetraivalent clusters they synthesized, likely due to the higher valency and larger size of the protein scaffold vs the small molecules. The low valency sialoside design with short spacer arms was not able to reach three binding sites of HA indicating that proper spacing between the trivalent inhibitor arms is an important design aspect.

The three-armed system **5** was based on three-way junction DNA as a well-defined rigid scaffold for the display of  $\alpha$ -2,3-SiaLac units,<sup>73</sup> This DNA molecule had a similar topology to the sialic acid binding sites on HA. Evaluation in whole virus hemagglutination inhibition experiments indicated strong enhancement, i.e.  $8.0 \times 10^4$ -fold higher potency for IAV A/Puerto Rico/8/1934 (H1N1) over free 3'SL, but only a factor of 8 (i.e. less than 2 per sugar) over a reference compound that only has a glycoligand in one of its three arms. This indicates that multivalency effects were minor but that HA binding to the DNA component was an important factor contributing to the observed enhancements.

A system based on rigid self-assembled peptide nucleic acid (PNA)-DNA complexes displaying two  $\alpha$ -2,6-SiaLacNAc units at various distances was also reported.<sup>45</sup> An optimal distance between the glycoligands of approximately 50Å was observed with a 30-fold enhancement (15-fold per sugar) over a DNA-PNA reference architecture containing only a single glycoligand. The data were also in agreement with experiments using whole virus and hemagglutination inhibition assays. Notably, more flexible polyethylene glycol linked molecules showed no enhancement which was supported by a theoretical model indicating that the distance-affinity relationships for interactions of the HA with bivalent SiaLacNAc ligands.

## 1.4 Conclusions

Multivalent protein-carbohydrate interactions play a very important role in the pathogen adhesion to cells. Understanding the unique interactions on the molecular level is of prime importance for developing optimized multivalent ligands to achieve strong inhibitory effects. Suitable protein targets with relatively close binding sites such as the influenza A virus HA have been investigated.

Although there are already two families of antiviral drugs being used to treat IAV infections, the emergence of drug-resistant viral strains makes it more urgent to find other ways to block the infection. Despite the research focusing on vaccines<sup>74-76</sup> and NA,<sup>77-81</sup> HA is an important target for investigating new IAV inhibitor strategies. Larger molecular entities such as glycopolymers, nanoparicles, dendrimers, DNA moieties, taking advantage of their size to bridge multiple HA trimers, have exhibited high inhibitory potencies. On the other hand, relatively small trivalent molecules also showed potential based on proper structural design, which may have advantages for development into clinical drugs. All these

examples provide inspiration for investigating multivalent ligands as new antiviral drugs and also as drugs for other diseases.

## Outline of the thesis

In this chapter, a variety of multivalent systems from small to large molecules were described which showed potent inhibitory effects against several pathogens. Anti-flu (influenza) applications in the lungs using multivalent carbohydrates particularly has potential because of the high binding affinities. By understanding the mechanism of multivalent interactions, we discussed glycopolymers, nanoparticles, dendrimers, calixarenes, liposomes, DNA derivatives etc. as multivalent inhibitors, targeting pathogens especially the hemagglutinin protein (HA) on the surface of the influenza A virus. Smaller molecules containing proper carbohydrate units can in principle be effective IAV inhibitors depending on whether their topological design allows them to bind simultaneously to several binding sites of a single HA trimer,<sup>6,67</sup> or even to binding sites on nearby trimers. These ligands could potentially be used as new anti-pathogenic agents or complementary to the current drugs and improve therapy.

HA binds only with millimolar affinities to its sialylated glycan receptors. These low affinities are a challenging starting point for a carbohydrate based drug development program, but also non-carbohydrate approaches have faced this challenge.<sup>82</sup> The virus, however, binds with high affinity to tissue surfaces by using multivalency,<sup>5</sup> which increases its avidity to levels that enable the infection. The multivalency effects involve the simultaneous binding of glycans to more than one of the three binding sites per HA trimer on the IAV surface, but also the simultaneous binding of cell surface glycans to multiple HA protein trimers on the viral surface. Based on the nature of HA binding, we aimed to design multivalent HA inhibitors that mimic these interactions between HA and the sialyl-oligosaccharides. In **Chapter 2**, efforts to obtain suitable building blocks to be used in the synthesis of multivalent HA inhibitors are described based on the goals mentioned above. Three types of building blocks are discussed: the scaffold, the ligand and the spacer to bridge these two parts. The main scaffold was an amino functionalized 1,3,5-triphenyl benzene,<sup>83</sup> which has a propeller shape that may be ideal for the available area on the top area of the HA protein, taking advantage of the groove areas for the spacer arms. The ligands were  $\alpha$ -2,6-sialyl-LacNAc moieties, in the form that allows the conjugation via CuAAC involving alkyne or

azide unit moieties. A triazole-phenyl-alkyne moiety with a LacNAc-Lac tetrasaccharide was introduced as the spacer of our HA inhibitors. Besides the rigidity, the additional elongation also added length to the arms, that might very well be important for optimal binding.

In **Chapter 3**, we showed the successful synthesis and characterization of multivalent sialic acid containing glycoconjugates based on two synthesis strategies. One of the proposed inhibitor designs is based on the trimeric structure of the “head” of hemagglutinin protein which will also be trivalent and consists of a ligand that contains an  $\alpha$ -2,6-sialylated glycan (3 copies), a propeller shaped scaffold, and a short rigid spacer that links the ligands to the scaffold. Another inhibitor design strategy is based on similar research within our group in which we have designed a series of divalent ligands presenting galactose residues with variations in the length of the spacer to fit a divalent binding mode.<sup>84-86</sup> Here we aim to introduce the triazole-phenyl-alkyne moieties to link two sialylated ligands. These syntheses were possible by a combination of chemical scaffold synthesis, enzymatic carbohydrate synthesis and CuAAC ‘click’ conjugation. We also discussed the synthesis of the final inhibitors and the identification of these molecules by NMR, LC-MS, IR, *et al.*, which confirmed the purities of the compounds for activity evaluation.

Besides the development of optimal molecular designs to inhibit HA, effective methods to evaluate the inhibition activities are also crucial for the research. The study of molecular binding processes is a key aspect to many fields of research. Determining which molecules interact, how they interact, and why they interact can ultimately lead to more effective drugs. Here in **Chapter 4**, we focused on evaluation of the di- & trivalent hemagglutinin inhibitors that have been described in **Chapter 3**, performed on two kinds of Influenza virus: WU95 and VI75 which contain the HA gene of A/Netherlands/178/95 H3N2 or A/Bilthoven/1761/76 H3N2, respectively, in the background of A/Puerto Rico/8/34/Mount Sinai H1N1 (Taxonomy ID: 183764), with the technology of a bio-layer interferometry (BLI) binding assay, a hemagglutination inhibition (HAI) assay and infection-inhibition experiments involving a cell line. BLI is a label-free technology for measuring real-time biomolecular interactions. This technique provides the ability to monitor binding specificity, rates of association and dissociation, or concentration with precision and accuracy. All these assays gave us interesting results that are discussed with respect to the structural features of the inhibitors in this chapter.

Finally, **Chapter 5** summarizes the main results and interesting findings described in this thesis. In addition, perspectives for the future of this field of research are

given. Proper strategies could be introduced to the application of this type of compounds. The multivalent approach may not be limited to IAV inhibitor discovery, but can likely be extended to other biological systems as previously shown as well.

## References

- 1 V. Wittmann and R. J. Pieters, Bridging lectin binding sites by multivalent carbohydrates, *Chem. Soc. Rev.*, 2013, **42**, 4492–4503.
- 2 Y. C. Lee, Biochemistry of carbohydrate-protein interactions, *FASEB J.*, 1992, **13**, 3193–3200.
- 3 Y. C. Lee and R. T. Lee, Carbohydrate-protein interactions: basis of glycobiology, *Acc. Chem. Res.*, 1995, **28**, 321–327.
- 4 R. Webster, W. Bean, O. Gorman, T. Chambers and Y. Kawaoka, Evolution and ecology of influenza A viruses., *Microbiol. Rev.*, 1992, **56**, 152–179.
- 5 M. Mammen, S. K. Choi and G. M. Whitesides, Polyvalent interactions in biological systems: implications for design and use of multivalent ligands and inhibitors, *Angew. Chemie Int. Ed.*, 1998, **37**, 2755–2794.
- 6 J. E. Gestwicki, C. W. Cairo, L. E. Strong, K. A. Oetjen and L. L. Kiessling, Influencing receptor-ligand binding mechanisms with multivalent ligand architecture, *J. Am. Chem. Soc.*, 2002, **124**, 14922–14933.
- 7 L. L. Kiessling, J. E. Gestwicki and L. E. Strong, Synthetic multivalent ligands as probes of signal transduction, *Angew. Chem. Int. Ed.*, 2006, **45**, 2348–2368.
- 8 W. P. Jencks, On the attribution and additivity of binding energies, *Proc. Natl. Acad. Sci.*, 1981, **78**, 4046–4050.
- 9 R. J. Pieters, Toward multivalent carbohydrate drugs, *Drug Discov. Today Technol.*, 2009, **6**, e27–e31.
- 10 A. L. Banerjee, D. Eiler, B. C. Roy, X. Jia, M. K. Haldar, S. Mallik and D. K. Srivastava, Spacer-based selectivity in the binding of ‘two-prong’ ligands to recombinant human carbonic anhydrase I, *Biochemistry*, 2005, **44**, 3211–3224.
- 11 C. R. Bertozzi and L. L. Kiessling, Chemical glycobiology, *Science*, 2001, **291**, 2357–2364.
- 12 K. De Schutter and E. J. M. Van Damme, Protein-carbohydrate interactions as part of plant defense and animal immunity, *Molecules*, 2015, **20**, 9029–9053.
- 13 J. Holgersson, A. Gustafsson and M. E. Breimer, Characteristics of protein-carbohydrate interactions as a basis for developing novel carbohydrate-based antirejection therapies, *Immunol. Cell Biol.*, 2005, **83**, 694–708.

- 14 A. V. Grishin, M. S. Krivozubov, A. S. Karyagina and A. L. Gintsburg, *Pseudomonas Aeruginosa* lectins as targets for novel antibacterials, *Acta Naturae*, 2015, **7**, 51–63.
- 15 R. U. Kadam, M. Bergmann, M. Hurley, D. Garg, M. Cacciarini, M. A. Swiderska, C. Nativi, M. Sattler, A. R. Smyth, P. Williams, M. Camara, A. Stocker, T. Darbre and J.-L. Reymond, A glycopeptide dendrimer inhibitor of the galactose-specific lectin LecA and of *Pseudomonas aeruginosa* biofilms, *Angew. Chem. Int. Ed.*, 2011, **50**, 10631–10635.
- 16 S. Cecioni, R. Lalor, B. Blanchard, J.-P. Praly, A. Imberty, S. E. Matthews and S. Vidal, Achieving high affinity towards a bacterial lectin through multivalent topological isomers of Calix[4]arene glycoconjugates, *Chem. Eur. J.*, 2009, **15**, 13232–13240.
- 17 Z. H. Soomro, S. Cecioni, H. Blanchard, J. P. Praly, A. Imberty, S. Vidal and S. E. Matthews, CuAAC synthesis of resorcin[4]arene-based glycoclusters as multivalent ligands of lectins, *Org. Biomol. Chem.*, 2011, **9**, 6587–6597.
- 18 S. Cecioni, V. Oerthel, J. Iehl, M. Holler, D. Goyard, J.-P. Praly, A. Imberty, J.-F. Nierengarten and S. Vidal, Synthesis of dodecavalent fullerene-based glycoclusters and evaluation of their binding properties towards a bacterial lectin, *Chem. Eur. J.*, 2011, **17**, 3252–3261.
- 19 M. L. Gening, D. V. Titov, S. Cecioni, A. Audfray, A. G. Gerbst, Y. E. Tsvetkov, V. B. Krylov, A. Imberty, N. E. Nifantiev and S. Vidal, Synthesis of multivalent carbohydrate-centered glycoclusters as nanomolar ligands of the bacterial lectin LecA from *Pseudomonas aeruginosa*, *Chem. Eur. J.*, 2013, **19**, 9272–9285.
- 20 F. Pertici and R. J. Pieters, Potent divalent inhibitors with rigid glucose click spacers for *Pseudomonas aeruginosa* lectin LecA, *Chem. Commun.*, 2012, **48**, 4008–4010.
- 21 F. Pertici, N. J. De Mol, J. Kemmink, R. J. Pieters and N. J. de Mol, Optimizing divalent inhibitors of *Pseudomonas aeruginosa* lectin leca by using a rigid spacer, *Chem. Eur. J.*, 2013, **19**, 16923–16927.
- 22 R. Visini, X. Jin, M. Bergmann, G. Michaud, F. Pertici, O. Fu, A. Pukin, T. R. Branson, D. M. E. Thies-Weesie, J. Kemmink, E. Gillon, A. Imberty, A. Stocker, T. Darbre, R. J. Pieters and J.-L. Reymond, Structural insight into multivalent galactoside binding to *Pseudomonas aeruginosa* lectin LecA, *ACS Chem. Biol.*, 2015, 2455–2462.
- 23 J. E. Heggelund, A. Mackenzie, T. Martinsen, J. B. Heim, P. Cheshev, A. Bernardi and U. Krengel, Towards new cholera prophylactics and treatment: crystal structures of bacterial enterotoxins in complex with GM1 mimics, *Sci. Rep.*, 2017, **7**, 1–11.
- 24 E. Fan, E. A. Merritt, C. L. M. J. Verlinde and W. G. J. Hol, AB 5 toxins: structures and inhibitor design, *Curr. Opin. Struct. Biol.*, 2000, **10**, 680–686.
- 25 E. H. Enterotoxin, E. A. Merritt, Z. Zhang, J. C. Pickens, M. Ahn, W. G. J. Hol and E. Fan, Characterization and crystal structure of a high-affinity pentavalent receptor

- binding inhibitor for Cholera Toxin and *E. coli* heat-labile enterotoxin, *J. Am. Chem. Soc.*, 2002, 8818–8824.
- 26 J. Garcia-Hartjes, S. Bernardi, C. A. G. M. Weijers, T. Wennekes, M. Gilbert, F. Sansone, A. Casnati and H. Zuilhof, Picomolar inhibition of cholera toxin by a pentavalent ganglioside GM1os-calix[5]arene, *Org. Biomol. Chem.*, 2013, **11**, 4340–4349.
- 27 M. Mattarella, J. Garcia-Hartjes, T. Wennekes, H. Zuilhof and J. S. Siegel, Nanomolar cholera toxin inhibitors based on symmetrical pentavalent ganglioside GM1os-sym-corannulenes., *Org. Biomol. Chem.*, 2013, **11**, 4333–9.
- 28 T. R. Branson, T. E. Mcallister, J. Garcia-hartjes, M. A. Fascione, J. F. Ross, S. L. Warriner, T. Wennekes, H. Zuilhof and W. B. Turnbull, A protein-based pentavalent inhibitor of the Cholera Toxin B subunit, *Angew. Chem. Int. Ed.*, 2014, 8323–8327.
- 29 A. V Pukin, H. M. Branderhorst, C. Sisu, C. C. A. G. M. Weijers, M. Gilbert, R. M. J. Liskamp, G. M. Visser, H. Zuilhof and R. J. Pieters, Strong inhibition of cholera toxin by multivalent GM1 derivatives, *ChemBioChem*, 2007, **8**, 1500–1503.
- 30 H. M. Branderhorst, R. M. J. Liskamp, G. M. Visser and R. J. Pieters, Strong inhibition of cholera toxin binding by galactose dendrimers, *Chem. Commun.*, 2007, 5043–5045.
- 31 D. D. Zomer-van Ommen, A. V. Pukin, O. Fu, L. H. C. Quarles van Ufford, H. M. Janssens, J. M. Beekman and R. J. Pieters, Functional characterization of Cholera Toxin inhibitors using human intestinal organoids, *J. Med. Chem.*, 2016, **59**, 6968–6972.
- 32 A. Muñoz, D. Sigwalt, B. M. Illescas, J. Luczkowiak, L. Rodríguez-Pérez, I. Nierengarten, M. Holler, J. S. Remy, K. Buffet, S. P. Vincent, J. Rojo, R. Delgado, J. F. Nierengarten and N. Martín, Synthesis of giant globular multivalent glycofullerenes as potent inhibitors in a model of Ebola virus infection, *Nat. Chem.*, 2016, **8**, 50–57.
- 33 N. C. Kaarsholm, S. Lin, L. Yan, T. Kelly, M. Van Heek, J. Mu, M. Wu, G. Dai, Y. Cui, Y. Zhu, E. Carballo-Jane, V. Reddy, P. Zafian, P. Huo, S. Shi, V. Antochshuk, A. Ogawa, F. Liu, S. C. Souza, W. Seghezzi, J. L. Duffy, M. Erion, R. P. Nargund and D. E. Kelley, Engineering glucose responsiveness into insulin, *Diabetes*, 2018, **67**, 299–308.
- 34 A. W. Krug, S. A. G. Visser, K. Tsai, B. Kandala, C. Fancourt, B. Thornton, L. Morrow, N. C. Kaarsholm, H. S. Bernstein, S. A. Stoch, M. Crutchlow, D. E. Kelley and M. Iwamoto, Clinical evaluation of MK-2640: an insulin analog with glucose-responsive properties, *Clin. Pharmacol. Ther.*, 2018, 1–9.
- 35 K. Nishikawa, K. Matsuoka, E. Kita, N. Okabe, M. Mizuguchi, K. Hino, S. Miyazawa, C. Yamasaki, J. Aoki, S. Takashima, Y. Yamakawa, M. Nishijima, D. Terunuma, H. Kuzuhara and Y. Natori, A therapeutic agent with oriented carbohydrates for treatment of infections by Shiga toxin-producing *Escherichia coli* O157:H7, *Proc. Natl. Acad. Sci. U. S. A.*, 2002, **99**, 7669–7674.



- 36 G. L. Mulvey, P. Marcato, P. I. Kitov, J. Sadowska, D. R. Bundle and G. D. Armstrong, Assessment in mice of the therapeutic potential of tailored, multivalent Shiga toxin carbohydrate ligands, *J. Infect. Dis.*, 2003, **187**, 640–649.
- 37 R. J. Pieters, H.-C.-C. Slotved, H. M. Mortensen, L. Arler, J. Finne, S. Haataja, J. a F. Joosten, H. M. Branderhorst and K. A. Krogfelt, Use of tetravalent galabiose for inhibition of *streptococcus suis* serotype 2 infection in a mouse model, *Biology (Basel)*, 2013, **2**, 702–718.
- 38 P. Palese, Influenza: Old and new threats, *Nat. Med.*, 2004, **10**, S82–S87.
- 39 S. Pöhlmann, *Viral Entry into Host Cells*, 2013, vol. 790.
- 40 M. de Graaf and R. A. Fouchier, Role of receptor binding specificity in influenza A virus transmission and pathogenesis, *Embo J*, 2014, **33**, 823–841.
- 41 Y. Ji, Y. J. White, J. A. Hadden, O. C. Grant and R. J. Woods, New insights into influenza A specificity: an evolution of paradigms, *Curr. Opin. Struct. Biol.*, 2017, **44**, 219–231.
- 42 M. von Itzstein, The war against influenza: discovery and development of sialidase inhibitors., *Nat. Rev. Drug Discov.*, 2007, **6**, 967–74.
- 43 A. Moscona, Oseltamivir Resistance — Disabling Our Influenza Defenses, *N. Engl. J. Med.*, 2005, **353**, 2633–2636.
- 44 A. Loregian, B. Mercorelli, G. Nannetti, C. Compagnin and G. Pal, Antiviral strategies against influenza virus: towards new therapeutic approaches., *Cell. Mol. Life Sci.*, 2014, **71**, 3659–3683.
- 45 V. Bandlow, S. Liese, D. Lauster, K. Ludwig, R. R. Netz, A. Herrmann and O. Seitz, Spatial screening of hemagglutinin on Influenza A Virus particles: Sialyl-LacNAc displays on DNA and PEG scaffolds reveal the requirements for bivalency enhanced interactions with weak monovalent binders, *J. Am. Chem. Soc.*, 2017, **139**, 16389–16397.
- 46 N. K. Sauter, M. D. Bednarski, B. A. Wurzburg, J. E. Hanson, G. M. Whitesides, J. J. Skehel and D. C. Wiley, Hemagglutinins from two influenza virus variants bind to sialic acid derivatives with millimolar dissociation constants: A 500-MHz Proton nuclear magnetic resonance study, *Biochemistry*, 1989, **28**, 8388–8396.
- 47 M. N. Matrosovich, L. V. Mochalova, V. P. Marinina, N. E. Byramova and N. V. Bovin, Synthetic polymeric inhibitors of influenza virus receptor-binding activity suppress virus replication, *FEBS Lett.*, 1990, **272**, 209–21.
- 48 W. J. Lees, A. Spaltenstein, J. E. Kingery-Wood and G. M. Whitesides, Polyacrylamides bearing pendant  $\alpha$ -sialoside groups strongly inhibit agglutination of erythrocytes by influenza A virus: Multivalency and steric stabilization of particulate biological systems, *J. Med. Chem.*, 1994, **37**, 3419–3433.
- 49 S. K. Choi, M. Mammen and G. M. Whitesides, Generation and in situ evaluation of libraries of poly(acrylic acid) presenting sialosides as side chains as polyvalent inhibitors of influenza-mediated hemagglutination, *J. Am. Chem. Soc.*, 1997, **119**, 4103–4111.

- 50 G. B. Sigal, M. Mammen, G. Dahmann and G. M. Whitesides, Polyacrylamides bearing pendant  $\alpha$ -sialoside groups strongly inhibit agglutination of erythrocytes by influenza virus: The strong inhibition reflects enhanced binding through cooperative polyvalent interactions, *J. Am. Chem. Soc.*, 1996, **118**, 3789–3800.
- 51 H. Kamitakahara, T. Suzuki, Y. Suzuki, O. Kanie and C. Wong, A lysoganglioside /poly-L-glutamic acid conjugate as a picomolar inhibitor of Influenza hemagglutinin, *Angew. Chemie Int. Ed.*, 1998, **37**, 1524–1528.
- 52 I. Papp, C. Sieben, A. L. Sisson, J. Kostka, C. Böttcher, K. Ludwig, A. Herrmann and R. Haag, Inhibition of influenza virus activity by multivalent glycoarchitectures with matched sizes, *ChemBioChem*, 2011, **12**, 887–895.
- 53 S. Bhatia, D. Lauster, M. Bardua, K. Ludwig, S. Angioletti-Uberti, N. Popp, U. Hoffmann, F. Paulus, M. Budt, M. Stadtmüller, T. Wolff, A. Hamann, C. Böttcher, A. Herrmann and R. Haag, Linear polysialoside outperforms dendritic analogs for inhibition of influenza virus infection *in vitro* and *in vivo*, *Biomaterials*, 2017, **138**, 22–34.
- 54 X. Li, P. Wu, G. F. Gao and S. Cheng, Carbohydrate-functionalized chitosan fiber for influenza virus capture, *Biomacromolecules*, 2011, **12**, 3962–3969.
- 55 H. W. Yeh, T. S. Lin, H. W. Wang, H. W. Cheng, D. Z. Liu and P. H. Liang, S-Linked sialyloligosaccharides bearing liposomes and micelles as influenza virus inhibitors, *Org. Biomol. Chem.*, 2015, **13**, 11518–11528.
- 56 X.-L. Sun, Y. Kanie, C.-T. Guo, O. Kanie, Y. Suzuki and C.-H. Wong, Syntheses of C-3-Modified sialylglycosides as selective inhibitors of influenza hemagglutinin and neuraminidase, *European J. Org. Chem.*, 2000, **2000**, 2643–2653.
- 57 R. Roy, D. Zanini, S. J. Meunier and A. Romanowska, Solid-phase synthesis of dendritic sialoside inhibitors of influenza A virus hemagglutinin, *Chem. Commun.*, 1993, 1869–1872.
- 58 H. Kamitakahara, T. Suzuki, N. Nishigori, Y. Suzuki, O. Kanie and C. H. Wong, A lysoganglioside poly-L-glutamic acid conjugate as a picomolar inhibitor of influenza hemagglutinin, *Angew. Chemie. Int. Ed.*, 1998, **37**, 1524–1528.
- 59 I. Papp, C. Sieben, K. Ludwig, M. Roskamp, C. Böttcher, S. Schlecht, A. Herrmann and R. Haag, Inhibition of influenza virus infection by multivalent sialic-acid-functionalized gold nanoparticles, *Small*, 2010, **6**, 2900–2906.
- 60 S. J. Kwon, D. H. Na, J. H. Kwak, M. Douaisi, F. Zhang, E. J. Park, J. H. Park, H. Youn, C. S. Song, R. S. Kane, J. S. Dordick, K. B. Lee and R. J. Linhardt, Nanostructured glycan architecture is important in the inhibition of influenza A virus infection, *Nat. Nanotechnol.*, 2017, **12**, 48–54.
- 61 J. D. Reuter, A. Myc, M. M. Hayes, Z. Gan, R. Roy, D. Qin, R. Yin, L. T. Piehler, R. Esfand, D. A. Tomalia and J. R. Baker, Inhibition of viral adhesion and infection by sialic-acid-conjugated dendritic polymers, 1999, 271–278.
- 62 S. Xiao, L. Si, Z. Tian, P. Jiao, Z. Fan, K. Meng, L. Zhang and D. Zhou, Pentacyclic triterpenes grafted on CD cores to interfere with influenza virus entry: A dramatic multivalent effect, 2016, **78**, 74–85.

- 63 R. R. Kale, H. Mukundan, D. N. Price, J. F. Harris, D. M. Lewallen, B. I. Swanson, J. G. Schmidt and S. S. Iyer, Detection of intact influenza viruses using biotinylated biantennary S-sialosides, *J. Am. Chem. Soc.*, 2008, **130**, 8169–8171.
- 64 A. Marra, L. Moni, D. Pazzi, A. Corallini, D. Bridi and A. Dondoni, Synthesis of sialoclusters appended to calix[4]arene platforms via multiple azide-alkyne cycloaddition. New inhibitors of hemagglutination and cytopathic effect mediated by BK and influenza A viruses, *Org. Biomol. Chem.*, 2008, **6**, 1396–1409.
- 65 Y. Yang, H. P. Liu, Q. Yu, M. B. Yang, D. M. Wang, T. W. Jia, H. J. He, Y. He, H. X. Xiao, S. S. Iyer, Z. C. Fan, X. Meng and P. Yu, Multivalent S-sialoside protein conjugates block influenza hemagglutinin and neuraminidase, *Carbohydr. Res.*, 2016, **435**, 68–75.
- 66 P. Kiran, S. Bhatia, D. Lauster, S. Aleksić, C. Fleck, N. Peric, W. Maison, S. Liese, B. G. Keller, A. Herrmann and R. Haag, Exploring rigid and flexible core trivalent sialosides for influenza virus inhibition, *Chem. Eur. J.*, 2018, 1–14.
- 67 P. I. Kitov, J. M. Sadowska, G. Mulvey, G. D. Armstrong, H. Ling, N. S. Pannu, R. J. Read and D. R. Bundle, Shiga-like toxins are neutralized by tailored multivalent carbohydrate ligands, *Nature*, 2000, **403**, 669–672.
- 68 G. D. Glick and J. R. Knowles, Molecular recognition of bivalent sialosides by influenza virus, *J. Am. Chem. Soc.*, 1991, **113**, 4701–4703.
- 69 S. Sabesan, J. O. Duus, P. Domaille, S. Kelm and J. C. Paulson, Synthesis of cluster sialoside inhibitors for influenza virus, *J. Am. Chem. Soc.*, 1991, **113**, 5865–5866.
- 70 T. Ohta, N. Miura, N. Fujitani, F. Nakajima, K. Niikura, R. Sadamoto, C. T. Guo, T. Suzuki, Y. Suzuki, K. Monde and S. I. Nishimura, Glycotentacles: Synthesis of cyclic glycopeptides, toward a tailored blocker of influenza virus hemagglutinin, *Angew. Chemie-Int. Ed.*, 2003, **42**, 5186–5189.
- 71 F. Feng, N. Miura, N. Isoda, Y. Sakoda, M. Okamatsu, H. Kida and S.-I. Nishimura, Novel trivalent anti-influenza reagent, *Bioorg. Med. Chem. Lett.*
- 72 M. Waldmann, K. Hoelscher, M. Wienke, F. C. Niemeyer, D. Rehders and B. Meyer, A nanomolar multivalent ligand as entry inhibitor of the hemagglutinin of avian influenza, *J. Am. Chem. Soc.*, 2014, **136**, 783–788.
- 73 M. Yamabe, K. Kaihatsu and Y. Ebara, Sialyllactose-modified three-way junction DNA as binding inhibitor of influenza virus hemagglutinin, *Bioconjug. Chem.*, 2018, **29**, 1490–1494.
- 74 F. Krammer and P. Palese, Influenza virus hemagglutinin stalk-based antibodies and vaccines, *Curr. Opin. Virol.*, 2013, **3**, 521–530.
- 75 D. J. Dilillo, G. S. Tan, P. Palese and J. V. Ravetch, Broadly neutralizing hemagglutinin stalk-specific antibodies require FcR interactions for protection against influenza virus *in vivo*, *Nat. Med.*, 2014, **20**, 143–151.
- 76 H. Memczak, D. Lauster, P. Kar, S. Di Lella, R. Volkmer, V. Knecht, A. Herrmann, E. Ehrentreich-Förster, F. F. Bier and W. F. M. Stöcklein, Anti-hemagglutinin antibody derived lead peptides for inhibitors of influenza virus binding, *PLoS One*, 2016, **11**, 1–24.

- 77 E. Feng, D. Ye, J. Li, D. Zhang, J. Wang, F. Zhao, R. Hilgenfeld, M. Zheng, H. Jiang and H. Liu, Recent advances in neuraminidase inhibitor development as anti-influenza drugs, *ChemMedChem*, 2012, **7**, 1527–1536.
- 78 Z.-L. Yang, X.-F. Zeng, H.-P. Liu, Q. Yu, X. Meng, Z.-L. Yan, Z.-C. Fan, H.-X. Xiao, S. S. Iyer, Y. Yang and P. Yu, Synthesis of multivalent difluorinated zanamivir analogs as potent antiviral inhibitors, *Tetrahedron Lett.*, 2016, 15–18.
- 79 L. Fu, Y. Bi, Y. Wu, S. Zhang, J. Qi, Y. Li, X. Lu, Z. Zhang, X. Lv, J. Yan, G. F. Gao and X. Li, Structure-based tetravalent Zanamivir with potent inhibitory activity against drug-resistant influenza viruses, *J. Med. Chem.*, 2016, **59**, 6303–6312.
- 80 T. Heise, C. Büll, D. M. Beurskens, E. Rossing, M. I. De Jonge, G. J. Adema, T. J. Boltje and J. D. Langereis, Metabolic oligosaccharide engineering with alkyne sialic acids confers Neuraminidase resistance and inhibits influenza reproduction, *Bioconj. Chem.*, 2017, **28**, 1811–1815.
- 81 X. Meng, M. Yang, Y. Li, X. Li, T. Jia, H. He, Q. Yu, N. Guo, Y. He, P. Yu and Y. Yang, Multivalent neuraminidase hydrolysis resistant triazole-sialoside protein conjugates as influenza-adsorbents, *Chinese Chem. Lett.*, 2018, **29**, 76–80.
- 82 R. U. Kadam and I. A. Wilson, A small-molecule fragment that emulates binding of receptor and broadly neutralizing antibodies to influenza A hemagglutinin, *Proc. Natl. Acad. Sci.*, 2018, 1801999115.
- 83 R. J. Pieters, J. Cuntze, M. Bonnet and F. Diederich, Enantioselective recognition with C3-symmetric cage-like receptors in solution and on a stationary phase, *J. Chem. Soc. Perkin Trans. 2*, 1997, 1891–1900.
- 84 F. Pertici and R. J. Pieters, Potent divalent inhibitors with rigid glucose click spacers for *Pseudomonas aeruginosa* lectin LecA, *Chem. Commun.*, 2012, **48**, 4008–4010.
- 85 F. Pertici, N. J. De Mol, J. Kemmink and R. J. Pieters, Optimizing divalent inhibitors of *Pseudomonas aeruginosa* lectin leca by using a rigid spacer, *Chem. A Eur. J.*, 2013, **19**, 16923–16927.
- 86 R. Visini, X. Jin, M. Bergmann, G. Michaud, F. Pertici, O. Fu, A. Pukin, T. R. Branson, D. M. E. Thies-Weesie, J. Kemmink, E. Gillon, A. Imberty, A. Stocker, T. Darbre, R. J. Pieters and J. L. Reymond, Structural Insight into Multivalent Galactoside Binding to *Pseudomonas aeruginosa* Lectin LecA, *ACS Chem. Biol.*, 2015, **10**, 2455–2462.

# *Chapter 2*

*Synthesis of building blocks  
for hemagglutinin inhibitors of Influenza A virus*

## 2.1 Introduction

Influenza A virus (IAV) is the cause of the flu infection which poses a serious threat to human health. History has shown that the flu can lead to serious pandemics, with millions of deaths in 1918<sup>1</sup> and a risk of future outbreaks of deadly variants.<sup>2</sup> The influenza A virus contains two major virulence factors on its surface, hemagglutinin (HA) and neuraminidase (NA), that both bind to sialylated glycans.<sup>3</sup> The HA is responsible for attachment of the virus to the tissue surface which triggers the infection process (Figure 1a), and its specificity lies at the origin of the species specificity and tissue tropism of the virus and is also of importance for the viral fusion with the endosome.<sup>4</sup> The NA is a glycosidase enzyme that removes the sialic acid group from glycans which leads to a release of the HA-based attachment and allows the virus to burrow through the protective mucosa and enter the cell. Most importantly, the NA also allows the next generation of newly produced virus to be released from the cell surface to infect other cells (Figure 1b).<sup>5,6</sup>

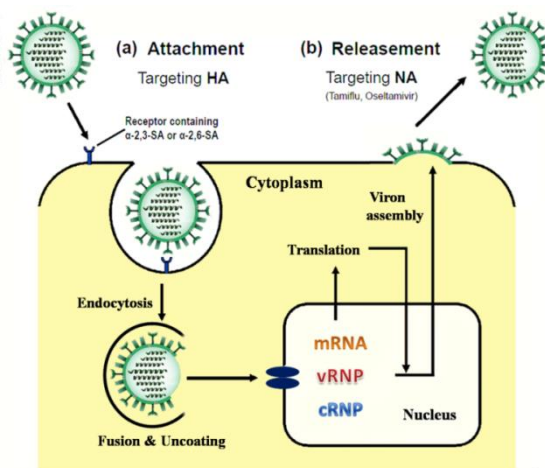


**Figure 1. Life cycle of the Influenza A virus.** The infection is triggered by recognition between the HA and the host cell surface by attachment of the  $\alpha$ -2,3- or  $\alpha$ -2,6-linked sialyl moieties, then the IAV enters the cell by receptor-mediated endocytosis. With the change of pH in the cell, a pH-dependent fusion and uncoating of the ribonucleoprotein (RNP) complexes occurs. After the translation step, new viral genomes are packaged and the virions bud to release from the host cell which is mediated by the activity of NA. The new generation of IAV will be produced to infect other cells.<sup>7</sup>

Several approaches are being used to interfere with the infection of the IAVs, and the most common of which is the vaccination strategy.<sup>8</sup> This is a valuable approach

for the seasonal IAV variants that are very common and infective, yet usually only life threatening for those with weakened immune systems like children and the elderly. The more dangerous IAV variants, are only common in an epidemic. In case of an epidemic, the NA inhibitors such as oseltamivir or zanamivir can be used to reduce the illness symptoms and infectivity.<sup>9</sup> Unfortunately, resistance of IAVs to these NA inhibitors has been observed<sup>10</sup> which greatly hampers the effectiveness of the therapy. Inspired by the treatment for HIV infections, it might be more effective to use a combination therapy that addresses both HA and NA and possibly additional targets.

HA is a glycoprotein which contains two major domains: the immunodominant globular head (HA1) domain (receptor-binding region), and the stalk (HA2) domain, which remains relatively conserved between influenza virus strains<sup>11-13</sup> (Figure 2). Binding of HA to sialic acid (SA) terminated glycan receptors on the surface of host cells is the first crucial step of infection and transmission.<sup>14</sup> It has been established that human-adapted HA prefers the  $\alpha$ -2,6-linked sialyl-glycans expressed in the upper respiratory tract of humans, whereas the avian-adapted HA preferentially binds to the  $\alpha$ -2,3-linked regioisomer.<sup>15-17</sup>

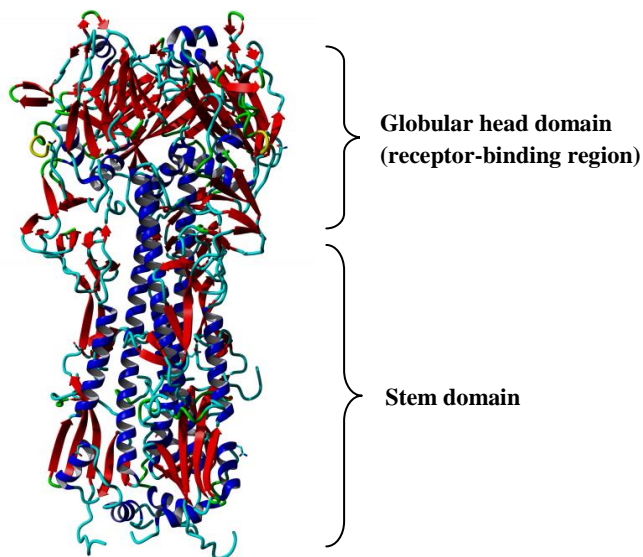


**Figure 2.** Structure of HA protein which containing two major domains (PDB ID: 1HGG), the figure was generated with YASARA.

As the NA inhibitor-resistant viruses have already emerged because of the high mutation rate of IAV,<sup>18,19</sup> HA is currently one of the ideal alternative targets to create anti-influenza drugs. Such drugs would be complementary with drugs that

target NA. However, the situation for new drug development is different. HA binds only with millimolar affinities to its sialylated glycan receptors. These low affinities are a challenging starting point for a carbohydrate based drugs development program, but also non-carbohydrate approaches have faced this challenge.<sup>20</sup> The virus, however, binds with high affinity to tissue surfaces by using multivalency,<sup>21</sup> which increases its avidity to levels that enable the infection. The multivalency effects involve the simultaneous binding of glycans to more than one of the three binding sites per HA trimer on the IAV surface, but also the simultaneous binding of cell surface glycans to multiple HA protein trimers on the viral surface. The overall avidity effects are very strong and crucial for IAV. Based on the nature of HA binding, we aimed to design multivalent HA inhibitors that mimic these interactions between HA and the sialyl-oligosaccharides.

One of the proposed inhibitor designs is based on the trimeric structure of the “head” of the hemagglutinin protein which will also be trivalent and consists of three different parts: a ligand that contains an  $\alpha$ -2,6-sialylated glycan (3 copies), a propeller shaped scaffold, and a short rigid spacer that links the ligands to the scaffold (Figure 3). The synthetic strategy to combine these three parts is based on the efficient copper catalyzed azide alkyne cycloaddition (CuAAC, “click”) reaction under microwave irradiation.

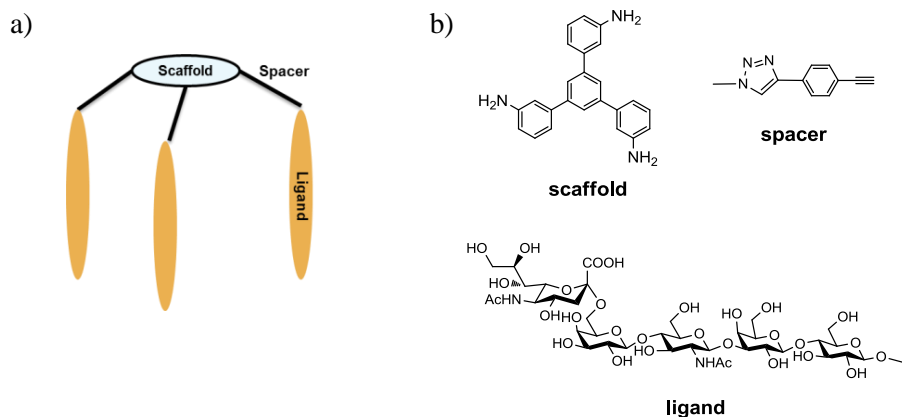


**Figure 3.** Schematic representation of the proposed trimeric inhibitor of Influenza A virus.

Another inhibitor design strategy is based on similar research within our group in which we have designed a series of divalent ligands presenting galactose residues with variations in the length of the spacer to fit a divalent binding mode.<sup>22–24</sup> A relatively rigid and straight spacer based on the alternation of glucose moieties linked by a 1,2,3-triazole unit via ‘click’ chemistry was designed and evaluated and



showed potent inhibition effect of the *Pseudomonas aeruginosa* lectin LecA. Here we aim to introduce a longer rigid spacer to link two sialylated ligands (Figure 4), by comparing different inhibitory effects of dimers and trimers, we may learn more to optimize anti-flu drugs in the future studies.

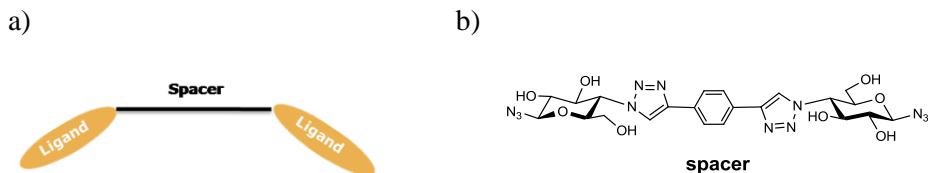


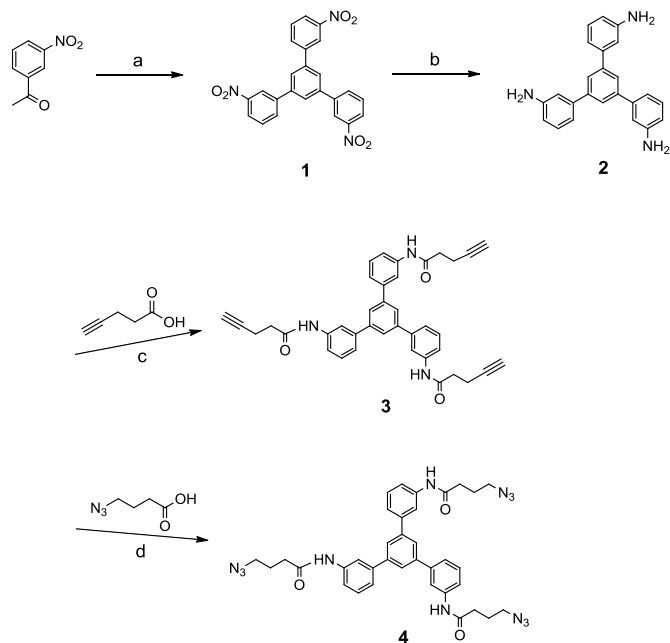
**Figure 4.** Schematic representation of the proposed dimeric inhibitor of Influenza A virus.

In this chapter, efforts to obtain suitable building blocks to be used in the synthesis of multivalent HA inhibitors are described based on the structure designs mentioned above.

## 2.2 Results and discussion

### 2.2.1 Design and synthesis of the trimeric scaffolds

Since HA is a symmetrical trimer, the scaffold reflects this geometry. The amino functionalized 1,3,5-triphenyl benzene<sup>25</sup> is particularly attractive, and its propeller shape may be ideal for the available area on the top area of the HA protein, taking advantage of the groove areas for the spacer arms. The synthetic strategy followed to obtain the scaffolds is shown in Scheme 1. They can subsequently be coupled to 3 copies of the spacer via the CuAAC reaction.



**Scheme 1.** Synthesis of the 1,3,5-triphenyl benzene-based scaffolds of trivalent hemagglutinin inhibitors. Reagents and conditions: a)  $K_2S_2O_7$ ,  $H_2SO_4$ , 85 °C, 8 h, 25 %; b)  $H_2$ , Pd/C, DMF, 14 h, 77 %; c) EDC HCl, DMAP, DCM, 48 h, 59 %; d) EDC HCl, DMAP, DCM, 48 h, 40 %.

The synthesis procedure started with the commercially available 3-nitroacetophenone. The first step was a polycondensation reaction which was first published in 1936<sup>26</sup> by Müller and Bernhauer. The 3-nitroacetophenone was first ground with solid potassium pyrosulfate ( $K_2S_2O_7$ ) and then heated together with concentrated sulfuric acid at 85 °C conditions to form the 1,3,5-trinitrophenyl benzene (compound 1). After 8 h of the reaction, the mixture was washed with ethanol and  $H_2O$ , then recrystallized by using xylenes-chlorobenzene solution to give a 25 % yield. The high melting point (298-299 °C) matched with the literature. Further characterizations were also performed by measuring  $^1H$  and  $^{13}C$  NMR which gave us more structural evidence of the very poorly soluble compound 1 for the first time (Figure 5).

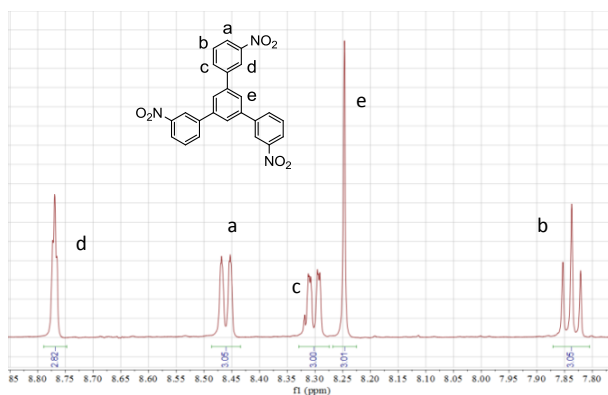


**Figure 5.**  $^1\text{H-NMR}$  spectra of compound **1** indicating the typical chemical shifts of the protons from the nitro-substituted benzene rings.

The nitro reduction was catalyzed by using 10 % palladium on carbon and used hydrogen to turn the three nitro groups into aromatic amino groups (compound **2**). Once the amines were formed, 4-pentanoic acid or 4-azidobutanoic acid<sup>27</sup> were introduced by an EDC mediated coupling reaction to obtain two versions of the scaffold (compound **3** & **4**), containing an alkyne or an azide unit, respectively. The coupling reaction to get compound **3** used the commercially available 4-pentanoic acid with a yield of 59 %. For compound **4**, the first step was to synthesize 4-azidobutanoic acid from the amino acid by a diazotransfer reaction by imidazole-1-sulfonyl azide hydrochloride. Then the azido-containing unit and compound **2** were coupled to give compound **4** with a yield of 40 %. The relatively low yield of compounds **3** & **4** may be caused by the low reactivity of the three aromatic amino groups, that all have to react to obtain the product. Analysis and characterization were also performed by measuring HPLC (Figure 6), HRMS,  $^1\text{H}$  and  $^{13}\text{C}$  NMR which confirmed the structures of compound **3** & **4**. These two versions of the trivalent scaffold can be used for elongations using the CuAAC reactions with additional azide/alkyne containing groups.

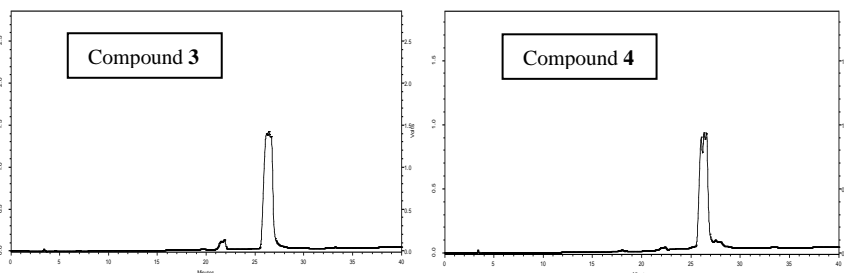
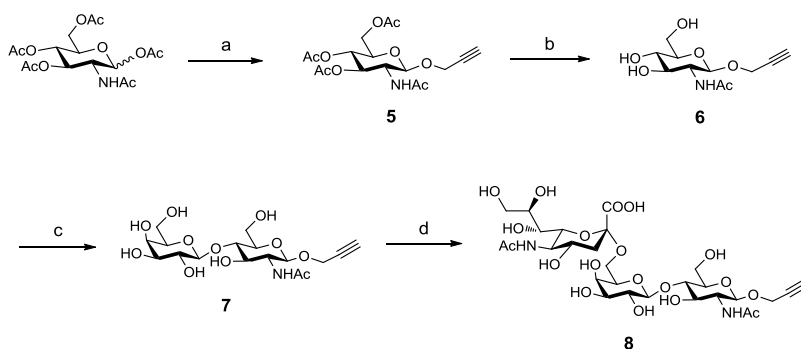


**Figure 6.** HPLC traces of scaffolds **3** & **4** after purification by column chromatography.

## 2.2.2 Design and synthesis of the ligands

The ligands that were made were  $\alpha$ -2,6-sialyl-LacNAc moieties (Scheme 2 & 3), in the form that allows the conjugation via CuAAC reaction (containing alkyne or azide units). The choice for the 2,6-variant of the sialyl-LacNAc ligand is due to the occurrence of the epitope on human cells, i.e. this is to target the matching viral specificity of the viruses that infect humans.

The first synthesis was aimed at the sialyl-LacNAc ligand containing a  $\beta$ -linked propargyl group at the reducing end, i.e. compound **8** (Scheme 2). The formation of a propargyl-containing moiety at the anomeric position with a  $\beta$  configuration in a lactose derivative is well described in the literature.<sup>28</sup>



**Scheme 2.** Synthesis of  $\alpha$ 2,6-sialyl-LacNAc ligand **8** for hemagglutinin inhibitors. Reagents and conditions: a) Propargyl alcohol,  $\text{BF}_3 \cdot \text{Et}_2\text{O}$ ,  $\text{DCM}$ ,  $4 \text{ \AA}$  sieves, overnight, 65 %; b)  $\text{NaOMe}$ ,  $\text{MeOH}$ , overnight, quant.; c)  $\text{UDP-Gal}$ , *LgtB*,  $\text{MES}$  buffer,  $37^\circ\text{C}$ , 3 h, 85 %; d)  $\text{CMP-NANA}$ , *PmST1* mutant P34H/M144L,  $\text{Tris-HCl}$  buffer,  $\text{pH } 7.5$ ,  $37^\circ\text{C}$ , 4 h, 77 %.

Starting from peracetylated N-acetyl-glucosamine, the propargyl group was introduced by a glycosylation reaction using propargyl alcohol and  $\text{BF}_3 \cdot \text{OEt}_2$  as the mediator of the reaction. The first attempt of the reaction failed seemingly because insufficient propargyl alcohol (2 equiv) was present, and when the amount was increased to 4 equiv, product **5** was formed without any  $\alpha$ -isomer with a yield of 65 % after silica gel column chromatography. Then the acetyl groups were removed using  $\text{NaOMe}$  in  $\text{MeOH}$  in an overnight reaction at room temperature to obtain compound **6**.  $\beta$ -1,4-galactosyltransferase from *Neisseria meningitidis* (*LgtB*)<sup>29</sup> was used to produce disaccharide **7**. *LgtB* is an efficient enzyme to produce galactosylated oligosaccharides on a multigram scale. Compound **6** and 1.5 equiv  $\text{UDP-Gal}$  were dissolved in 100 mM  $\text{MES}$  buffer, containing 20 mM  $\text{MnCl}_2$  and were incubated with the galactosyltransferase for 3 h at  $37^\circ\text{C}$  while the

reaction was monitored by TLC. When the reaction was complete, the mixture was first centrifuged to remove the insoluble parts. After lyophilizing the solution, about 50  $\mu\text{L}$  of the reaction mixture was loaded on to a Bio-gel P-2 column which has efficient separation power for hydrophobic molecules with a molecular weight of less than 1800. The fractions containing compound **7** were collected and lyophilized to give a white solid with 85 % yield without further purification. After that,  $\alpha$ -2,6-sialyltransferase (PmST1 double mutant P34H/M144L)<sup>30</sup> from *Pasteurella multocida* was used to produce compound **8** as our first ligand for the HA inhibitors. PmST1 is a bacterial enzyme that is commonly used in catalyzing  $\alpha$ -2,3-sialylation to only the terminal galactose residues in glycans. McArthur and co-workers found a mutant version of PmST1 which gave high yields of  $\alpha$ -2,6-sialylated products in a cheap and efficient way compared to other enzymes that could be used for this type of sialylation. Compound **7** and 1.2 equiv of CMP-NANA were dissolved in 100 mM Tris-HCl buffer (pH 7.5) containing 20 mM  $\text{MgCl}_2$  and incubated with the  $\alpha$ -2,6-sialyltransferase for 4 h at 37 °C while the reaction was also monitored by TLC. Following the same purification procedure than for compound **7**, compound **8** was then characterized by HRMS, <sup>1</sup>H NMR (Figure 7), <sup>13</sup>C NMR, and the final yield of the product was 77 % after purification.

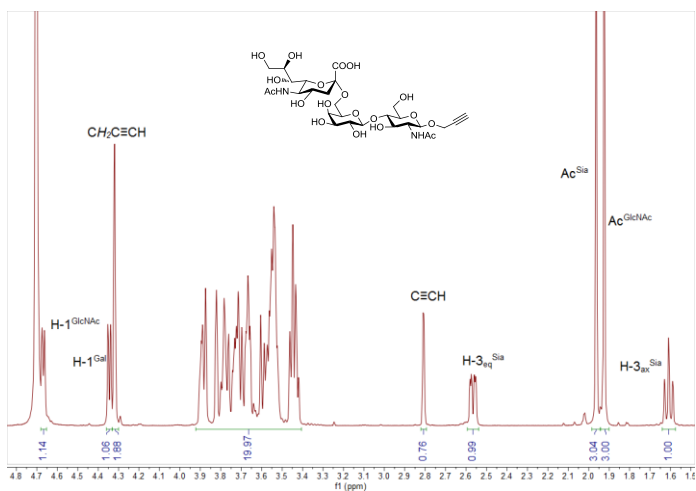
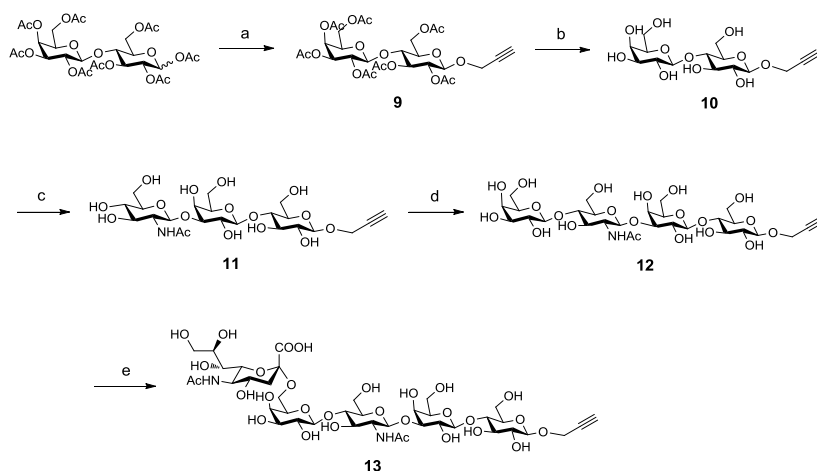


**Figure 7.** <sup>1</sup>H NMR spectra of compound **8** indicating the typical chemical shifts of the protons from the sugar units.

Besides compound **8**, we also synthesized a longer version of the ligand, i.e. the  $\alpha$ -2,6-sialyl-LacNAc-Lactose to be linked to the scaffolds, and likely better capable of reaching the three HA binding sites simultaneously. Paulson *et al.* showed in their study of human HA binding by sialylated poly-N-acetyllactosamine chains,<sup>31</sup>

that the binding is stronger for sialylated glycans containing di-LacNAc in comparison with mono-LacNAc. However, Tian *et al.* investigated the fluorescence response to influenza A virus by using sialyl-Lactose and LacNAc. In their research, the sialyl-Lactose based glycofoldamer showed a better response compared to sialyl-LacNAc version.<sup>32</sup> These results showed that there is no clear answers as to what is the most suitable monovalent ligand for all HA's. We decided to synthesize an elongated ligand, i.e.  $\alpha$ -2,6-sialyl-LacNAc-Lactose. This elongated ligand could also be used for comparison with the  $\alpha$ -2,6-sialyl-LacNAc ligand **8**.



**Scheme 3.** Synthesis of  $\alpha$ 2,6-sialyl-LacNAc-Lactose ligand for hemagglutinin inhibitors. Reagents and conditions: a) Propargyl alcohol,  $\text{BF}_3 \cdot \text{Et}_2\text{O}$ , Dry DCM, 48 h, 39 %; b) NaOMe, MeOH, overnight, quant.; c) UDP-GlcNAc, *H. Pylori* $\beta$ 3GlcNAcT, CIAP, HEPES buffer, pH 7.3, 37 °C, overnight, 70 %; d) UDP-Gal, *LgtB*, MES buffer, 37 °C, 3 h, 81 %; e) CMP-NANA, PmST1 mutant P34H/M144L, Tris-HCl buffer, pH 7.5, 37 °C, 4 h, 27 %.

The synthesis approach started with peracetylated lactose, when the reagent propargyl alcohol and the solvent dry DCM and later the Lewis acid  $\text{BF}_3 \cdot \text{Et}_2\text{O}$  were added for reaction. The work up of this step and silica gel column chromatography resulted in lactoside **9** as a transparent oil with a yield of 39 % following a method described in the literature.<sup>28</sup> Then, the acetyl groups were removed using NaOMe in MeOH to obtain the unprotected lactoside **10** in quantitative yield. The subsequent attachment of GlcNAc linked in a  $\beta$ -1,4 fashion was realized enzymatically, using a  $\beta$ -1,3-N-acetylglucosaminyltransferase of bacterial origin, i.e. from *Helicobacter pylori*.<sup>33</sup> This bacterial GlcNAc transferase (*H. Pylori* $\beta$ 3GlcNAcT) together with 10 mU Calf intestine Alkaline Phosphatase

(CIAP) were added to the solution of **10** and 1.5 equiv UDP-GlcNAc. CIAP was added to hydrolyze the free UDP to uridine and inorganic phosphate, preventing the free nucleotide's inhibitory effects on the enzyme activity. The reaction mixture was incubated at 37 °C overnight to produce the fully glycosylated trisaccharide **11** in 70 % yield after purification by Bio-gel P-2 column using an automatic fraction collector. Then, the galactosyltransferase (*LgtB*) was used for the attachment of another galactose and  $\alpha$ -2,6-sialyltransferase (PmST1 double mutant P34H/M144L) was used to elongate the final ligand (compound **13**) with an  $\alpha$ -2,6-linked sialic acid. After the final enzymatic reaction, **13** was first purified by a Bio-gel P-2 column eluting with H<sub>2</sub>O. Further purification with preparative HPLC was performed using a HILIC column. Despite all these procedures of purification, the desired pentasaccharide **13** (Table 1) was obtained in 27 % yield.

**Table 1.** Method for preparation HPLC using HILIC column to purify compound **13**.

Time (min)	Buffer A (%)	Buffer B (%)	Flow rate (mL/min)
0.0	10	90	3.6
5.0	28	72	3.6
7.0	28	72	3.6
10.0	31	69	3.6
14.0	31	69	3.6
14.1	50	50	3.6
18.0	50	50	3.6

Analysis and characterization were performed by measuring LC-MS, HRMS, <sup>1</sup>H NMR (Figure 8), COSY, and HSQC. Based on that, the signals of the anomeric centers of these sugar units were assigned as shown in the <sup>1</sup>H NMR spectrum.

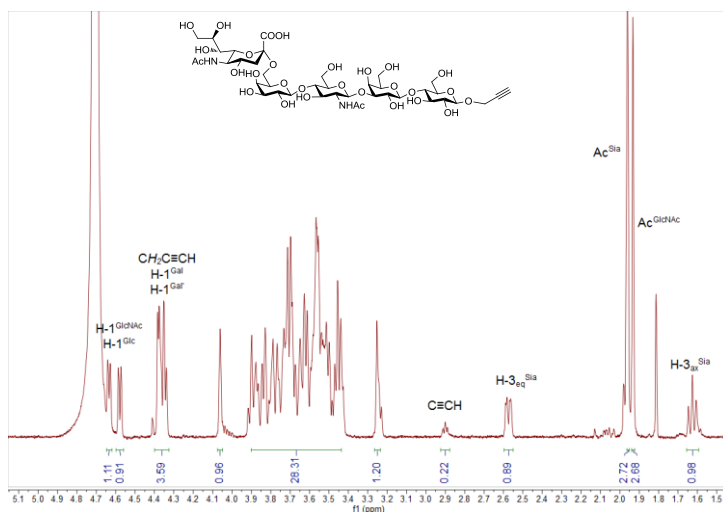
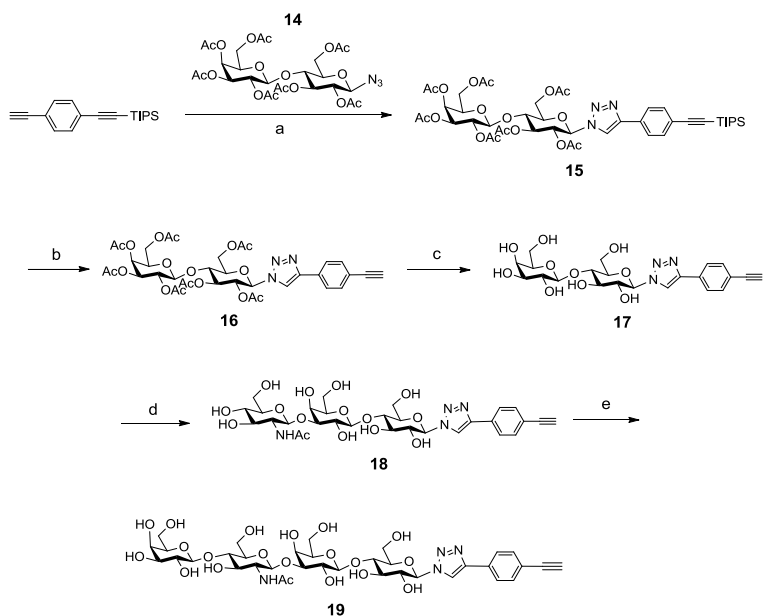


**Figure 8.**  $^1\text{H}$  NMR spectra of compound **13** with annotations of the typical chemical shift pattern of the indicated protons.

### 2.2.3 Design and synthesis of the spacer

In the design and synthesis of the *Pseudomonas aeruginosa* lectin LecA inhibitors,<sup>23,24</sup> the use of rigid or conformationally well-defined spacers based on directly fused glucose-triazole units has led to a ca. 7500-fold potency enhancement in the inhibition, for the best matched divalent ligand. In other words, introducing a proper designed rigid spacer can play an important role in the inhibition of biological processes involving multi-binding site proteins. Inspired by these findings from our group, a rigid elongation was also introduced to the design of our HA inhibitors. Besides the rigidity, the additional elongation also added length to the arms, that might very well be important for optimal binding. To this end a synthesis was started that contained a triazole-phenyl-alkyne moiety to the reducing end of a LacNAc-Lac tetrasaccharide. The synthesis procedure of the rigid spacer was shown in Scheme 4.





**Scheme 4.** Synthesis of LacNAc-Lactose glycan with rigid elongation for hemagglutinin inhibitors. Reagents and conditions: a) **14**, CuSO<sub>4</sub> 5H<sub>2</sub>O, Na-ascorbate, DMF/H<sub>2</sub>O (9:1), microwave 80 °C, 30 min; b) TBAF 3H<sub>2</sub>O, THF, 97 % ; c) NaOMe, MeOH, overnight, quant.; d) UDP-GlcNAc, *H. Pylori*β3GlcNAcT, CIAP, HEPES buffer, pH 7.3, 37 °C, overnight, 71 %; e) UDP-Gal, *LgtB*, MES buffer, 37 °C, 3 h, 82 %.

The synthesis procedure started with the CuAAC ‘click’ reaction of the 1-((triisopropylsilyl)ethynyl)-4-ethynylbenzene to per-acetyl-azidolactose **14**. **14** was obtained by following the procedure of the literature<sup>34</sup> transferring the azido unit to the anomeric centre of the glycan. Then the cycloaddition reaction was performed with these two starting materials, catalyzed by CuSO<sub>4</sub> 5H<sub>2</sub>O and Na-ascorbate in the solution of a DMF/H<sub>2</sub>O mixture under microwave irradiation at 80 °C for 30 min. With an excess amount of **14** added to the reaction mixture, 1-((triisopropylsilyl)ethynyl)-4-ethynylbenzene showed complete conversion into compound **15**. After evaporation of the solvents, **15** was characterized by HRMS (Figure 9) and used directly for the next step which was the deprotection of the other alkyne unit.

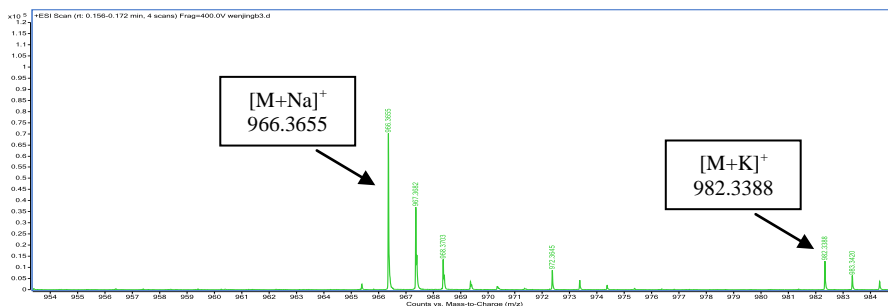


**Figure 9.** HRMS spectra of compound **15** giving the MS of 966.3655 which referred to  $C_{45}H_{61}N_3O_{17}Si$   $[M+Na]^+$  and 982.3388 referred to  $[M+K]^+$ .

TBAF deprotection of **15** in THF solution yielded **16** in 97 %. Deprotection of the acetyl groups on the sugar chain was performed as the third step, with 0.1 equiv NaOMe stirring at room temperature overnight. Compound **17** was obtained as a white solid with a quantitative yield which dissolved much better in MeOH than in  $H_2O$  and was used without further purification. Enzymatic elongation was followed after the chemosynthetic part. The first glycosylation processed with 1.5 equiv of UDP-GlcNAc. CIAP (10 mU) and *H. Pylori*  $\beta 3GlcNAcT$  ( $\beta 1-3GlcNAc$  Transferase) were added and the mixture was incubated at 37 °C overnight for full glycosylation. Completion of the reaction was monitored by TLC and the purification was performed by gel filtration over Bio-gel P-2 (eluent  $H_2O$ ). Compound **18** was obtained in a 71 % yield after this purification procedure. The final step to synthesize **19** was to introduce the galactose unit. By dissolving **18** and 1.5 equiv UDP-Gal in 100 mM MES buffer, *LgtB* was added to the solution and the reaction was finished efficiently in 3 h. The reaction mixture was also purified following the same method by using the Bio-gel column which gave compound **19** as an amorphous white solid with 82 % yield. Further characterization was performed by measuring HRMS,  $^1H$  NMR, COSY and HSQC which confirmed the structure of compound **19** (Figure 10). Although part of the spectrum within the  $\delta$  3.92 – 3.42 range was quite crowded, the signals of the triazole, phenyl group and anomeric protons were clearly identified.

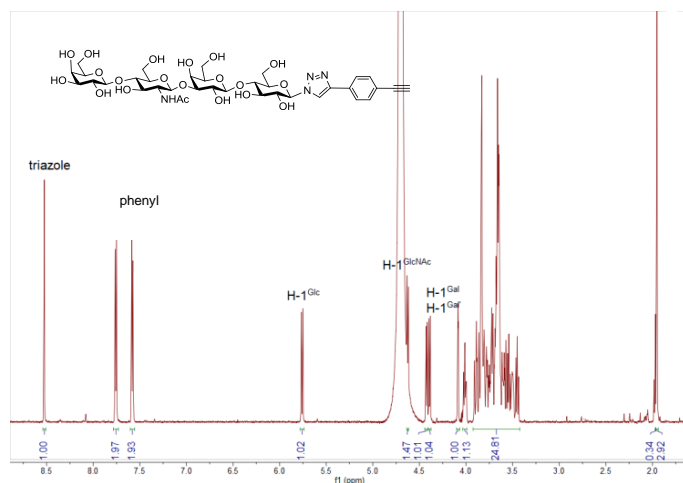


**Figure 10.**  $^1\text{H}$  NMR spectra of compound **18** indicating the typical chemical shifts of the protons.

### 2.3 Conclusion and outlook

A reliable pathway for the synthesis of suitable building blocks to build up hemagglutinin inhibitors was found. Different strategies were investigated. And we successfully managed to synthesize all the building blocks we need for the assembly of the proposed HA inhibitors. For the first time, a rigid spacer attachment was introduced in the design of a HA inhibitor to hopefully enhance the binding affinity between the sugar moiety and the virus surface protein. Enzymes like  $\beta$ -1,3-N-acetylglucosaminyltransferase (*H. Pylori*  $\beta$ 3GlcNAcT),  $\beta$ -1,4-galactosyltransferase (*LgtB*) and  $\alpha$ 2,6-sialyltransferase (PmST1 mutant P34H/M144L) were made in house by Robert P. de Vries and used efficiently for getting the desired compounds as we designed. By further CuAAC conjugation and enzymatic elongation, we would get the target trivalent HA inhibitors at the next stage of the research program. The building blocks are also important reference compounds for the subsequent biological activity analysis. This synthetic strategy presented here also have some drawbacks which have to be taken into account. The biggest problem encountered during the synthesis route was the small quantities that could be used in the enzymatic reactions which limited the amounts of the targeted products. Chemical synthesis typically is run on a larger scale, but would in these case require many more steps involving protecting group manipulations, as well as precarious glycosylation reactions. Furthermore, there is no inherent reason why the enzymatic synthesis could not be scaled up.

## 2.4 Experimental procedure

### 2.4.1 General

#### 2.4.1.1 Chemical synthesis and identification

Chemicals were used as obtained from commercial sources without further purification unless stated otherwise. Compound **1**, **2**, **5**, **6**, **9**, **10** and **14** were prepared as reported in the literature procedures.<sup>25,26,28,34</sup> The solvents were obtained as synthesis grade and stored on molecular sieves (4 Å). Column chromatography was performed using Silica-P Flash silica gel (60 Å, particle size 40-63µm) from Silicycle. TLC was performed on Merck precoated silica gel 60F254 glass plates and compound spots were visualized with UV light and/or 10 % H<sub>2</sub>SO<sub>4</sub> (MeOH). Melting points were measured by Buchi melting point determination apparatus. Microwave reaction was carried out in a Biotage Initiator (300 W) reactor. <sup>1</sup>H NMR spectra were recorded on a 400 MHz, 500 MHz or 600 MHz spectrometer. <sup>13</sup>C NMR analysis was recorded on a 100 MHz, 125 MHz or 151 MHz spectrometer. High resolution mass spectrometry (HRMS) analysis was recorded using Agilent 6560 Ion Mobility Q-TOF LC/MS. Analytical HPLC was performed on a Shimadzu-10AVP (Class-VP) system using a Phenomenex Gemini C18 column (110 Å, 5 µm, 250×4.6 mm) at a flow rate of 1 mL/min. The used buffers were 0.1 % trifluoroacetic acid in Buffer A CH<sub>3</sub>CN/H<sub>2</sub>O (5:95 v/v) and 0.1 % trifluoroacetic acid in Buffer B CH<sub>3</sub>CN/H<sub>2</sub>O (95:5 v/v). Runs were performed using a standard protocol: 100 % buffer A for 2 min, then a linear gradient of buffer B (0 – 100 % in 38 min) and UV-absorption was measured at 210 nm and 254 nm. Analytical LC-ESI-MS was performed on Thermo-Finnigan LCQ Deca XP Max using the same buffers and protocol as described for analytical HPLC.

#### 2.4.1.2 Enzymatic synthesis and identification

All enzymatic reactions were performed in aqueous buffered systems with the appropriate pH for each enzyme. The reactions were monitored by TLC performed on Silicycle aluminium backed silica F254 plates. After development with appropriate eluents, the spots were visualized by UV light and/or dipping in 10 % sulfuric acid in methanol. Gel filtration chromatography was performed with column packed with Bio-gel P-2 Fine (Bio-Rad), eluted with water. Water was purified by Milli-Q Gradient A10 Water Purification System. Lyophilization was performed on a Christ Alpha 1-2 apparatus. NMR spectra were recorded on the same equipment as 2.4.1.1. Analytical LC-MS was performed on Agilent 6560 Ion Mobility Q-TOF LC/MS using a Waters XBridge HILIC column (5 µm, 250×4.6 mm) at a flow rate of 0.6 mL/min. The used buffers were 50 mM formic acid in

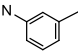
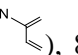
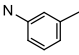
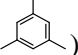
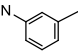
H<sub>2</sub>O (Buffer A, pH 4.4) and CH<sub>3</sub>CN (Buffer B). UV-absorption was measured at 210 nm and 254 nm. Purification using preparative HPLC was performed on an Shimadzu 20A HPLC system with a Waters XBridge BEH Prep Amide column (5 μm, 250×10 mm) at a flow rate of 3.6 mL/min.

β-1,3-N-acetylglucosaminyltransferase (*H. Pylori*β3GlcNAcT)<sup>33</sup> (0.7 mg/mL), β-1,4-galactosyltransferase (*LgtB*)<sup>29</sup> (71.3 mg/mL) and α-2,6-sialyltransferase (PmST1 mutant P34H/M144L)<sup>30</sup> (2.3 mg/mL) were made in house by cell free extract (measured by Thermo Scientific™ NanoDrop 2000). Alkaline Phosphatase from calf intestine (1,000 U/mL) was purchased from Invitrogen. Uridine 5'-diphospho-N-acetylglucosamine (UDP-GlcNAc) and Uridine 5'-diphosphogalactose (UDP-Gal) were purchased from Sigma-Aldrich. Cytidine-5'-monophospho-N-acetylneuraminic acid (CMP-NANA) was purchased from Roche Diagnostics GmbH.

## 2.4.2 Synthetic procedures and compound characterization

### 3,3''-dinitro-5'-(3-nitrophenyl)-1,1':3',1''-terphenyl (1)

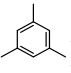
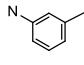
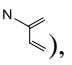
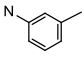
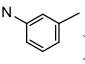
3'-nitroacetophenone (16.95 mmol, 2.8 g) and K<sub>2</sub>S<sub>2</sub>O<sub>7</sub> (17.69 mmol, 4.1 g) were mixed and ground in a mortar. Then the mixture was moved to a 250 mL round-bottomed flask. H<sub>2</sub>SO<sub>4</sub> (7.5 mmol, 0.4 mL) was added to the mixture. The reaction mixture was heated in an oil bath at 85 °C for 8 h. H<sub>2</sub>O and EtOH were used for washing the mixture. Then xylenes-chlorobenzene solution was used for recrystallization of compound **1** (1.86 g, 25 %).

Melting point : 298-299 °C. <sup>1</sup>H NMR (500 MHz, DMSO-d<sub>6</sub>): δ 8.77 (t, *J* = 2.0 Hz, 3H, ) , 8.46 (d, *J* = 7.8 Hz, 3H, ) , 8.30 (d, *J* = 8.2 Hz, 3H, ) , 8.25 (s, 3H, ) , 7.84 (t, *J* = 8.0 Hz, 3H, ) ; <sup>13</sup>C NMR (126 MHz, DMSO-d<sub>6</sub>): δ 149.0, 141.7, 140.3, 134.7, 130.9, 126.7, 123.1, 122.5; ESI-MS: calcd. for C<sub>24</sub>H<sub>15</sub>N<sub>3</sub>O<sub>6</sub> 441.10, found 464.09 *m/z* and this corresponds to [M+Na]<sup>+</sup>.

### 5'-(3-aminophenyl)-[1,1':3',1''-terphenyl]-3,3''-diamine (2)

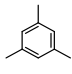
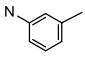
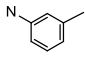
Compound **1** (1.00 g; 2.27 mmol) was dissolved in DMF (150 mL), then 0.10 g Pd/C (10 %) was added. A hydrogen balloon was connected, and the mixture was stirred for 14 h after which the catalyst was removed with a short column of celite. The column was washed with DCM and the combined solutions were concentrated *in vacuo*. The residue was dissolved in a minimal amount of DCM and precipitated with the addition of hexanes. The solid was filtered off and washed with hexanes

and dried to give 0.61 g (77 %) of a beige solid which was used as such in the next step.

$^1\text{H}$  NMR (600 MHz, DMSO- $d_6$ ):  $\delta$  7.65 (s, 3H, ) , 7.13 (t,  $J = 7.7$  Hz, 3H, ) , 6.97 (s, 3H, ) , 6.90 (d,  $J = 7.8$  Hz, 3H, ) , 6.60 (d,  $J = 8.1$  Hz, 3H, ) , 5.17 (s, 6H,  $\text{NH}_2$ );  $^{13}\text{C}$  NMR (151 MHz, DMSO- $d_6$ ):  $\delta$  149.7, 142.5, 141.4, 129.9, 124.0, 114.9, 113.8, 112.8. HRMS:  $m/z$  calcd for  $\text{C}_{24}\text{H}_{21}\text{N}_3$   $[\text{M}+\text{H}]^+$  352.1814, found 352.1821.

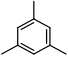
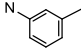
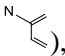
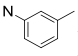
### Tri-alkyne 3

Compound **2** (80 mg, 0.28 mmol) was dissolved in DCM (5 mL). 4-pentanoic acid (100 mg, 1.00 mmol, 4 equiv) was added, followed by DMAP (12.0 mg, 0.10 mmol, 0.4 equiv), EDC HCl (277 mg, 1.45 mmol, 5 equiv). The mixture was stirred for 48 h at room temperature. Then the solution was washed with 1M HCl solution, followed by saturated  $\text{NaHCO}_3$  solution and brine. After drying ( $\text{Na}_2\text{SO}_4$ ) the solvent was removed, and the residue was purified using column chromatography over silica gel (eluent DCM/MeOH 75:1 v/v) to give 100 mg (59 %) of an off-white solid.

$^1\text{H}$  NMR (500 MHz,  $\text{CDCl}_3$ ):  $\delta$  8.14 (s, 3H,  $\text{NH}$ ), 7.71 (s, 3H, ) , 7.55 – 7.50 (m, 6H, ) , 7.35 – 7.28 (m, 6H, ) , 2.71 – 2.62 (q,  $J = 4.0, 3.6$  Hz, 12H,  $\text{CH}_2\text{CH}_2\text{CH}$ );  $^{13}\text{C}$  NMR (126 MHz,  $\text{CDCl}_3$ ):  $\delta$  170.2 ( $\text{C}=\text{O}$ ), 141.7, 141.5, 137.9, 129.4, 125.2, 123.7, 119.5, 119.1, 82.7, 69.9, 36.2, 14.9. HRMS:  $m/z$  calcd for  $\text{C}_{39}\text{H}_{33}\text{N}_3\text{O}_3$   $[\text{M}+\text{H}]^+$  592.2600, found 592.2599.

### Tri-azide 4

Compound **2** (70 mg, 0.2 mmol) was dissolved in DCM (5 mL). 4-azidobutanoic acid (77 mg, 0.6 mmol, 3 equiv) was added, followed by DMAP (7.3 mg, 0.06 mmol, 0.3 equiv), EDC HCl (190 mg, 1.0 mmol, 5 equiv). The mixture was stirred for 48 h at room temperature. Then the solution was washed with 1 M HCl solution, followed by saturated  $\text{NaHCO}_3$  solution and by a saturated NaCl solution. After drying ( $\text{Na}_2\text{SO}_4$ ) the solvent was removed and the residue was purified using column chromatography over silica gel (eluent DCM/MeOH 75:1 v/v) to give 55 mg (40 %) of an off-white solid.

<sup>1</sup>H NMR (600 MHz, CDCl<sub>3</sub>): δ 7.81(s, 3H, NH), 7.72 (s, 3H, ) , 7.60 (s, 3H, ) , 7.52 (d, 3H, ) , 7.35-7.33 (m, 6H, ) , 3.43-3.40 (t, *J* = 6.5 Hz, 6H, CH<sub>2</sub>N<sub>3</sub>), 2.52-2.49 (t, *J* = 7.2 Hz, 6H, COCH<sub>2</sub>), 2.05-2.00 (m, 6H, CH<sub>2</sub>CH<sub>2</sub>N<sub>3</sub>); <sup>13</sup>C NMR (151 MHz, CDCl<sub>3</sub>): δ 170.5 (C=O), 141.8, 141.7, 138.2, 129.5, 125.3, 123.5, 119.2, 118.9, 50.8, 34.2, 24.7. HRMS: *m/z* calcd for C<sub>36</sub>H<sub>36</sub>N<sub>12</sub>O<sub>3</sub> [M+H]<sup>+</sup> 685.3106, found 685.3107.

### Peracetylated GlcNAc derivative 5

Peracetylated N-glucosamine (1.0 g, 2.57 mmol) was dissolved in DCM (10 mL) with molecular sieves and propargyl alcohol (0.6 mL, 10.28 mmol, 4 equiv). When this was completed, BF<sub>3</sub>·Et<sub>2</sub>O (1.6 mL, 12.85 mmol, 5 equiv) was added to the reaction mixture. The yellow mixture was stirred overnight at room temperature. The brown mixture was extracted with EtOAc and aqueous sat. NaHCO<sub>3</sub> until no gas evolution was seen anymore. Then the mixture was dried over Na<sub>2</sub>SO<sub>4</sub>, filtered and concentrated *in vacuo*. Silica gel column chromatography (EtOAc/hexane 9:1 v/v) resulted in a white solid (0.64 g, 1.67 mmol, 65 %).

<sup>1</sup>H NMR (400 MHz, CDCl<sub>3</sub>): δ 5.64 (d, *J* = 9.0 Hz, 1H, NH), 5.26 (dd, *J* = 10.6, 9.3 Hz, 1H, H-3), 5.06 (dd, *J* = 9.6 Hz, 1H, H-4), 4.83 (d, *J* = 8.4 Hz, 1H, H-1), 4.35 (d, *J* = 2.4 Hz, 2H, CH<sub>2</sub>C≡CH), 4.24 (dd, *J* = 12.3, 4.7 Hz, 1H, H-6), 4.11 (dd, *J* = 12.3, 2.4 Hz, 1H, H-6), 3.93 (m, 1H, H-2), 3.70 (m, 1H, H-2), 2.45 (t, *J* = 2.4 Hz, 1H, C≡CH), 2.06 (s, 3H, Ac), 2.00 (d, *J* = 3.0 Hz, 6H, Ac), 1.93 (s, 3H, Ac); <sup>13</sup>C NMR (101 MHz, CDCl<sub>3</sub>): δ 170.9, 170.7, 170.3, 169.3, 98.3, 78.4, 75.4, 72.4, 71.9, 68.4, 61.9, 55.9, 54.2, 23.3, 20.7, 20.7, 20.6. HRMS: *m/z* calcd for C<sub>17</sub>H<sub>23</sub>NO<sub>9</sub> [M+H]<sup>+</sup> 386.1451, found 386.1456.

### GlcNAc derivative 6

Compound **5** (0.2 g, 0.52 mmol) was dissolved in MeOH (20 mL) and 2.8 mg NaOMe (0.052 mmol, 0.1 equiv) was added. The reaction mixture was stirred overnight at room temperature. This resulted in complete conversion according to TLC analysis and the reaction was quenched by adding Dowex H<sup>+</sup>-resin to a pH of ca.7 when the resin was removed by filtration. The reaction mixture was concentrated *in vacuo* which resulted in compound **6** as a white solid (0.13 g, 0.52 mmol, quant.).

<sup>1</sup>H NMR (400 MHz, CD<sub>3</sub>OD): δ 4.58 (d, *J* = 8.4 Hz, 1H, H-1), 4.34 (d, *J* = 1.6 Hz, 2H, CH<sub>2</sub>C≡CH), 3.86 (dd, *J* = 12.0, 2.0 Hz, 1H, H-6), 3.73 – 3.59 (m, 2H, H-2,

H-6), 3.46 (dd,  $J = 10.3, 8.0$  Hz, 1H, H-3), 3.31 – 3.21 (m, 2H, H-4, H-5), 2.83 (t,  $J = 2.4$  Hz, 1H,  $C\equiv CH$ ), 1.96 (s, 3H, Ac);  $^{13}C$  NMR (101 MHz,  $CD_3OD$ ):  $\delta$  172.4, 99.0, 78.4, 76.6, 74.7, 74.5, 70.6, 61.3, 55.6, 55.0, 21.5. HRMS: calcd. for  $C_{11}H_{17}NO_6$  259.1056, found 260.1138  $m/z$  and this corresponds to  $[M+H]^+$ .

### LacNAc derivative 7

Compound **6** (22 mg, 0.085 mmol) and UDP-Gal (77 mg, 0.13 mmol, 1.5 equiv) were dissolved in 5 mL Tris-HCl buffer (50 mM, pH 7.5) containing  $MnCl_2$  (20 mM). To this, *lgtB* ( $\beta$ 1-4Gal Transferase, 71.3 mg/mL, 100  $\mu$ L) was added to the reaction mixture. The resulting reaction mixture was incubated at 37 °C for 3 h. The reaction mixture was centrifuged, and the supernatant subjected to gel filtration over Bio-gel P-2 (eluent  $H_2O$ ). Fractions containing product were combined and lyophilized to give the respective product as amorphous white solid (30 mg, 85 % yield).

$^1H$  NMR (400 MHz,  $D_2O$ ):  $\delta$  4.58 (d,  $J = 7.8$  Hz, 1H, H-1<sup>GlcNAc</sup>), 4.31 (d,  $J = 7.8$  Hz, 1H, H-1<sup>Gal</sup>), 4.25 (d,  $J = 2.3$  Hz, 2H,  $CH_2C\equiv CH$ ), 3.83 (dd,  $J = 12.3, 2.2$  Hz, 1H, H-6<sup>GlcNAc</sup>), 3.76 (dd,  $J = 4.2$  Hz, 1H, H-6<sup>GlcNAc</sup>), 3.72 – 3.33 (m, 10H), 2.74 (t,  $J = 2.4$  Hz, 1H,  $C\equiv CH$ ), 1.88 (s, 3H,  $CH_3$ );  $^{13}C$  NMR (101 MHz,  $D_2O$ ):  $\delta$  174.6, 102.8, 99.2, 79.6, 78.2, 75.9, 75.3, 74.8, 73.6, 72.4, 70.9, 68.4, 60.5, 59.9, 55.2, 54.8, 22.1. HRMS:  $m/z$  calcd for  $C_{17}H_{27}NO_{11}$   $[M+Na]^+$  444.1482, found 444.1484.

### $\alpha$ -2,6-SialyllacNAc derivative 8

Compound **7** (5.0 mg, 0.012 mmol) and CMP-NANA (10.0 mg, 0.015 mmol, 1.2 equiv) were dissolved in 500  $\mu$ L Tris-HCl buffer (100 mM, pH 7.5) containing  $MgCl_2$  (20 mM). To this, PmST1 mutant P34H/M144L ( $\alpha$ -2,6-sialyltransferase, 2.3 mg/mL, 50  $\mu$ L) was added to the reaction mixture. Then the resulting reaction mixture was incubated at 37 °C for 4 h. The reaction mixture was centrifuged and the supernatant subjected to gel filtration over Bio-gel P-2 (eluent  $H_2O$ ). Fractions containing product were combined and lyophilized to give the respective product as amorphous white solid (6.5 mg, 77 % yield).

$^1H$  NMR (600 MHz,  $D_2O$ ):  $\delta$  4.67 (d,  $J = 7.1$  Hz, 1H, H-1<sup>GlcNAc</sup>), 4.34 (d,  $J = 8.1$  Hz, 1H, H-1<sup>Gal</sup>), 4.33 – 4.30 (m, 2H,  $CH_2C\equiv CH$ ), 3.92 – 3.39 (m, 20H), 2.81 (t,  $J = 2.4$  Hz, 1H,  $C\equiv CH$ ), 2.57 (dd,  $J = 12.6, 4.4$  Hz, 1H, H-3<sub>eq</sub><sup>Sia</sup>), 1.96 (s, 3H, Ac<sup>Sia</sup>), 1.92 (s, 3H, Ac<sup>GlcNAc</sup>), 1.61 (t,  $J = 12.4$  Hz, 1H, H-3<sub>ax</sub><sup>Sia</sup>);  $^{13}C$  NMR (151 MHz,  $D_2O$ ):  $\delta$  174.9 (C=O), 174.7 (C=O), 173.5 (C=O), 103.5, 100.1, 99.1, 80.6, 76.2, 74.6, 73.6, 72.5, 72.4, 72.4, 71.7, 70.7, 68.4, 68.3, 68.2, 63.3, 62.6, 60.2, 56.6, 54.6, 51.9, 40.1



(C-3<sup>Sia</sup>), 22.3 (CH<sub>3</sub>CO), 22.0 (CH<sub>3</sub>CO). HRMS:  $m/z$  calcd for C<sub>28</sub>H<sub>44</sub>N<sub>2</sub>O<sub>19</sub> [M+H]<sup>+</sup> 713.2611, found 713.2618.

### Peracetylated Lactoside 9

Acetylated lactoside (3.0 g, 4.42 mmol) was dissolved in dry DCM (30 mL) and propargyl alcohol (2.5 mL, 42.9 mmol, 9.71 equiv) and when this was completed, the BF<sub>3</sub>·Et<sub>2</sub>O (10 mL, 81.0 mmol, 18.3 equiv) was added to the reaction mixture. The yellow mixture was stirred for 48 h at room temperature and completion was determined by TLC. The brown mixture was diluted with DCM and solid NaHCO<sub>3</sub> was added portion-wise. The mixture became yellow and was stirred for 2 h until all CO<sub>2</sub> formation ceased. The mixture was extracted with DCM (3×) and the organic layer was washed with NaHCO<sub>3</sub> (2×), H<sub>2</sub>O (1×) and brine (1×), dried over Na<sub>2</sub>SO<sub>4</sub>, filtered and concentrated *in vacuo*. Silica gel column chromatography (EtOAc/hexane 1:1 v/v) resulted in a transparent oil (1.17 g, 1.73 mmol, 39 %).

<sup>1</sup>H NMR (400 MHz, CDCl<sub>3</sub>): δ 5.65 (d,  $J$  = 8.1 Hz, 1H, H-1<sup>Glc</sup>), 5.26 – 5.16 (t,  $J$  = 9.0 Hz, 1H), 5.09 (dd,  $J$  = 10.3, 7.8 Hz, 1H), 4.97 – 4.85 (m, 2H, H-2), 4.72 (d,  $J$  = 7.8 Hz, 1H, H-1<sup>Gal</sup>), 4.53 – 4.43 (m, 2H), 4.32 (d,  $J$  = 2.4 Hz, 2H, CH<sub>2</sub>C≡CH), 4.16 – 4.01 (m, 3H), 3.89 – 3.75 (m, 2H), 3.66 – 3.58 (m, 1H), 2.43 (t,  $J$  = 2.4 Hz, 1H, C≡CH), 2.13 (s, 3H), 2.10 (s, 3H), 2.06 – 2.00 (m, 12H), 1.94 (s, 3H); <sup>13</sup>C NMR (101 MHz, CDCl<sub>3</sub>): δ 170.3, 170.1, 170.1, 170.0, 169.7, 169.7, 169.0, 101.0, 97.8, 78.0, 76.1, 75.4, 72.7, 72.6, 71.3, 70.7, 69.1, 66.6, 61.8, 55.8, 53.4, 20.8, 20.7, 20.7, 20.6, 20.6, 20.6, 20.5; ESI-MS: calcd. for C<sub>29</sub>H<sub>38</sub>O<sub>18</sub> 674.60, found 697.20  $m/z$  and this corresponds to [M+Na]<sup>+</sup>.

### Lactoside 10

Compound **9** (0.5 g, 0.74 mmol) was dissolved in MeOH (20 mL) and a solution of NaOMe in MeOH (200 μL, 6 g/100 mL) was added. The reaction mixture was stirred overnight at room temperature. This resulted in complete conversion according to TLC analysis and the reaction was quenched by adding Dowex H<sup>+</sup>-resin to a pH of ca.7 when the resin was removed by filtration. The reaction mixture was concentrated *in vacuo* which resulted in compound **10** as a white solid (0.28 g, quant.).

<sup>1</sup>H NMR (400 MHz, D<sub>2</sub>O): δ 4.51 (d,  $J$  = 8.0 Hz, 1H, H-1<sup>Glc</sup>), 4.39 – 4.25 (m, 3H, H-1<sup>Gal</sup>, CH<sub>2</sub>C≡CH), 3.82 (dd,  $J$  = 12.3, 2.1 Hz, 1H, H-6), 3.76 (d,  $J$  = 3.4 Hz, 1H, H-4), 3.71 – 3.44 (m, 7H), 3.38 (dd,  $J$  = 10.0, 7.8 Hz, 1H, H-2<sup>Gal</sup>), 3.19 (m, 1H, H-2<sup>Glc</sup>), 2.76 (t,  $J$  = 2.5 Hz, 1H, C≡CH); <sup>13</sup>C NMR (101 MHz, D<sub>2</sub>O): δ 102.8, 100.3,

78.6, 78.1, 76.2, 75.3, 74.8, 74.2, 72.5, 72.4, 70.8, 68.4, 60.9, 59.9, 56.5; ESI-MS: calcd. for C<sub>15</sub>H<sub>24</sub>O<sub>11</sub> 380.34, found 381.14 *m/z* and this corresponds to [M+H]<sup>+</sup>.

### GlcNAc-Lac derivative 11

Compound **10** (12 mg, 0.031 mmol) and UDP-GlcNAc (30 mg, 0.046 mmol, 1.5 equiv) were dissolved in HEPES buffer (2.5 mL, 50 mM, pH 7.3) containing KCl (25 mM), MgCl<sub>2</sub> (2 mM), and dithiothreitol (1 mM). To this, CIAP (20 μL, 10 mU) and *H. Pylori* β3GlcNAcT (β1-3GlcNAc Transferase, 0.7 mg/mL, 50 μL) were added. The resulting reaction mixture was incubated at 37 °C overnight. The reaction mixture was centrifuged and the supernatant was subjected to gel filtration over Bio-gel P-2 (eluent H<sub>2</sub>O). Fractions containing product were combined and lyophilized. Then the crude product was purified by using column chromatography over silica gel (eluent EtOAc/MeOH/H<sub>2</sub>O 7:2:1 v/v/v) to give compound **11** as an amorphous white solid (12.8 mg, 70 % yield).

<sup>1</sup>H NMR (600 MHz, D<sub>2</sub>O): δ 4.58 (d, *J* = 8.5 Hz, 1H, H-1<sup>GlcNAc</sup>), 4.57 (d, *J* = 8.1 Hz, 1H, H-1<sup>Glc</sup>), 4.37 (d, *J* = 5.7 Hz, 2H), 4.33 (d, *J* = 7.8 Hz, 1H, H-1<sup>Gal</sup>), 4.05 (d, *J* = 3.4 Hz, 1H), 3.88 (dd, *J* = 12.3, 2.1 Hz, 1H), 3.79 (dd, *J* = 12.4, 2.1 Hz, 1H), 3.70 – 3.33 (m, 14H), 3.28 – 3.20 (m, 1H, H-2<sup>Glc</sup>), 2.81 (t, *J* = 2.4 Hz, 1H, C≡CH), 1.94 (s, 3H, Ac); <sup>13</sup>C NMR (151 MHz, D<sub>2</sub>O): δ 175.0 (C=O), 102.9 (C-1<sup>Gal</sup>), 102.8 (C-1<sup>GlcNAc</sup>), 100.3 (C-1<sup>Glc</sup>), 81.9, 78.2, 75.6, 74.9, 74.8, 74.8, 74.3, 73.5, 72.6, 72.5, 70.0, 69.7, 68.3, 60.9, 60.4, 59.9, 56.6, 55.6, 22.1 (CH<sub>3</sub>CO). HRMS: *m/z* calcd for C<sub>23</sub>H<sub>37</sub>NO<sub>16</sub> [M+Na]<sup>+</sup> 606.2005, found 606.2011.

### LacNAcLac derivative 12

Compound **11** (10 mg, 0.017 mmol) and UDP-Gal (15.7 mg, 0.026 mmol, 1.5 equiv) were dissolved in MES buffer (100 mM, 500 μL) containing MnCl<sub>2</sub> (20 mM). To this, *LgtB* (β1-4Gal Transferase, 71.3 mg/mL, 50 μL) were added. The resulting reaction mixture was incubated at 37 °C for 3 h. The reaction mixture was centrifuged, and the supernatant subjected to gel filtration over Bio-gel P-2 (eluent H<sub>2</sub>O). Fractions containing product were combined and lyophilized to give the respective product as an amorphous white solid (10.3 mg, 81 % yield).

<sup>1</sup>H NMR (600 MHz, D<sub>2</sub>O): δ 4.60 (d, *J* = 8.4 Hz, 1H, H-1<sup>GlcNAc</sup>), 4.57 (d, *J* = 8.0 Hz, 1H, H-1<sup>Glc</sup>), 4.40 – 4.36 (m, 3H, CH<sub>2</sub>C≡CH, H-1<sup>Gal'</sup>), 4.34 (d, *J* = 7.8 Hz, 1H, H-1<sup>Gal</sup>), 4.06 (d, *J* = 3.2 Hz, 1H), 3.91 – 3.82 (m, 3H), 3.78 – 3.41 (m, 20H), 3.27 – 3.21 (m, 1H, H-2<sup>Glc</sup>), 2.81 (t, *J* = 2.4 Hz, 1H, C≡CH), 1.93 (s, 3H, Ac); <sup>13</sup>C NMR (151 MHz, D<sub>2</sub>O): δ 174.9 (C=O), 102.9 (C-1<sup>Gal</sup>), 102.8 (C-1<sup>Gal'</sup>), 102.7 (C-1<sup>GlcNAc</sup>),

100.3 (C-1<sup>Glc</sup>), 82.0, 78.7, 78.2, 78.1, 76.3, 75.3, 74.9, 74.8, 74.5, 74.3, 72.5, 72.5, 72.1, 70.9, 69.9, 68.5, 68.3, 61.0, 60.9, 59.9, 59.8, 56.6, 55.2, 22.1 (CH<sub>3</sub>CO). HRMS: *m/z* calcd for C<sub>29</sub>H<sub>47</sub>NO<sub>21</sub> [M+Na]<sup>+</sup> 768.2538, found 768.2547.

### **$\alpha$ -2,6-SialyllacNAclac derivative 13**

Compound **12** (2 mg, 2.7  $\mu$ mol) and CMP-NANA (2.6 mg, 4.0  $\mu$ mol, 1.5 equiv) were dissolved in Tris-HCl buffer (100 mM, pH 7.5, 500  $\mu$ L) containing MgCl<sub>2</sub> (20 mM). To this, PmST1 mutant P34H/M144L ( $\alpha$ 2-6sialyltransferase, 2.3 mg/mL, 50  $\mu$ L) were added. The resulting reaction mixture was incubated at 37 °C for 4 h. The completion of the reaction was analyzed by TLC. The reaction mixture was centrifuged and the supernatant subjected to gel filtration over Bio-gel P-2 (eluent H<sub>2</sub>O). Fractions containing product were combined and lyophilized for further preparative HPLC using a HILIC column (**Table 1**). Then the fractions containing product were combined and lyophilized to give to the respective product as an amorphous white solid (0.75 mg, 27 % yield).

<sup>1</sup>H NMR (600 MHz, D<sub>2</sub>O):  $\delta$  4.63 (d, *J* = 7.2 Hz, 1H, H-1<sup>GlcNAc</sup>), 4.58 (d, *J* = 8.3 Hz, 1H, H-1<sup>Glc</sup>), 4.39 – 4.33 (m, 4H, CH<sub>2</sub>C $\equiv$ CH, H-1<sup>Gal'</sup>, H-1<sup>Gal</sup>), 4.06 (d, *J* = 3.2 Hz, 1H), 3.90 – 3.42 (m, 28H), 3.27 – 3.24 (m, 1H, H-2<sup>Glc</sup>), 2.90 (t, *J* = 2.4 Hz, 1H, C $\equiv$ CH), 2.57 (dd, *J* = 12.2, 4.1 Hz, 1H, H-3<sup>Sia<sub>eq</sub></sup>), 1.96 (s, 3H, Ac<sup>Sia</sup>), 1.93 (s, 3H, Ac<sup>GlcNAc</sup>), 1.63 (t, *J* = 12.2 Hz, 1H, H-3<sup>Sia<sub>ax</sub></sup>); <sup>13</sup>C NMR (151 MHz, D<sub>2</sub>O, extracted from HSQC):  $\delta$  103.3 (C-1<sup>Gal</sup>), 103.3 (C-1<sup>Gal'</sup>), 102.7 (C-1<sup>GlcNAc</sup>), 100.4 (C-1<sup>Glc</sup>), 82.1, 80.6, 78.4, 75.0, 74.6, 74.5, 73.8, 72.7, 72.5, 72.4, 71.8, 70.8, 70.1, 68.5, 68.5, 68.4, 63.4, 63.4, 62.8, 62.7, 61.0, 60.3, 60.2, 56.6, 55.0, 51.9, 40.1 (C-3<sup>Sia</sup>), 22.4 (CH<sub>3</sub>CO), 22.1 (CH<sub>3</sub>CO). HRMS: *m/z* calcd for C<sub>40</sub>H<sub>64</sub>N<sub>2</sub>O<sub>29</sub> [M+Na]<sup>+</sup> 1059.3487, found 1059.3490.

### **Peracetylated azido lactoside 14**

Acetylated lactoside (6.21 g, 9.15 mmol) was dissolved in dry DCM (30 mL) and HMDS (1.87 mL, 9.15 mmol) and solid iodine (2.32 g, 9.15 mmol) were added and the reaction mixture was stirred for 2 h at room temperature. The mixture was diluted with DCM and was stirred with a 10 % aqueous Na<sub>2</sub>S<sub>2</sub>O<sub>3</sub> solution for 15 min. The organic layer was washed with NaHCO<sub>3</sub>, H<sub>2</sub>O and brine, dried over Na<sub>2</sub>SO<sub>4</sub>, filtered and concentrated *in vacuo*. Then the product was dissolved in acetone (35 mL) and a solution of NaN<sub>3</sub> (5 equiv) in H<sub>2</sub>O (10 mL) was added drop-wise. The mixture turned from yellow to orange to red and acetone/H<sub>2</sub>O was added to obtain a homogenous solution. The mixture was stirred for 19 h at room temperature. Work up followed by adding ice and DCM to dilute the reaction

mixture. The mixture was extracted with DCM (3×) and the organic layer was washed with NaHCO<sub>3</sub>, H<sub>2</sub>O and brine, dried over Na<sub>2</sub>SO<sub>4</sub>, filtered and concentrated *in vacuo* which resulted in a white solid compound **14** (5.46 g, 83 %).

<sup>1</sup>H NMR (400 MHz, CDCl<sub>3</sub>): δ 5.34 – 5.25 (m, 1H), 5.17 (t, *J* = 9.2 Hz, 1H), 5.07 (dd, *J* = 10.4, 7.8 Hz, 1H), 4.92 (dd, *J* = 10.4, 3.4 Hz, 1H), 4.87 – 4.76 (m, 1H), 4.60 (d, *J* = 8.8 Hz, 1H), 4.51 – 4.42 (m, 2H), 4.16 – 4.00 (m, 3H), 3.84 (td, *J* = 6.8, 1.3 Hz, 1H), 3.78 (dd, *J* = 9.9, 8.9 Hz, 1H), 3.67 (ddd, *J* = 9.9, 5.1, 2.1 Hz, 1H), 2.11 (d, *J* = 5.7 Hz, 6H), 2.12 – 1.92 (m, 13H), 1.93 (s, 3H); <sup>13</sup>C NMR (101 MHz, CDCl<sub>3</sub>): δ 170.29, 170.26, 170.07, 169.99, 169.58, 169.44, 169.02, 101.06, 87.66, 75.74, 74.76, 72.49, 70.95, 70.89, 70.72, 69.02, 66.55, 61.69, 60.75, 20.85, 20.84, 20.75, 20.68, 20.58, 20.56, 20.55, 20.50, 20.47, 20.45.

### Triazole-phenyl-peracetylated lactoside **16**

1-((triisopropylsilyl)ethynyl)-4-ethynylbenzene (0.14 g, 0.5 mmol), **14** (0.5 g, 0.76 mmol, 1.5 equiv), CuSO<sub>4</sub>·5H<sub>2</sub>O (12.5 mg, 0.05 mmol, 0.1 equiv), sodium L-ascorbate (0.1 g, 0.5 mmol, 1.0 equiv) were dissolved in DMF/H<sub>2</sub>O (9:1, 5 mL). The reaction was performed under microwave irradiation at 80 °C for 30 min. Then the mixture was concentrated *in vacuo*. The residue was used in the next step without further purification. HRMS: *m/z* calcd for C<sub>45</sub>H<sub>61</sub>N<sub>3</sub>O<sub>17</sub>Si [M+Na]<sup>+</sup> 966.3662, found 966.3655, was consistent with the structure of **15**.

Then compound **15** (244 mg, 0.26 mmol) was dissolved in THF (10 mL) and to this solution TBAF·3H<sub>2</sub>O (122 mg, 0.39 mmol) was added. The obtained reaction mixture was stirred for 2 h as the reaction was complete, based on TLC. H<sub>2</sub>O (10 mL) was added to the reaction mixture for quenching. The mixture was extracted with DCM and washed with H<sub>2</sub>O and brine, then dried over Na<sub>2</sub>SO<sub>4</sub>, filtered and concentrated *in vacuo*. The residue was purified using column chromatography over silica gel (eluent DCM/MeOH 9:1 v/v) to give the Compound **16** as a white solid (198 mg, 97 % yield).

<sup>1</sup>H NMR (400 MHz, CDCl<sub>3</sub>): δ 7.92 (s, 1H, H-triazole), 7.75 (d, *J* = 8.2 Hz, 2H, H-phenyl), 7.51 (d, *J* = 8.3 Hz, 2H, H-phenyl), 5.85 (d, *J* = 8.7 Hz, 1H, H-1<sup>Glc</sup>), 5.48 – 5.36 (m, 2H, H-2<sup>Glc</sup>, H-3<sup>Glc</sup>), 5.33 (d, *J* = 3.2 Hz, 1H, H-4<sup>Gal</sup>), 5.10 (dd, *J* = 10.4, 7.8 Hz, 1H, H-2<sup>Gal</sup>), 4.95 (dd, *J* = 10.4, 3.4 Hz, 1H, H-3<sup>Gal</sup>), 4.51 (d, *J* = 7.9 Hz, 1H, H-1<sup>Gal</sup>), 4.45 (d, *J* = 12.0 Hz, 1H, H-6a<sup>Glc</sup>), 4.17 – 4.03 (m, 4H, H-5<sup>Glc</sup>, 2H-6<sup>Gal</sup>, H-6b<sup>Glc</sup>), 3.99 – 3.85 (m, 2H, H-5<sup>Gal</sup>, H-4<sup>Glc</sup>), 3.11 (s, 1H, C≡CH), 2.13 (s, 3H, Ac), 2.06 (s, 3H, Ac), 2.04 (s, 6H, 2Ac), 1.94 (s, 3H, Ac), 1.84 (s, 3H, Ac); <sup>13</sup>C NMR (101 MHz, CDCl<sub>3</sub>): δ 170.3 (C=O), 170.2 (C=O), 170.0 (C=O), 170.0 (C=O), 169.4 (C=O), 169.2 (C=O), 169.0 (C=O), 147.5, 132.6, 132.6 (C-phenyl), 130.2,

125.6, 125.6 (C-phenyl), 122.1, 118.2 (C-triazole), 101.1 (C-1<sup>Gal</sup>), 85.5 (C-1<sup>Glc</sup>), 83.3, 78.2, 75.9, 75.6, 72.6, 70.9, 70.8, 70.4, 69.0, 66.6, 61.8, 60.8, 20.8 (CH<sub>3</sub>CO), 20.7 (CH<sub>3</sub>CO), 20.6 (CH<sub>3</sub>CO), 20.6 (CH<sub>3</sub>CO), 20.5 (CH<sub>3</sub>CO), 20.2 (CH<sub>3</sub>CO). HRMS: *m/z* calcd for C<sub>36</sub>H<sub>41</sub>N<sub>3</sub>O<sub>17</sub> [M+H]<sup>+</sup> 788.2509, found 788.2509.

### Triazole-phenyl lactoside 17

NaOMe (0.69 mg, 0.013 mmol, 0.1 equiv) was added to a solution of compound **16** (100 mg, 0.13 mmol) in methanol (10 mL) and the mixture was stirred overnight at room temperature. The solution was neutralized with Dowex-H<sup>+</sup> resin to a pH of ca.7 when the resin was removed by filtration. The residue was concentrated *in vacuo*. Compound **17** was obtained as a white solid (62 mg, quant.).

<sup>1</sup>H NMR (400 MHz, CD<sub>3</sub>OD): δ 8.60 (s, 1H, H-triazole), 7.82 (d, *J* = 8.1 Hz, 2H, H-phenyl), 7.52 (d, *J* = 8.5 Hz, 2H, H-phenyl), 5.68 (d, *J* = 9.2 Hz, 1H, H-1<sup>Glc</sup>), 4.42 (d, *J* = 7.6 Hz, 1H, H-1<sup>Gal</sup>), 4.00 (t, *J* = 9.1 Hz, 1H, H-2<sup>Glc</sup>), 3.90 (d, *J* = 2.8 Hz, 2H), 3.83 – 3.70 (m, 6H), 3.63 – 3.54 (m, 2H), 3.51 – 3.47 (m, 1H), 2.13 (s, 1H, C≡CH); <sup>13</sup>C NMR (101 MHz, CD<sub>3</sub>OD): δ 146.6, 132.2, 132.2 (C-phenyl), 130.5, 125.2, 125.2 (C-phenyl), 130.5, 125.2, 122.3, 120.4 (C-triazole), 103.7 (C-1<sup>Gal</sup>), 88.1 (C-1<sup>Glc</sup>), 78.2, 78.2, 75.7, 75.4, 73.4, 72.3, 71.1, 68.9, 61.1, 60.1. HRMS: *m/z* calcd for C<sub>22</sub>H<sub>27</sub>N<sub>3</sub>O<sub>10</sub> [M+H]<sup>+</sup> 494.1775, found 494.1782.

### Triazole-phenyl-Lac-GlcNAc 18

Compound **17** (9 mg, 0.018 mmol) and UDP-GlcNAc (17 mg, 0.027 mmol, 1.5 equiv) were dissolved in HEPES buffer (50 mM, pH 7.3, 500 μL) containing KCl (25 mM), MgCl<sub>2</sub> (2 mM), and dithiothreitol (1 mM). To this, CIAP (10 mU, 20 μL) and *H. Pylori* β3GlcNAcT (β1-3GlcNAc Transferase, 0.7 mg/mL, 50 μL) were added. The resulting reaction mixture was incubated at 37 °C overnight. The reaction mixture was centrifuged and the supernatant subjected to gel filtration over Bio-gel P-2 (eluent H<sub>2</sub>O). Fractions containing product were combined and lyophilized to give Compound **18** as an amorphous white solid (8.9 mg, 71 % yield).

<sup>1</sup>H NMR (600 MHz, D<sub>2</sub>O): δ 8.50 (s, 1H, H-triazole), 7.73 (d, *J* = 8.4 Hz, 2H, H-phenyl), 7.56 (d, *J* = 8.4 Hz, 2H, H-phenyl), 5.75 (d, *J* = 9.2 Hz, 1H, H-1<sup>Glc</sup>), 4.61 (d, *J* = 8.4 Hz, 1H, H-1<sup>GlcNAc</sup>), 4.42 (d, *J* = 7.8 Hz, 1H, H-1<sup>Gal</sup>), 4.08 (d, *J* = 3.4 Hz, 1H), 4.01 (t, *J* = 9.0 Hz, 1H, H-2<sup>Glc</sup>), 3.90 (d, *J* = 12.0 Hz, 1H), 3.84 – 3.64 (m, 11H), 3.83 – 3.70 (m, 6H), 3.63 – 3.54 (m, 2H), 3.51 – 3.47 (m, 1H), 3.41 – 3.34 (m, 2H), 1.98 (s, 1H, C≡CH), 1.96 (s, 3H, Ac); <sup>13</sup>C NMR (151 MHz, D<sub>2</sub>O): δ 175.0

(C=O), 147.0, 132.8, 132.8 (C-phenyl), 129.7, 125.8, 125.8 (C-phenyl), 122.5, 121.7 (C-triazole), 102.9 (C-1<sup>Gal</sup>), 102.9 (C-1<sup>GlcNAc</sup>), 87.4 (C-1<sup>Glc</sup>), 81.9, 77.7, 77.7, 77.2, 75.6, 74.9, 74.5, 73.5, 72.0, 70.0, 69.7, 69.6, 68.3, 61.0, 60.4, 59.7, 55.6, 22.1 (CH<sub>3</sub>CO). HRMS: *m/z* calcd for C<sub>30</sub>H<sub>40</sub>N<sub>4</sub>O<sub>15</sub> [M+Na]<sup>+</sup> 719.2382, found 719.2388.

### Triazole-phenyl-Lac-LacNAc 19

Compound **18** (5 mg, 0.007 mmol) and UDP-Gal (6.5 mg, 0.01 mmol, 1.5 equiv) were dissolved in MES buffer (100 mM, 300  $\mu$ L) containing MnCl<sub>2</sub> (20 mM). To this, *LgtB* ( $\beta$ 1-4Gal Transferase, 71.3 mg/mL, 30  $\mu$ L) were added. The resulting reaction mixture was incubated at 37 °C for 3 h. The reaction mixture was centrifuged and the supernatant subjected to gel filtration over Bio-gel P-2 (eluent H<sub>2</sub>O). Fractions containing product were combined and lyophilized to give the respective product as an amorphous white solid (4.9 mg, 82 % yield).

<sup>1</sup>H NMR (600 MHz, D<sub>2</sub>O):  $\delta$  8.53 (s, 1H, H-triazole), 7.76 (d, *J* = 8.4 Hz, 2H, H-phenyl), 7.58 (d, *J* = 8.0 Hz, 2H, H-phenyl), 5.76 (d, *J* = 9.1 Hz, 1H, H-1<sup>Glc</sup>), 4.63 (d, *J* = 8.4 Hz, 1H, H-1<sup>GlcNAc</sup>), 4.42 (d, *J* = 7.8 Hz, 1H, H-1<sup>Gal</sup>), 4.39 (d, *J* = 7.8 Hz, 1H, H-1<sup>Gal'</sup>), 4.08 (d, *J* = 3.2 Hz, 1H), 4.01 (t, *J* = 8.8 Hz, 1H, H-2<sup>Glc</sup>), 3.92 – 3.52 (m, 21H), 3.47 – 3.43 (m, 1H), 1.97 (s, 1H, C $\equiv$ CH), 1.95 (s, 3H, Ac); <sup>13</sup>C NMR (151 MHz, D<sub>2</sub>O, extracted from HSQC):  $\delta$  132.9, 125.9, 121.7 (C-triazole), 102.9 (C-1<sup>Gal</sup>), 102.9 (C-1<sup>Gal'</sup>), 102.8 (C-1<sup>GlcNAc</sup>), 87.3 (C-1<sup>Glc</sup>), 82.0, 78.3, 77.6, 75.4, 75.1, 74.6, 74.6, 72.6, 72.3, 72.0, 71.0, 70.0, 69.6, 68.6, 68.4, 61.0, 58.9, 59.9, 55.2, 22.0 (CH<sub>3</sub>CO). HRMS: *m/z* calcd for C<sub>36</sub>H<sub>50</sub>N<sub>4</sub>O<sub>20</sub> [M+H]<sup>+</sup> 859.3091, found 859.3090.

### References

- 1 P. Palese, Influenza: Old and new threats, *Nat. Med.*, 2004, **10**, S82–S87.
- 2 M. Richard and R. A. M. Fouchier, Influenza A virus transmission via respiratory aerosols or droplets as it relates to pandemic potential, *FEMS Microbiol. Rev.*, 2015, **40**, 68–85.
- 3 F. Krammer and P. Palese, Influenza virus hemagglutinin stalk-based antibodies and vaccines, *Curr. Opin. Virol.*, 2013, **3**, 521–530.
- 4 B. S. Hamilton, G. R. Whittaker and S. Daniel, Influenza virus-mediated membrane fusion: Determinants of hemagglutinin fusogenic activity and experimental approaches for assessing virus fusion, *Viruses*, 2012, **4**, 1144–1168.

- 5 S. J. Gamblin and J. J. Skehel, Influenza hemagglutinin and neuraminidase membrane glycoproteins, *J. Biol. Chem.*, 2010, **285**, 28403–28409.
- 6 J. S. Rossman and R. A. Lamb, Influenza virus assembly and budding, *Virology*, 2011, **411**, 229–236.
- 7 F. Krammer, G. J. D. Smith, R. A. M. Fouchier, M. Peiris, K. Kedzierska, P. C. Doherty, P. Palese, M. L. Shaw, J. Treanor, R. G. Webster and A. Garc ía-Sastre, Influenza, *Nat. Rev. Dis. Prim.*, 2018, **4**, 3.
- 8 F. Krammer and P. Palese, Advances in the development of influenza virus vaccines, *Nat. Rev. Drug Discov.*, 2015, **14**, 167–182.
- 9 M. von Itzstein, The war against influenza: discovery and development of sialidase inhibitors., *Nat. Rev. Drug Discov.*, 2007, **6**, 967–74.
- 10 A. Moscona, Oseltamivir resistance — disabling our influenza defenses, *N. Engl. J. Med.*, 2005, **353**, 2633–2636.
- 11 S. J. Gamblin, The structure and receptor binding properties of the 1918 influenza hemagglutinin, *Science*, 2004, **303**, 1838–1842.
- 12 T. T. Wang and P. Palese, Biochemistry. Catching a moving target, *Science*, 2011, **333**, 834–835.
- 13 R. J. Russell, P. S. Kerry, D. J. Stevens, D. A. Steinhauer, S. R. Martin, S. J. Gamblin and J. J. Skehel, Structure of influenza hemagglutinin in complex with an inhibitor of membrane fusion, *Proc. Natl. Acad. Sci.*, 2008, **105**, 17736–17741.
- 14 W. Weis, J.H. Brown, S. Cusack, J.C. Paulson, J.J. Skehel, Structure of the influenza virus haemagglutinin complexed with its receptor, sialic acid, *Nature*, 1988, **333**, 426–431.
- 15 Y. Suzuki, T. Ito, T. Suzuki, R. E. Holland, T. M. Chambers, M. Kiso, H. Ishida and Y. Kawaoka, Sialic acid species as a determinant of the host range of Influenza A Viruses, *J. Virol.*, 2000, **74**, 11825–11831.
- 16 J. Stevens, O. Blixt, L. Glaser, J. K. Taubenberger, P. Palese, J. C. Paulson and I. A. Wilson, Glycan microarray analysis of the hemagglutinins from modern and pandemic influenza viruses reveals different receptor specificities, *J. Mol. Biol.*, 2006, **355**, 1143–1155.
- 17 N. K. Sauter, J. E. Hanson, G. D. Glick, J. H. Brown, R. L. Crowther, S. J. Park, J. J. Skehel and D. C. Wiley, Binding of influenza virus hemagglutinin to analogs of its cell-surface receptor, sialic acid: Analysis by Proton Nuclear Magnetic Resonance Spectroscopy and X-ray Crystallography, *Biochemistry*, 1992, **31**, 9609–9621.
- 18 Q. M. Le, M. Kiso, K. Someya, Y. T. Sakai, T. H. Nguyen, K. H. L. Nguyen, N. D. Pham, H. H. Ngyen, S. Yamada, Y. Muramoto, T. Horimoto, A. Takada, H. Goto, T. Suzuki, Y. Suzuki and Y. Kawaoka, Avian flu: Isolation of drug-resistant H5N1 virus, *Nature*, 2005, **437**, 1108–1108.
- 19 J. Yang, M. Li, X. Shen and S. Liu, Influenza A virus entry inhibitors targeting the hemagglutinin, *Viruses*, 2012, **5**, 352–373.

- 20 R. U. Kadam and I. A. Wilson, A small-molecule fragment that emulates binding of receptor and broadly neutralizing antibodies to influenza A hemagglutinin, *Proc. Natl. Acad. Sci.*, 2018, 1801999115.
- 21 M. Mammen, S. K. Choi and G. M. Whitesides, Polyvalent interactions in biological systems: Implications for design and use of multivalent ligands and inhibitors, *Angew. Chemie Int. Ed.*, 1998, **37**, 2755–2794.
- 22 F. Pertici and R. J. Pieters, Potent divalent inhibitors with rigid glucose click spacers for *Pseudomonas aeruginosa* lectin LecA, *Chem. Commun.*, 2012, **48**, 4008–4010.
- 23 F. Pertici, N. J. De Mol, J. Kemmink and R. J. Pieters, Optimizing divalent inhibitors of *Pseudomonas aeruginosa* lectin leca by using a rigid spacer, *Chem. A Eur. J.*, 2013, **19**, 16923–16927.
- 24 R. Visini, X. Jin, M. Bergmann, G. Michaud, F. Pertici, O. Fu, A. Pukin, T. R. Branson, D. M. E. Thies-Weesie, J. Kemmink, E. Gillon, A. Imberty, A. Stocker, T. Darbre, R. J. Pieters and J. L. Reymond, Structural insight into multivalent galactoside binding to *Pseudomonas aeruginosa* lectin LecA, *ACS Chem. Biol.*, 2015, **10**, 2455–2462.
- 25 R. J. Pieters, J. Cuntze, M. Bonnet and F. Diederich, Enantioselective recognition with C3-symmetric cage-like receptors in solution and on a stationary phase, *J. Chem. Soc. Perkin Trans. 2*, 1997, 1891–1900.
- 26 P. M. and F. N. K. Bernhauer, Über die kondensation aromatischer methylketone, *J. Prakt. Chem.*, 1936, **145**, 301–308.
- 27 E.D.Goddard-Borger and R.V.Stick, An efficient, inexpensive, and shelf-stable diazotransfer reagent: Imidazole-1-sulfonyl azide hydrochloride, *Org. Lett.*, 2007, **9**, 3797–3800.
- 28 H. B. Mereyala and S. R. Gurrula, A highly diastereoselective, practical synthesis of allyl, propargyl 2,3,4,6-tetra-O-acetyl- $\beta$ -D-gluco,  $\beta$ -D-galactopyranosides and allyl, propargyl heptaacetyl- $\beta$ -D-lactosides, *Carbohydr. Res.*, 1998, **307**, 351–354.
- 29 O. Blixt, J. Brown, M. J. Schur, W. Wakarchuk and J. C. Paulson, Efficient preparation of natural and synthetic galactosides with a recombinant  $\beta$ -1,4-galactosyltransferase-/UDP-4'-gal epimerase fusion protein, *J. Org. Chem.*, 2001, **66**, 2442–2448.
- 30 J. B. McArthur, H. Yu, J. Zeng and X. Chen, Converting *Pasteurella multocida*  $\alpha$ 2-3-sialyltransferase 1 (PmST1) to a regioselective  $\alpha$ 2-6-sialyltransferase by saturation mutagenesis and regioselective screening, *Org. Biomol. Chem.*, 2017, **15**, 1700–1709.
- 31 C. M. Nycholat, R. McBride, D. C. Ekiert, R. Xu, J. Rangarajan, W. Peng, N. Razi, M. Gilbert, W. Wakarchuk, I. A. Wilson and J. C. Paulson, Recognition of sialylated poly-N-acetyllactosamine chains on N- and O-linked glycans by human and avian influenza A virus hemagglutinins, *Angew. Chemie - Int. Ed.*, 2012, **51**, 4860–4863.



- 32 Z. Tian, L. Si, K. Meng, X. Zhou, Y. Zhang, D. Zhou and S. Xiao, Inhibition of influenza virus infection by multivalent pentacyclic triterpene-functionalized per-O-methylated cyclodextrin conjugates, *Eur. J. Med. Chem.*, 2017, **134**, 133–139.
- 33 W. Peng, J. Pranskevich, C. Nycholat, M. Gilbert, W. Wakarchuk, J. C. Paulson and N. Razi, *Helicobacter pylori* 1,3-N-acetylglucosaminyltransferase for versatile synthesis of type 1 and type 2 poly-LacNAcs on N-linked, O-linked and I-antigen glycans, *Glycobiology*, 2012, **22**, 1453–1464.
- 34 M.D.Chander, Synthesis of glycopeptides from Tolerogenic peptides & carbohydrates by the click reaction, 2014.



# *Chapter 3*

*Synthesis of the di- & trivalent hemagglutinin  
inhibitors of Influenza A virus*

### 3.1 Introduction

Multivalent interactions between different interfaces or molecules play a vital role in many biological systems such as recognition, adhesion, and signaling processes.<sup>1-3</sup> It is of importance to understand multivalent interactions on the molecular level because of the dramatically different effects when comparing monovalent and multivalent interactions. Monovalent interactions between receptors and ligands are too weak which usually appear with a dissociation constant ( $K_d$ ) ranging from millimolar to micromolar, while multivalency can enhance binding or inhibitory potencies by orders of magnitude. Multivalency as a strategy to enhance binding and inhibition has been widely explored in protein-carbohydrate interactions<sup>4</sup> to bridge binding sites,<sup>5</sup> or to inhibit pathogen binding<sup>6</sup> by mechanisms such as chelation and statistical rebinding.<sup>7,8</sup> Research focusing on multivalent effects on the molecular level is important for developing optimized multivalent ligands.

As for the Influenza A virus (IAV), a single hemagglutinin (HA) ligand binding site has only millimolar affinity for sialylated sugars, but the multivalent engagement of receptor-ligand interactions allows the virus to attach at much lower concentrations. The overall avidity effects are very strong and a crucial aspect for developing potent inhibitors for IAV infection. In that sense it is a logical step to attempt to block the viral infection via the HA protein with a multivalent inhibitor. Indeed several examples of multivalent sialic acid containing glycans have been reported. Relatively large molecular entities can take advantage of their size to bridge multiple HA trimers. Some of these have yielded potency enhancements of 3-4 orders of magnitude. Large systems like a polyacrylate carrier,<sup>9</sup> polyacrylamide,<sup>10,11</sup> polyglutamic acid,<sup>12</sup> polyglycerol-based nanoparticles,<sup>13,14</sup> chitosan<sup>15</sup> and liposomes<sup>16</sup> were explored as HA inhibitors.

However, it would be an advantage for drug development if monodisperse, small well-defined molecular entities can be used, with no risk of immunogenicity. Reaching this goal has proven considerably more difficult in the situation for anti-HA drugs. For such molecules bridging binding sites seems an obvious goal, but potency enhancements may also be obtained from bridging trimers. Reported studies showed divalent sialosides,<sup>17</sup> such as two  $\alpha$ -2,6-SiaLacNAc units linked via a single galactoside moiety,<sup>18</sup> dendrimers presenting sialic acids,<sup>19</sup> cyclic peptides presenting sialyl lactosides,<sup>20</sup> calixarene linked to 4 sialic acids<sup>21</sup> and three  $\alpha$ -2,3-SiaLac units linked to a triphenyl methyl scaffold.<sup>22</sup> These constructs resulted in moderate enhancements and no clear evidence of chelating/bridging HA binding sites. The same is true for a trisubstituted benzene ring linked to sialic acids via

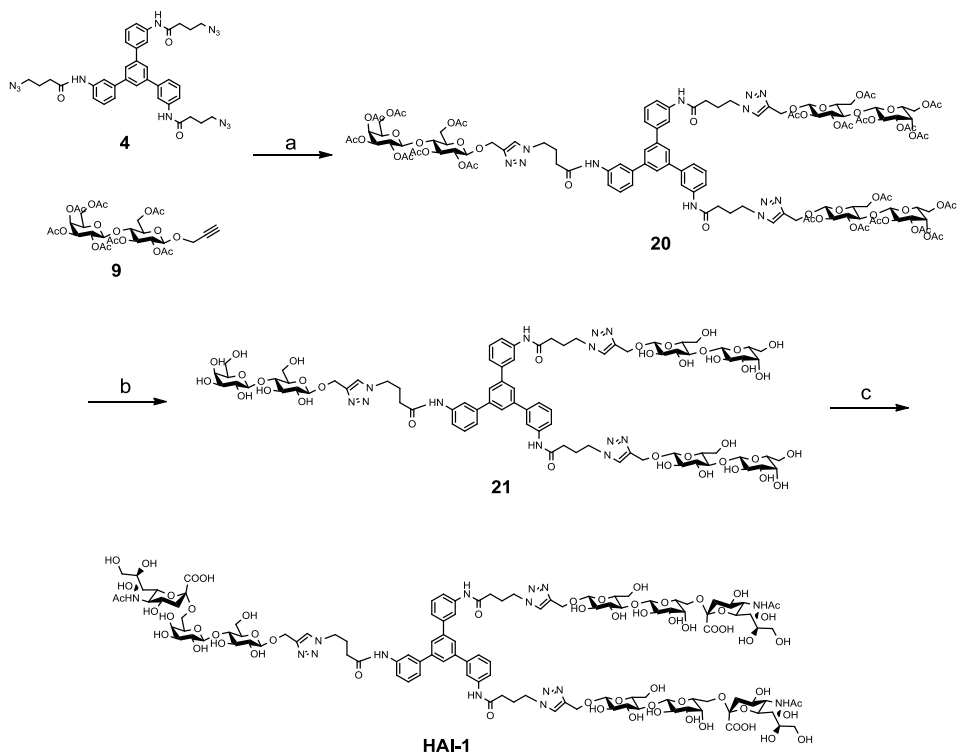
peptidic spacer arms. This construct was reported to bind to immobilized HA by surface plasmon resonance (SPR) with a  $K_d$  of 450 nM,<sup>23</sup> but the peptidic component showed significant binding and was more than just a spacer. In another system, a three way junction DNA for the display of  $\alpha$ -2,3-SiaLac units was shown to be potent, but a single arm was not much less potent.<sup>24</sup> A system based on PNA-DNA complexes displaying two  $\alpha$ -2,6-SiaLacNAc units at various distances was also reported.<sup>25</sup> Evidence for a true chelation effect was provided with a ca. 30-fold enhancement (15-fold per sugar) over a DNA-PNA reference construct containing only a single glyco-ligand. Unfortunately, these noncovalent constructs of ca. 21 kDa are not small molecules and also susceptible to degradation. Other indications that chelation of HA binding sites is indeed possible comes from carbohydrate array experiments with bi-antennary glycans. It was shown that glycans with at least three LacNAc units in each of the arms, bound more strongly to human type specific HA's.<sup>26</sup> Molecular modeling supported the chelation mode, and indicated that two LacNAc units would be too short to reach two sialic acid binding pockets of HA. This chelation-type binding was shown to only be possible for the human type specific HA binding to  $\alpha$ -2,6-linked sialic acid for geometrical reasons and is precluded for the  $\alpha$ -2,3-linked ones.<sup>27</sup>

As has already been mentioned in Chapter 2, our structural design of HA inhibitors include were divalent or trivalent moieties that seem to fit the geometry of the HA protein. As we already synthesized building blocks successfully, the next step of the research would be the assembly of the building blocks to produce divalent and trivalent inhibitors. Here in this chapter, we discuss the synthesis of the final inhibitors and the characterization of these molecules. Compounds with different sugar chain lengths were synthesized through chemical reaction then sialylated by using an efficient  $\alpha$ -2,6-sialyltransferase (PmST1 double mutant P34H/M144L)<sup>28</sup> from *Pasteurella multocida*. The largest of the compounds had longer arms than a biantennary Sia(LacNAc)<sub>3</sub> linked to a tri-mannose core, known for its chelation binding mode to HA.

## 3.2 Results and discussion

### 3.2.1 Synthesis of the short version of trivalent HA inhibitor

In order to work through the synthesis pathway of the trivalent HA inhibitors, we first started with the shortest version (**Scheme 1**).



**Scheme 1.** Synthesis of the shortest version of a trivalent HA inhibitor. Reagents and conditions: a)  $\text{CuSO}_4 \cdot 5\text{H}_2\text{O}$ , Na-ascorbate, DMF/ $\text{H}_2\text{O}$  (9:1), microwave  $100\text{ }^\circ\text{C}$ , 1.5 h, 97 %; b) NaOMe, MeOH, 14 h, 90 %; c) CMP-NANA, PmST1 mutant P34H/M144L, Tris-HCl buffer, pH 8.0,  $37\text{ }^\circ\text{C}$ , 14 h, 57 %.

The azido-scaffold **4** was reacted with 5 equiv of acetylated propargyl lactoside **9** by a CuAAC 'click' cycloaddition reaction under microwave irradiation. In order to achieve higher yield of the first trivalent compound **20**, we added an excess amount of lactoside **9** and heated the reaction mixture at  $100\text{ }^\circ\text{C}$  for 1.5 h. The completion was checked by TLC using UV light as the scaffold has a strong UV-absorption. A silica gel chromatography with a 97 % yield of compound **20** was obtained. The deacetylation was performed with 0.1 equiv NaOMe in MeOH solution and reacted overnight. Then the solution was neutralized with Dowex- $\text{H}^+$  resin to a pH of ca.7 when the resin was removed by filtration. After that, the residue was concentrated *in vacuo* and used directly for next step. The final sialylation was achieved by using the sialyltransferase PmST1 double mutant P34H/M144L, that was mutated to get the desired  $\alpha$ -2,6-specificity.<sup>28</sup> This reaction was incubated in 100 mM Tris-HCl buffer (pH 8.0) under  $37\text{ }^\circ\text{C}$ . Different from the sialylation of compounds **8** and **13** (Chapter 2), a solution with a different pH was

used as a literature report mentioned that for sialylation of lactose moieties, the pH should be more basic (ca. 8.0) than for LacNAc moieties. In that case, pH 7.5 is more appropriate as the acetyl group is sensitive to basic conditions.<sup>29</sup> 50  $\mu$ L enzyme solution was used to catalyze the conversion of 1 mg of substrate for 14 h to make sure all three arms of the molecule were being sialylated. The reaction mixture was purified first by a polyacrylamide gel column and then by preparative HPLC using a HILIC column with a specific method shown in Table 1. This reaction only yielded the trisubstituted product **HAI-1** i.e. no mono- or disubstituted variants were observed.

**Table 1.** Method to purify **HAI-1** by preparation HPLC using HILIC column.

Time (min)	Buffer A (%)	Buffer B (%)	Flow rate (mL/min)
0.0	30	70	3.6
11.0	32	68	3.6
14.0	33	67	3.6
17.0	36	64	3.6
23.0	37	63	3.6
23.1	50	50	3.6
27.0	50	50	3.6

After collecting all of the purified fractions of **HAI-1**, <sup>1</sup>H NMR, HPLC and HRMS were performed to characterize the product. Comparing the proton NMRs of compound **21** and **HAI-1** (Figure 1), it was possible to identify e.g. the H-3 peaks of the sialic acid which confirmed that the tri-sialylation reaction worked.

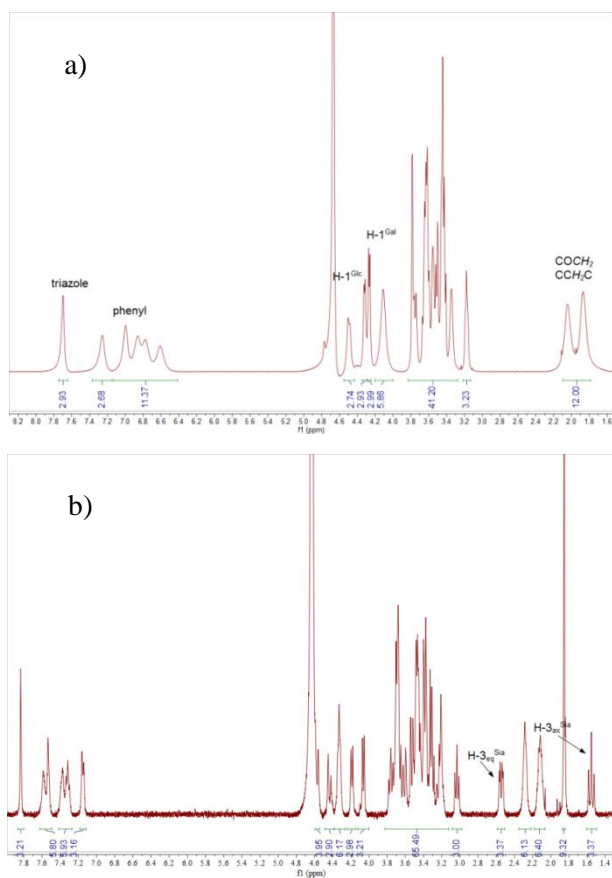


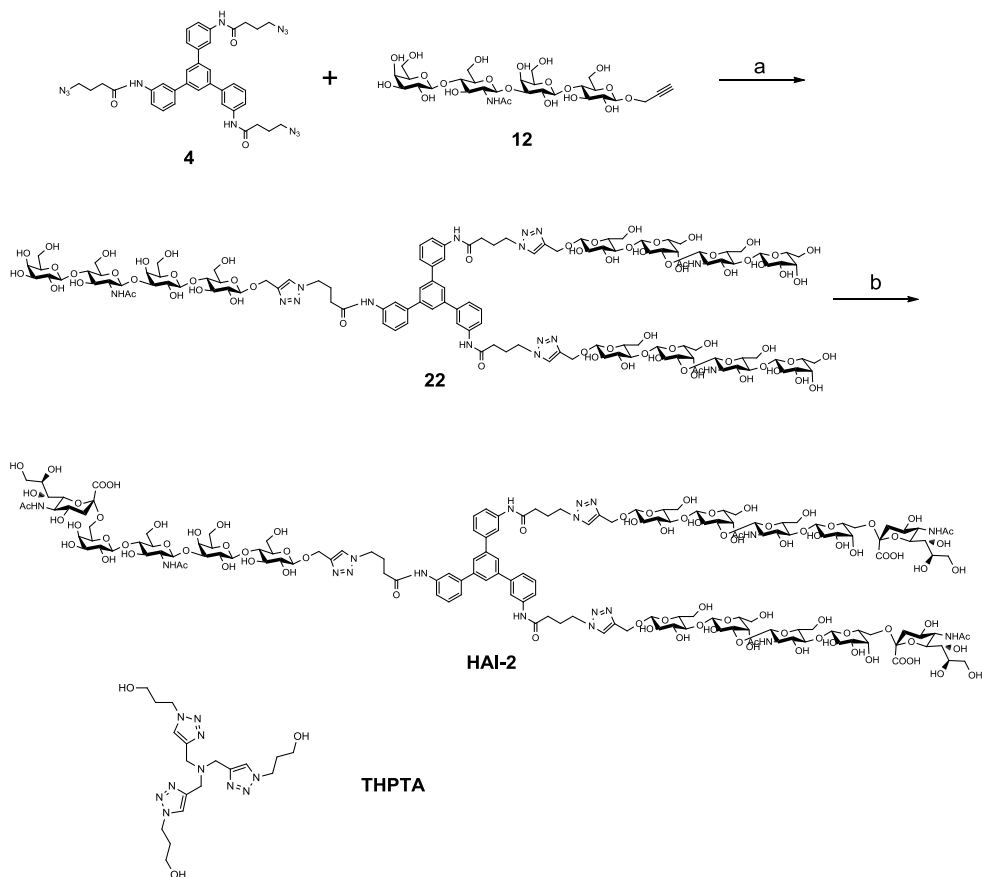
**Figure 1.** <sup>1</sup>H NMR spectra of compound **21** and **HAI-1** in D<sub>2</sub>O indicating the typical chemical shifts of the protons.

### 3.2.2 Synthesis of a tri- $\alpha$ 2,6Sia-LacNAc-Lac HA inhibitor

As already mentioned above, the LacNAc-repeats seem to have benefits for enhancing the interaction between sialyl-oligosaccharides and HA.<sup>26</sup> We therefore introduced the LacNAc-Lactose sugar chain into our second HA inhibitor design. Several methods were tested in the beginning of this synthesis route. The first thought was an enzymatic elongation starting from the tri-lactoside **21**. This should be possible by using the  $\beta$ -1,3-N-acetylglucosaminyltransferase from *Helicobacter pylori* (HP39)<sup>30</sup> and the  $\beta$ -1,4-galactosyltransferase from *Neisseria meningitidis* (*LgtB*).<sup>31</sup> This way we planned to add a LacNAc unit to **21**, and then finally attach a sialic acid in the last step. The first reaction was performed with UDP-GlcNAc and catalyzed by HP39 and was successful monitored by LC-MS, but the second reaction with UDP-Gal failed as only product was obtained with one galactose



attached to it instead of three. As this synthetic route was not working, another strategy was applied in which the sugarchain was elongated to a trisaccharide first (Chapter 2) and then linked to the trivalent scaffold (**Scheme 2**).



**Scheme 2.** Synthesis of tri- $\alpha$ 2,6Sia-LacNAc-Lac HA inhibitor. Reagents and conditions: a) THPTA,  $\text{CuSO}_4 \cdot 5\text{H}_2\text{O}$ , Na-ascorbate, DMF/ $\text{H}_2\text{O}$  (1:2), microwave  $80^\circ\text{C}$ , 1.5 h, 63 %; b) CMP-NANA, PmST1 mutant P34H/M144L, Tris-HCl buffer, pH 7.5,  $37^\circ\text{C}$ , 14 h, 44 %.

The CuAAC conjugation was performed between the azido-scaffold **4** and the alkyne-linked LacNAc-lactose building block **12**. The first attempt of this ‘click’ reaction followed the same method of **Scheme 1**, but there was no product observed by TLC. Then another method was used by adding a water soluble triazole ligand tris(3-hydroxypropyltriazolylmethyl)amine (THPTA), which can stabilize Cu(I), protecting it from oxidation and disproportionation, thus enhancing its catalytic activity in the CuAAC reaction. By doing so, and also the changing ratio of the DMF- $\text{H}_2\text{O}$ , adding more catalysts,<sup>32,33</sup> the trimeric product **22** was

finally obtained. Purification by a using Bio-gel P-2 column was possible, and the characterization of **22** was confirmed by  $^1\text{H}$  NMR, HPLC and HRMS, and a yield of 63 % was obtained. The final sialylation followed according to the former route described in scheme 1, catalyzed by the PmST1 mutant<sup>28</sup> at pH 7.5 this time, as there are sensitive acetyl groups in the substrate. The mixture was incubated overnight to maximize conversion and then purified by preparative HPLC using the method shown in Table 2.

**Table 2.** Method for preparation HPLC of **HAI-2** using HILIC column.

Time (min)	Buffer A (%)	Buffer B (%)	Flow rate (mL/min)
0.0	30	70	3.6
10.0	32	68	3.6
15.0	33	67	3.6
20.0	36	64	3.6
40.0	37	63	3.6
50.0	37	63	3.6
65.0	50	50	3.6
80.0	50	50	3.6

After collecting all the purified fractions of **HAI-2**,  $^1\text{H}$  NMR, HSQC (Figure 2), COSY, LCMS and HRMS were performed to characterize the product.

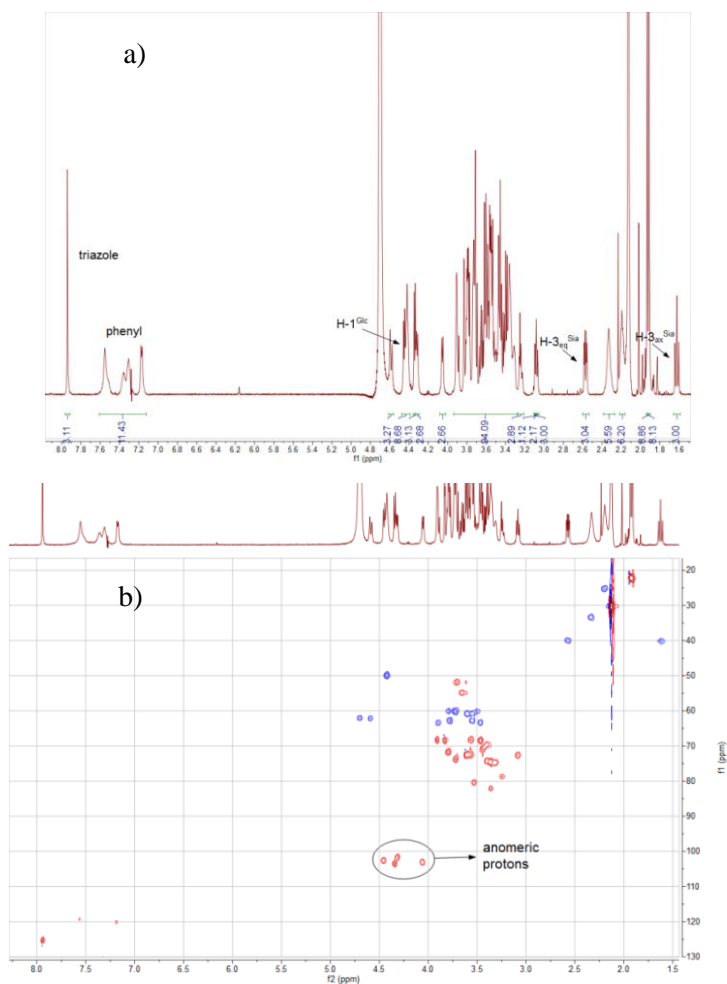
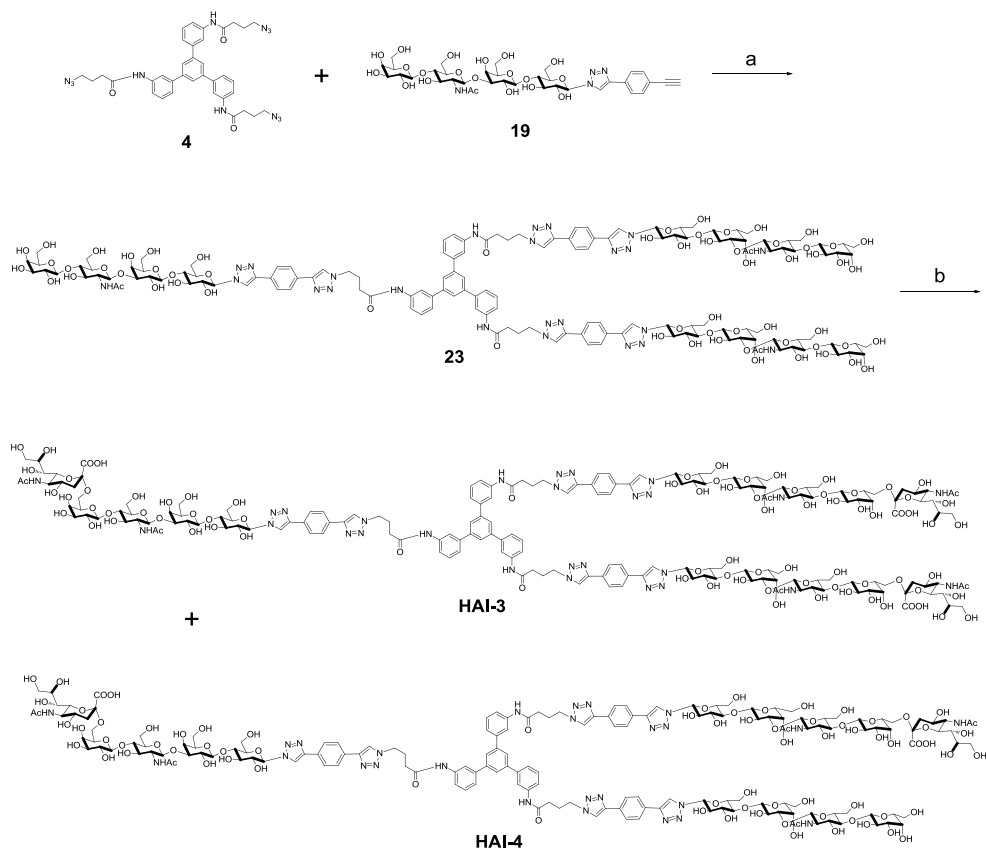


**Figure 2.** <sup>1</sup>H NMR (a) and HSQC (b) spectra of **HAI-2** indicating the typical chemical shifts of the protons and carbons.

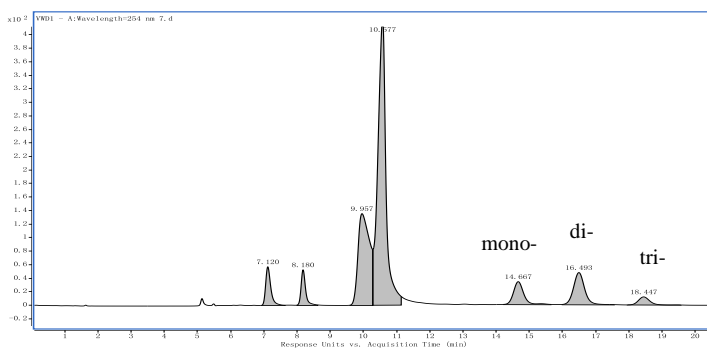
### 3.2.3 Synthesis of tri- $\alpha$ 2,6Sia-LacNAc-Lac HA inhibitor with extended rigid spacer

In order to investigate the influence of elongation and rigidity to the binding affinity, we also introduced a rigid spacer extension to the trivalent inhibitor design (**Scheme 3**).



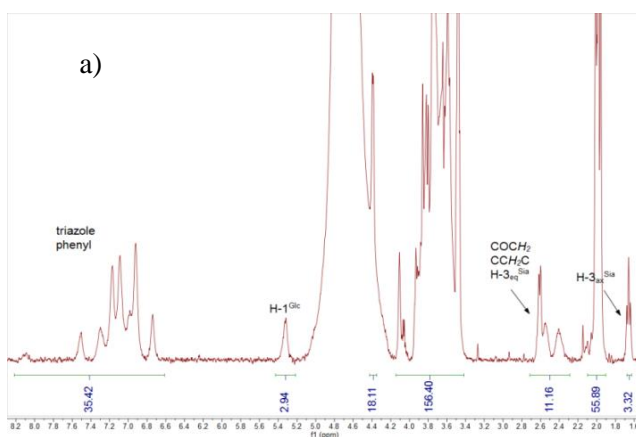
**Scheme 3.** Synthesis of tri- $\alpha$ 2,6Sia-LacNAc-Lac HA inhibitor with extended rigid spacer. Reagents and conditions: a) THPTA,  $\text{CuSO}_4 \cdot 5\text{H}_2\text{O}$ , Na-ascorbate, DMF/ $\text{H}_2\text{O}$  (1:2), microwave  $80^\circ\text{C}$ , 1.5 h, 77 %; b) CMP-NANA, PmST1 mutant P34H/M144L, Tris-HCl buffer, pH 7.5,  $37^\circ\text{C}$ , 4 h.

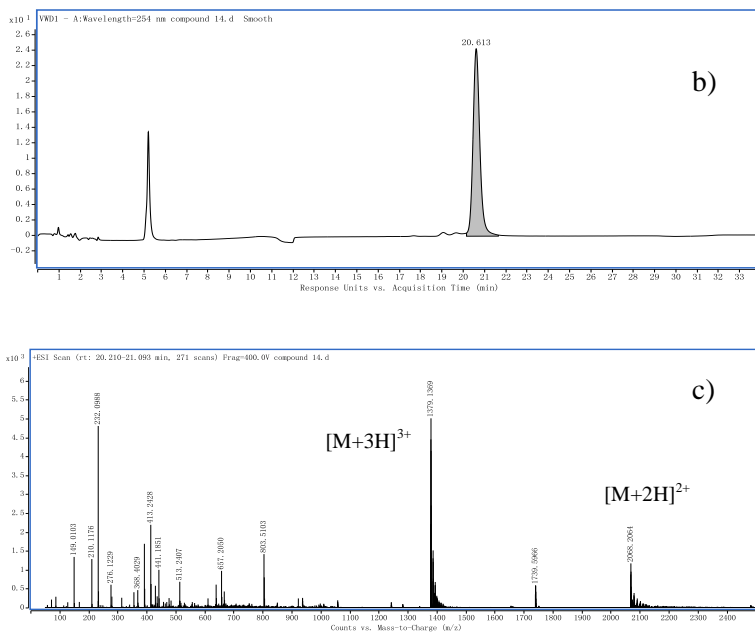
The synthesis followed a similar route to the **HAI-2** synthesis, starting with a CuAAC cycloaddition reaction between the azido-scaffold **4** and the alkyne-linked LacNAc-lactose spacer. The ligand THPTA was also used to enhance the activity. After 1.5 h of microwave irradiation, 77 % of compound **23** was obtained after purified by Bio-gel P-2 column. **23** was used directly for the next sialylation step without further purification. However, the sialylation of **23** did not proceed the same way as for **HAI-2**. The first trial was performed at the same condition shown in Scheme 2, but after 14 h of incubation, the presence of both the mono- and di-sialylated products was evident from the HPLC chromatogram (Figure 3).



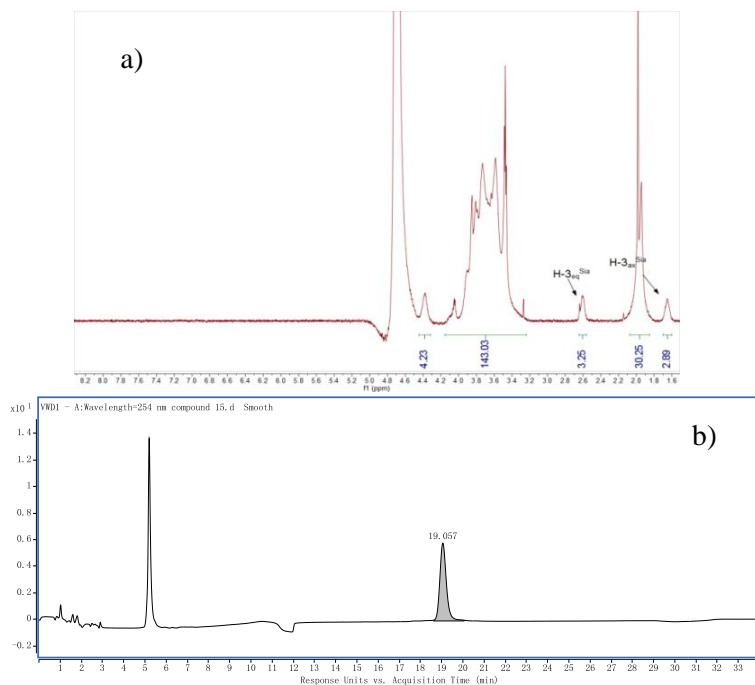
**Figure 3.** HPLC spectra of the reaction mixture of the sialylation of **23**.

Even when we added an excess amount of enzyme and CMP-NANA, the reaction still couldn't be pushed to a full conversion of the desired trivalent compounds in contrast to the synthesis of **HAI-2**. However, from another point of view, the incomplete coupling products might be useful reference compounds for the evaluation of these multivalent inhibitors. It was therefore decided to purify these compound and analyze them for future use by preparative HPLC following the same method shown in Table 2. As the sialylation of **23** was performed on a low miligram scale, only 0.38 mg of purified **HAI-3** and 0.86 mg purified **HAI-4** could be isolated. The reason for this result is difficult to say with certainty other than that the triazole substituted phenyl extension changes the properties of the construct to prevent a complete reaction. After collecting all the purified fractions of **HAI-3** & **4**,  $^1\text{H}$  NMR, LCMS (Figure 4 & 5) and HRMS were performed to characterize the product.





**Figure 4.** Characterization of the trivalent inhibitor **HAI-3**. a)  $^1\text{H}$  NMR spectra indicating the typical chemical shifts of the protons; b) LC spectra indicating the purity after the preparative HPLC; c) MS spectra indicating the right product with double and triple charges.



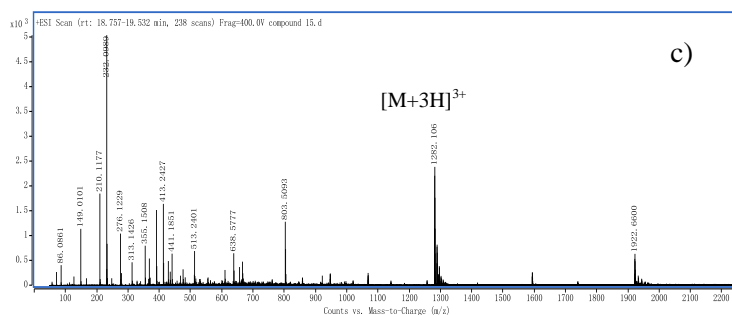
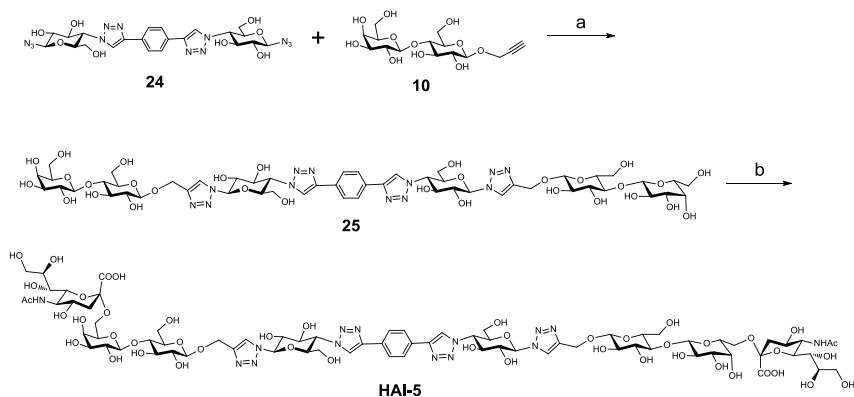


**Figure 5.** Characterization of the trivalent inhibitor **HAI-4**. a)  $^1\text{H}$  NMR spectra indicating the typical chemical shifts of the protons; b) LC spectra indicating the purity after the preparative HPLC; c) MS spectra indicating the right product with double and triple charges.

Although the  $^1\text{H}$  NMR spectra of **HAI-3** and especially **HAI-4** are not really clear, the LCMS gave us complementary information of the characterization of these inhibitors, which confirmed the synthesis results. The reason for the nature of the NMR spectra with broad (**HAI-3**) and even some absent peaks (**HAI-4**) is the slow exchange with respect to the NMR timescale that these molecules seem to move in. This can be caused by slow dynamic process, such as aggregation, likely involving the aromatic core of the molecules.

### 3.2.4 Synthesis of short version of the di- $\alpha$ 2,6Sia-Lac HA inhibitor

Besides the trivalent inhibitors we designed and synthesized, divalent rigid inhibitors are also synthesized for comparison purposes (**Scheme 4**). While binding simultaneously with three binding sites is conceptually very attractive, efficient binding with two sites can also yield very potent compounds and may be easier to achieve. Here we used a divalent spacer with rigid elements such as a direct linkage between glucose and triazole, a motif that was previously explored in rigid spacers for enhanced multivalency effects.<sup>34</sup>



**Scheme 4.** Synthesis of short version of the di- $\alpha$ 2,6Sia-Lac HA inhibitor. Reagents and conditions: a) THPTA, CuSO<sub>4</sub> 5H<sub>2</sub>O, Na-ascorbate, DMF/H<sub>2</sub>O (1:2), microwave 80 °C, 1.5 h, 79 %; b) CMP-NANA, PmST1 mutant P34H/M144L, Tris-HCl buffer, pH 8.0, 37 °C, 4 h, 52 %.

The rigid spacer **24** was a potent molecule that has been used in the research of the problematic pathogen *Pseudomonas aeruginosa* lectin LecA in our group. By following the similar synthetic route as before, propargyl lactoside **10** was conjugated with the spacer under microwave irradiation at 80 °C for 1.5 h. The reaction was monitored by TLC and then purified by Bio-gel P-2 column without further purification with a yield of 79 %. After that, the sialylation was performed with 3 equiv of CMP-NANA catalyzed by the PmST1 mutant incubating for 4 h for a full conversion to di-sialylated **HAI-5**. The product was purified by preparative HPLC following the method shown in Table 3.

**Table 3.** Method for preparation HPLC of **HAI-5** using HILIC column.

Time (min)	Buffer A (%)	Buffer B (%)	Flow rate (mL/min)
0.0	20	80	3.6
10.0	30	70	3.6
45.0	33	67	3.6
60.0	50	50	3.6
75.0	50	50	3.6



After collecting all the purified fractions of **HAI-5**,  $^1\text{H}$  NMR, HSQC (Figure 6), COSY, LCMS and HRMS were performed to characterize the product which was obtained in 52 % yield after purification.

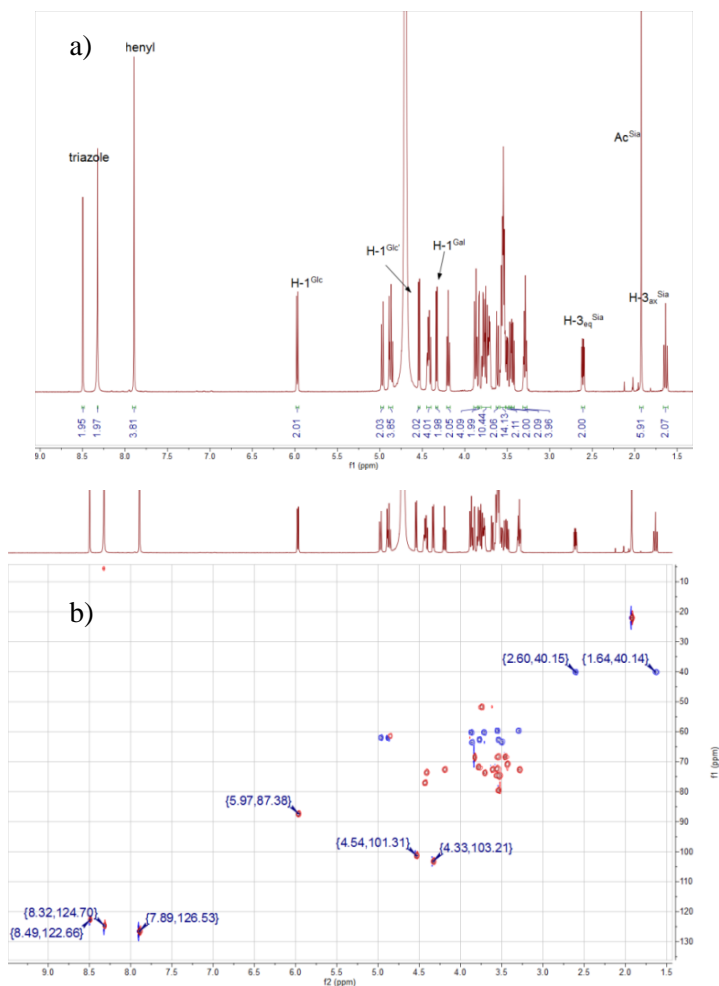
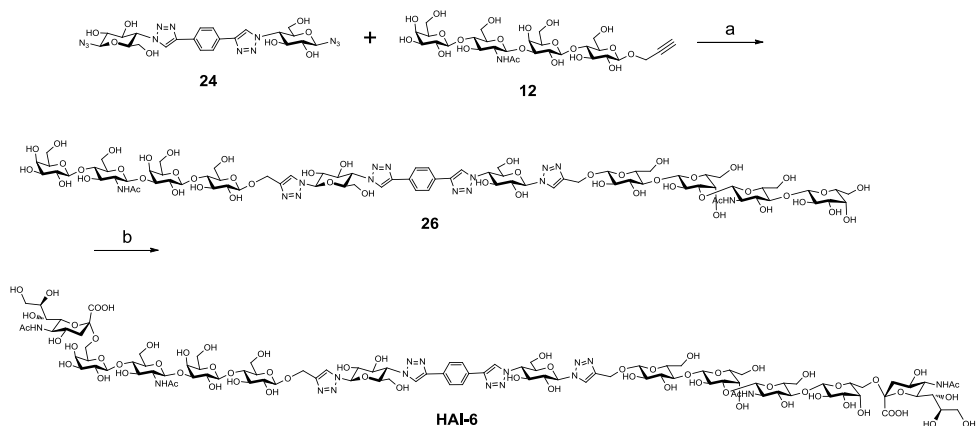


**Figure 6.**  $^1\text{H}$  NMR and HSQC spectra of **HAI-5** indicating the typical chemical shifts of the protons and carbons.

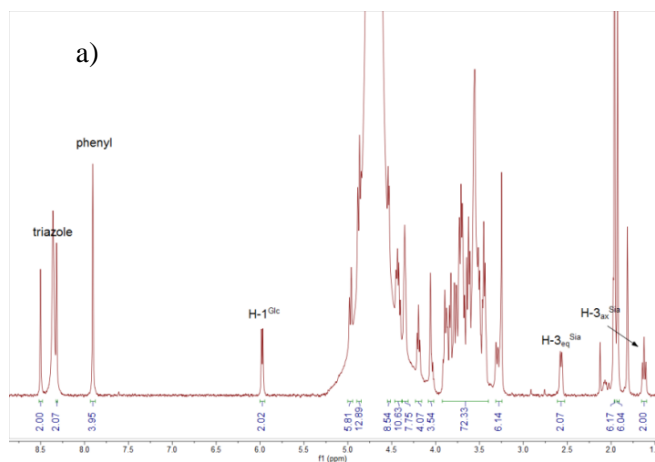
### 3.2.5 Synthesis of di- $\alpha$ 2,6Sia-LacNAc-Lac HA inhibitor

As literature reports showed that the presence of elongated LacNAc groups linked to the sialic acid<sup>35</sup> could benefit the binding to HA, a longer version of the divalent ligand was prepared as described in Scheme 5.



**Scheme 5.** Synthesis of di- $\alpha$ 2,6Sia-LacNAc-Lac HA inhibitor with a rigid divalent core. Reagents and conditions: a) THPTA,  $\text{CuSO}_4 \cdot 5\text{H}_2\text{O}$ , Na-ascorbate, DMF/ $\text{H}_2\text{O}$  (1:2), microwave  $80^\circ\text{C}$ , 1.5 h, 87 %; b) CMP-NANA, PmST1 mutant P34H/M144L, Tris-HCl buffer, pH 7.5,  $37^\circ\text{C}$ , 4 h, 55 %.

Also starting from the rigid spacer **24**, the CuAAC reaction was performed under microwave irradiation at the same conditions as before with 3 equiv propargyl tetrasaccharide **12** which resulted in product **26** with 87 % yield after Bio-gel P-2 column purification. After that, **26** was catalyzed by the PmST1 mutant with 3 equiv CMP-NANA for 4 h at pH 7.5, as there are sensitive acetyl groups in the substrate, which resulting in the di-sialylated compound **HAI-6**. The product was purified by preparative HPLC following the same method as shown in Table 3. After collecting all the purified fractions of **HAI-6**,  $^1\text{H}$  NMR, LCMS (Figure 7) and HRMS were performed to characterize the product which was obtained in 55 % yield after purification.



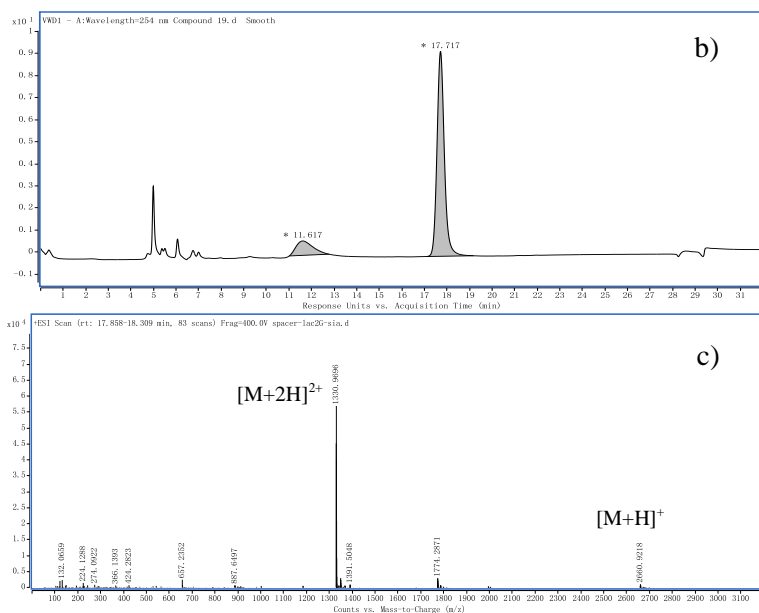
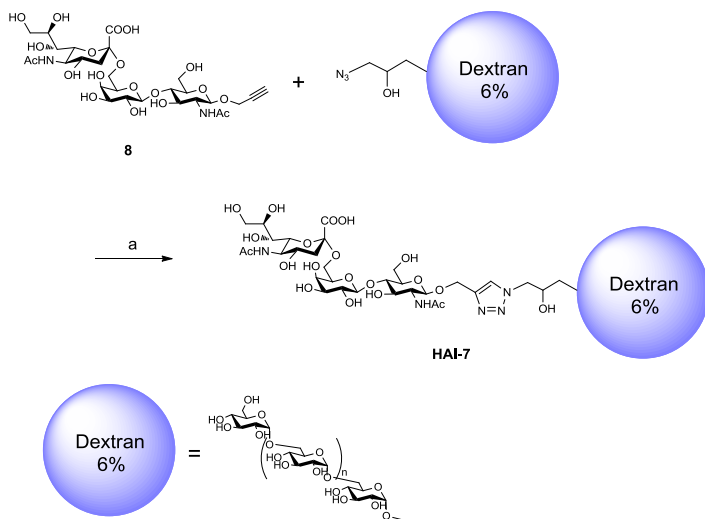


**Figure 7.** Characterization of the trivalent inhibitor **HAI-6**. a) <sup>1</sup>H NMR spectra indicating the typical chemical shifts of the protons; b) LC spectra indicating the purity after the preparative HPLC; c) MS spectra indicating the right product with single and double charges.

### 3.2.6 Synthesis of the polymeric $\alpha$ -2,6Sia-LacNAc-dextran construct

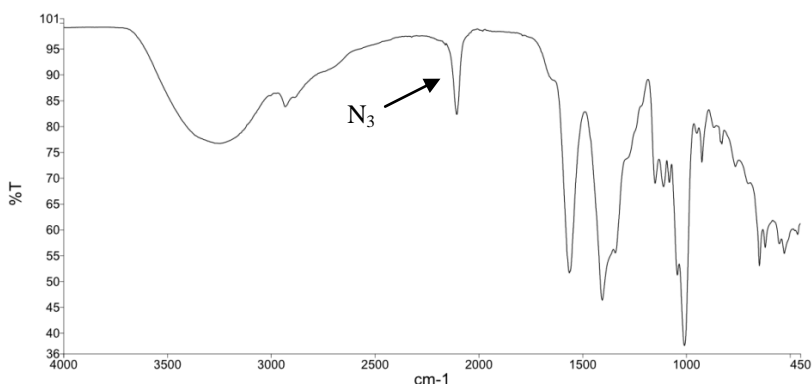
For comparison with the ‘small’ molecule scaffolds, a polymeric chitosan scaffold was also used for the synthesis of an HA inhibitor (**Scheme 6**). In this case the previously mentioned  $\alpha$ -2,6-Sia-LacNAc building block was coupled to a modified dextran polymer<sup>36</sup> with a degree of substitution of 6 % as determined by NMR.



**Scheme 6.** Synthesis of the polymeric  $\alpha$ -2,6Sia-LacNAc-dextran. Reagents and conditions: a)  $\text{CuSO}_4 \cdot 5\text{H}_2\text{O}$ , Na-ascorbate,  $\text{H}_2\text{O}$ , microwave  $100^\circ\text{C}$ , 60 min, 24 %.

The azido polymer was coupled with 1.3 equiv propargyl- $\alpha$ -2,6Sia-LacNAc **8** under microwave irradiation. After 1 h reaction, the solvent was evaporated and the crude mixture was purified by dialysis using a cellulose based dialysis cassette (MWCO: 2K) to obtain 3 mg (24 %) of **HAI-7**. During the course of CuAAC conjugation, IR spectroscopy, as an analytical tool, was particularly helpful to verify the completion of the reaction. As shown in **Figure 8A**, the IR data of azido-dextran showed a peak corresponding to azide (ca.  $2098\text{ cm}^{-1}$ ) residue, while the azide stretching peak disappeared after the reaction (**Figure 8B**).

#### A) 6 % dextran



## B) HAI-7

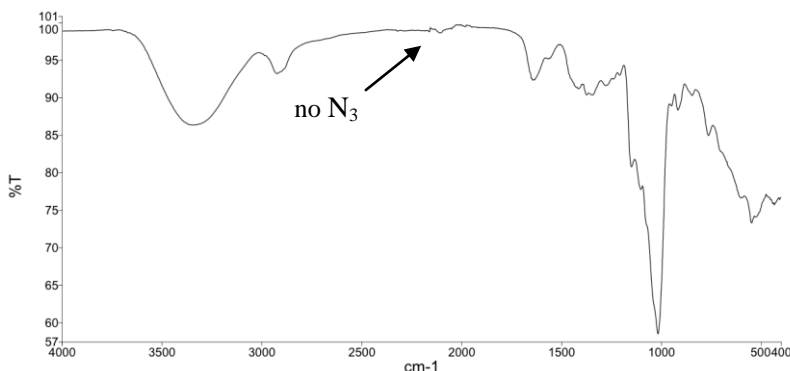


**Figure 8.** IR spectra of the 6 % functionalized dextran before and after glycosylation.

## 3.3 Conclusion and outlook

We here showed the successful synthesis and characterization of multivalent sialic acid containing glycoconjugates. Their synthesis was possible by a combination of chemical scaffold synthesis, enzymatic carbohydrate synthesis and CuAAC conjugation. Although the characterization of some of the HA inhibitors was difficult, we managed arrive at definitive characterizations by combining multiple analysis techniques. The syntheses were performed on a small low milligram scale, and future attempts on a larger scale should also be investigated. More importantly, variations of the conjugate structures based on the biological evaluation of these constructs, could to be performed to find the optimal designs for IAV inhibitors, to ultimately be used as anti-flu drugs.

## 3.4 Experimental procedure

### 3.4.1 General

#### 3.4.1.1 Chemical synthesis and identification

Chemicals were used as obtained from commercial sources without further purification unless stated otherwise. The solvents were obtained as synthesis grade and stored on molecular sieves (4 Å). Column chromatography was performed using Silica-P Flash silica gel (60 Å, particle size 40–63 μm) from Silicycle. TLC was performed on Merck precoated silica gel 60F254 glass plates and compound spots were visualized with UV light and/or 10 % H<sub>2</sub>SO<sub>4</sub> (MeOH). Microwave

reaction was carried out in a Biotage Initiator (300 W) reactor.  $^1\text{H}$  NMR spectra were recorded on a 400 MHz, 500 MHz or 600 MHz spectrometer.  $^{13}\text{C}$  NMR analysis was recorded on a 100 MHz, 125 MHz or 151 MHz spectrometer. High resolution mass spectrometry (HRMS) analysis was recorded using Agilent 6560 Ion Mobility Q-TOF LC/MS. Analytical HPLC was performed on a Shimadzu-10AVP (Class-VP) system using a Phenomenex Gemini C18 column (110 Å, 5  $\mu\text{m}$ , 250 $\times$ 4.6 mm) at a flow rate of 1 mL/min. The used buffers were 0.1 % trifluoroacetic acid in Buffer A  $\text{CH}_3\text{CN}/\text{H}_2\text{O}$  (5:95 v/v) and 0.1 % trifluoroacetic acid in Buffer B  $\text{CH}_3\text{CN}/\text{H}_2\text{O}$  (95:5 v/v). Runs were performed using a standard protocol: 100 % buffer A for 2 min, then a linear gradient of buffer B (0 – 100 % in 38 min) and UV-absorption was measured at 210 nm and 254 nm. Purification using preparative HPLC was performed on an Applied Biosystems workstation with a Phenomenex Gemini C18 column (10  $\mu\text{m}$ , 110 Å, 250 $\times$ 21.2 mm) at a flow rate of 6.25 mL/min. Runs were performed using a standard protocol: 100 % buffer A for 5 min, then a linear gradient of buffer B (0 – 100 % in 70 min) with the same buffers as described for the analytical HPLC. Analytical LC-ESI-MS was performed on Thermo-Finnigan LCQ Deca XP Max using the same buffers and protocol as described for analytical HPLC. FT-IR spectra were recorded on a PerkinElmer UATR TWO FT-IR spectrometer operating from 4000-650  $\text{cm}^{-1}$  on the Universal diamond ATR top-plate. Here I want to thank Diksha for performing the coupling reaction of the polymer which was also very important for this research.

#### **3.4.1.2 Enzymatic synthesis and identification**

All enzymatic reactions were performed in aqueous buffered system with the appropriate pH for each enzyme. The reactions were monitored by TLC performed on Silicycle aluminium backed silica F254 plates. After development with appropriate eluents, the spots were visualized by UV light and/or dipping in 10 % sulfuric acid in methanol. Gel filtration chromatography was performed with column packed with Bio-gel P-2 Fine (Bio-Rad), eluted with water. Water was purified by Milli-Q Gradient A10 Water Purification System. Lyophilization was performed on a Christ Alpha 1-2 apparatus. NMR spectra were recorded on the same equipment as 3.4.1.1. Analytical LC-ESI-MS was performed on Agilent 6560 Ion Mobility Q-TOF LC/MS using a Waters XBridge HILIC column (5  $\mu\text{m}$ , 250 $\times$ 4.6 mm) at a flow rate of 0.6 mL/min. The used buffers were 50 mM formic acid in  $\text{H}_2\text{O}$  (Buffer A, pH 4.4) and  $\text{CH}_3\text{CN}$  (Buffer B). UV-absorption was measured at 210 nm and 254 nm. Purification using preparative HPLC was performed on a Shimadzu 20A HPLC system with a Waters XBridge BEH Prep Amide column (5  $\mu\text{m}$ , 250 $\times$ 10 mm) at a flow rate of 3.6 mL/min.

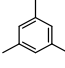
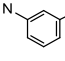
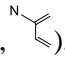
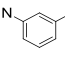
$\alpha$ -2,6-sialyltransferase (PmST1 double mutant P34H/M144L) from *Pasteurella multocida*<sup>28</sup> (2.3 mg/mL) were made in house by Robert P. de Vries. Cytidine-5'-monophospho-N-acetylneuraminic acid (CMP-NANA) was purchased from Roche Diagnostics GmbH.

### 3.4.2 Synthetic procedures and compound characterization

#### Acetylated-trivalent-Lac substrate **20**

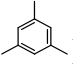
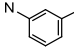
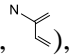
Compound **4** (12.3 mg, 0.018 mmol), **9** (61 mg, 0.09 mmol, 5 equiv), CuSO<sub>4</sub> · 5H<sub>2</sub>O (2.2 mg, 0.009 mmol, 0.5 equiv), sodium L-ascorbate (8.9 mg, 0.045 mmol, 2.5 equiv) were dissolved in DMF/H<sub>2</sub>O (9:1, 2 mL). The reaction was performed under microwave irradiation at 100 °C for 1.5 h. The completion of the reaction was analyzed by TLC (DCM/MeOH 7:1 v/v). Then the mixture was concentrated *in vacuo*. The residue was purified by silica chromatography (DCM/ MeOH 20:1 v/v) which gave the product **20** as a light yellow solid (47.3 mg, 97 % yield).

<sup>1</sup>H NMR (400 MHz, CDCl<sub>3</sub>):  $\delta$  8.14 (s, 3H, H-triazole), 7.80 (s, 3H, NH), 7.71 (s,

3H, , 7.58 (m, 6H, , , 7.40 (m, 6H, , 5.31 (d,  $J = 3.4$  Hz, 3H, H-4<sup>Gal</sup>), 5.15 (t,  $J = 9.3$  Hz, 3H, H-3<sup>Glc</sup>), 5.07 (dd,  $J = 10.4, 7.1$  Hz, 3H, H-2<sup>Gal</sup>), 4.94 – 4.72 (m, 12H, H-3<sup>Gal</sup>, CH<sub>2</sub>N, H-2<sup>Glc</sup>), 4.59 (d,  $J = 7.8$  Hz, 3H, H-1<sup>Glc</sup>), 4.52 – 4.42 (m, 12H, H-1<sup>Gal</sup>, H-6a<sup>Glc</sup>, OCH<sub>2</sub>C), 4.12 – 4.00 (m, 9H, 2H-6<sup>Gal</sup>, H-6b<sup>Glc</sup>), 3.82 (t,  $J = 7.0$  Hz, 3H, H-5<sup>Gal</sup>), 3.75 (t,  $J = 9.4$  Hz, 3H, H-4<sup>Glc</sup>), 3.61 – 3.53 (m, 3H, H-5<sup>Glc</sup>), 2.43 – 2.26 (m, 12H, COCH<sub>2</sub>, CCH<sub>2</sub>C), 2.14 – 2.08 (m, 18H, Ac), 2.03 – 1.92 (m, 45H, Ac); <sup>13</sup>C NMR (101 MHz, CDCl<sub>3</sub>):  $\delta$  170.5, 170.3, 170.1, 170.1, 170.1, 169.8, 169.7, 169.0, 141.7, 141.5, 138.5, 129.5, 125.1, 123.4, 123.1, 119.2, 118.7, 101.0(C-1<sup>Gal</sup>), 99.9(C-1<sup>Glc</sup>), 76.0, 72.8, 72.6, 71.6, 70.9, 70.6, 69.1, 66.6, 63.1, 61.8, 60.7, 49.4, 33.4, 29.7, 25.8, 20.9, 20.7, 20.7, 20.6, 20.6, 20.6, 20.5. HRMS:  $m/z$  calcd for C<sub>123</sub>H<sub>150</sub>N<sub>12</sub>O<sub>57</sub> [M+2H]<sup>2+</sup> 1354.4677, found 1354.4673.

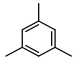
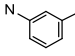
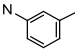
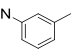
#### Trivalent-Lac substrate **21**

NaOMe (0.8 mg, 0.001 mmol, 0.1 equiv) was added to a solution of compound **9** (37 mg, 0.014 mmol) in MeOH (5 mL) and the mixture was stirred for 14 h at room temperature. The solution was neutralized with Dowex-H<sup>+</sup> resin to a pH of ca.7 when the resin was removed by filtration. The residue was concentrated *in vacuo*. Compound **21** was obtained as a white solid (23 mg, 90 % yield).

$^1\text{H}$  NMR (500 MHz,  $\text{D}_2\text{O}$ ):  $\delta$  7.70 (s, 3H, H-triazole), 7.26 (s, 3H, ) , 7.12 – 6.42 (m, 12H, , ) , 4.49 (d,  $J = 9.5$  Hz, 3H, H-6b<sup>Glc</sup>), 4.32 (d,  $J = 7.0$  Hz, 3H, H-1<sup>Glc</sup>), 4.27 (d,  $J = 7.3$  Hz, 3H, H-1<sup>Gal</sup>), 4.20 – 4.00 (m, 6H,  $\text{CH}_2\text{N}$ ), 3.83 – 3.27 (m, 36H), 3.18 (t,  $J = 8.1$  Hz, 3H, H-2<sup>Glc</sup>), 2.09 – 1.79 (m, 12H,  $\text{COCH}_2$ ,  $\text{CCH}_2\text{C}$ );  $^{13}\text{C}$  NMR (126 MHz,  $\text{D}_2\text{O}$ ):  $\delta$  171.9, 143.4, 140.4, 137.8, 129.0, 124.8, 123.9, 122.6, 118.9, 118.3, 102.9(C-1<sup>Gal</sup>), 101.5(C-1<sup>Glc</sup>), 78.4, 75.28, 74.71, 74.32, 72.66, 72.51, 70.89, 68.49, 61.84, 60.97, 60.05, 49.48, 33.05, 25.37; HRMS:  $m/z$  calcd. for  $\text{C}_{81}\text{H}_{108}\text{N}_{12}\text{O}_{36} [\text{M}+2\text{H}]^{2+}$  913.3567, found 913.3568.

### Trivalent- $\alpha$ 2,6Sia-Lac Ligand HAI-1

Compound **21** (1 mg, 0.55  $\mu\text{mol}$ ) and CMP-NANA (2.1 mg, 3.3  $\mu\text{mol}$ , 6 equiv) were dissolved in Tris-HCl buffer (100 mM, pH 8.0, 500  $\mu\text{L}$ ) containing  $\text{MgCl}_2$  (20 mM). To this, PmST1 mutant P34H/M144L ( $\alpha$ 2-6sialyltransferase, 2.3 mg/mL, 50  $\mu\text{L}$ ) was added. The resulting reaction mixture was incubated at 37  $^\circ\text{C}$  for 14 h. The reaction mixture was centrifuged and the supernatant subjected to gel filtration over Bio-gel P-2 (eluent  $\text{H}_2\text{O}$ ). Fractions containing product were combined and lyophilized for further preparation HPLC (HILIC column) using the standard protocol (**Table 1**) which then gave the respective product as an amorphous white solid (0.85 mg, 57 % yield).

$^1\text{H}$  NMR (400 MHz,  $\text{D}_2\text{O}$ ):  $\delta$  7.84 (s, 3H, H-triazole), 7.63 – 7.49 (m, 6H, ) , 7.42 – 7.27 (m, 6H, , ) , 7.18 – 7.11 (m, 3H, ) , 4.60 – 4.54 (d,  $J = 12.6$  Hz, 3H, H-6a<sup>Glc</sup>), 4.44 (d,  $J = 12.6$  Hz, 3H, H-6b<sup>Glc</sup>), 4.38 – 4.27 (m, 6H,  $\text{CH}_2\text{N}$ ), 4.19 (d,  $J = 8.3$  Hz, 3H, H-1<sup>Glc</sup>), 4.06 (d,  $J = 7.8$  Hz, 3H, H-1<sup>Gal</sup>), 3.77 – 3.60 (m, 18H), 3.55 – 3.31 (m, 33H), 3.23 – 3.19 (m, 3H), 3.03 (t,  $J = 8.6$  Hz, 3H, H-2<sup>Glc</sup>), 2.55 (dd,  $J = 12.4, 4.6$  Hz, 3H, H-3<sub>eq</sub><sup>Sia</sup>), 2.29 (t,  $J = 11.6$  Hz, 6H,  $\text{COCH}_2$ ), 2.12 (t,  $J = 11.3$  Hz, 6H,  $\text{CCH}_2\text{C}$ ), 1.85 (s, 9H,  $\text{Ac}^{\text{Sia}}$ ), 1.55 (t,  $J = 12.0$  Hz, 3H, H-3<sub>ax</sub><sup>Sia</sup>). HRMS:  $m/z$  calcd. for  $\text{C}_{114}\text{H}_{159}\text{N}_{15}\text{O}_{60} [\text{M}+2\text{H}]^{2+}$  1349.9999, found 1349.9967.

### Trivalent-LacNAc-Lac substrate **22**

Compound **4** (0.82 mg, 1.2  $\mu\text{mol}$ ), **12** (4 mg, 5.4  $\mu\text{mol}$ , 4.5 equiv),  $\text{CuSO}_4 \cdot 5\text{H}_2\text{O}$  (12.5  $\mu\text{g}$ , 0.05  $\mu\text{mol}$ , 0.04 equiv), sodium L-ascorbate (0.5 mg, 2.5  $\mu\text{mol}$ , 2 equiv) and THPTA (50  $\mu\text{g}$ , 0.1  $\mu\text{mol}$ , 0.08 equiv) were dissolved in DMF/ $\text{H}_2\text{O}$  (1:2, 0.5 mL)<sup>33</sup>. The reaction was performed under microwave irradiation at 80  $^\circ\text{C}$  for 1.5 h.



Then the mixture was concentrated *in vacuo*. The reaction mixture was dissolved in water (50  $\mu$ L) and centrifuged. Then the supernatant was subjected to gel filtration over Bio-gel P-2 (eluent H<sub>2</sub>O). Fractions containing product were combined and lyophilized without further purification which gave the respective product as an amorphous white solid (2.2 mg, 63 % yield).

HRMS:  $m/z$  calcd. for C<sub>123</sub>H<sub>177</sub>N<sub>15</sub>O<sub>66</sub> [M+2H]<sup>2+</sup> 1461.0550, found 1461.0551.

### Trivalent- $\alpha$ 2,6Sia-LacNAc-Lac Ligand HAI-2

Compound **22** (1 mg, 0.34  $\mu$ mol) and CMP-NANA (2.2 mg, 3.4  $\mu$ mol, 10 equiv) were dissolved in Tris-HCl buffer (100 mM, pH 7.5, 200  $\mu$ L) containing MgCl<sub>2</sub> (20 mM). To this, PmST1 mutant P34H/M144L ( $\alpha$ 2-6sialyltransferase, 2.3 mg/mL, 20  $\mu$ L) was added. The resulting reaction mixture was incubated at 37 °C for 14 h. The reaction mixture was centrifuged and the supernatant subjected to gel filtration over Bio-gel P-2 (eluent H<sub>2</sub>O). Fractions containing product were combined and lyophilized for further preparative HPLC (HILIC column) using the standard protocol (**Table 2**) which then gave the respective product as an amorphous white solid (0.57 mg, 44 % yield).

<sup>1</sup>H NMR (600 MHz, D<sub>2</sub>O):  $\delta$  7.94 (s, 3H, H-triazole), 7.61 – 7.12 (m, 15H, H-phenyl), 4.70 (d, 3H, H6), 4.58 (d,  $J$  = 12.2 Hz, 3H, H6), 4.48 – 4.39 (m, 9H, H-1, CH<sub>2</sub>N), 4.34 (d,  $J$  = 7.9 Hz, 3H, H-1), 4.32 (d,  $J$  = 7.7 Hz, 3H, H-1<sup>Glc</sup>), 4.05 (d,  $J$  = 7.7 Hz, 3H, H-1), 3.94 – 3.28 (m, 90H), 3.27 – 3.21 (m, 3H), 3.08 (t,  $J$  = 17.4, 8.6 Hz, 3H, H-2<sup>Glc</sup>), 2.57 (dd,  $J$  = 12.4, 4.7 Hz, 3H, H-3<sup>Sia</sup><sub>eq</sub>), 2.39 – 2.26 (m, 6H, COCH<sub>2</sub>), 2.22 – 2.16 (m, 6H, CCH<sub>2</sub>C), 1.93 (s, 9H, Ac<sup>Sia</sup>), 1.91 (s, 9H, Ac), 1.62 (t,  $J$  = 12.2 Hz, 3H, H-3<sup>Sia</sup><sub>ax</sub>); <sup>13</sup>C NMR (151 MHz, D<sub>2</sub>O, extracted from HSQC):  $\delta$  125.3, 120.2, 109.3, 103.5, 103.0, 102.6, 101.7, 82.1, 80.4, 78.7, 74.7, 74.6, 73.8, 72.6, 72.5, 72.5, 71.7, 70.8, 69.7, 68.5, 68.4, 68.3, 68.2, 63.4, 62.8, 62.1, 60.9, 60.8, 60.2, 60.1, 54.9, 51.9, 51.8, 49.9, 40.1, 33.4, 25.3, 22.3, 22.1. HRMS:  $m/z$  calcd. for C<sub>156</sub>H<sub>228</sub>N<sub>18</sub>O<sub>90</sub> [M+2H]<sup>2+</sup> 1897.6982, found 1897.6985.

### Trivalent-LacNAc-Lac-triazole-phenyl-triazole substrate 23

Compound **4** (0.79 mg, 1.0  $\mu$ mol), **19** (6 mg, 7.0  $\mu$ mol, 7 equiv), CuSO<sub>4</sub> 5H<sub>2</sub>O (25  $\mu$ g, 0.1  $\mu$ mol, 0.1 equiv), sodium L-ascorbate (0.5 mg, 2.5  $\mu$ mol, 2.5 equiv) and THPTA (50  $\mu$ g, 0.1  $\mu$ mol, 0.1 equiv) were dissolved in DMF/H<sub>2</sub>O (1:2, 0.2 mL). The reaction was performed under microwave irradiation at 80 °C for 1.5 h. Then the mixture was concentrated *in vacuo*. The reaction mixture was dissolved in water (50  $\mu$ L) and centrifuged. Then the supernatant was subjected to gel filtration

over Bio-gel P-2 (eluent H<sub>2</sub>O). Fractions containing product were combined and lyophilized without further purification which gave the respective product as an amorphous white solid (2.5 mg, 77 % yield).

HRMS:  $m/z$  calcd. for C<sub>144</sub>H<sub>186</sub>N<sub>24</sub>O<sub>63</sub> [M+3H]<sup>3+</sup> 1087.4102, found 1087.4070.

### **Trivalent- & divalent- $\alpha$ 2,6Sia-LacNAc-Lac-triazole-phenyl-triazole Ligands HAI-3 & -4**

Compound **23** (2.5 mg, 0.77  $\mu$ mol) and CMP-NANA (2.9 mg, 4.6  $\mu$ mol, 6 equiv) were dissolved in Tris-HCl buffer (100 mM, pH 7.5, 300  $\mu$ L) containing MgCl<sub>2</sub> (20 mM). To this, PmST1 mutant P34H/M144L ( $\alpha$ 2-6sialyltransferase, 2.3 mg/mL, 50  $\mu$ L) was added. The resulting reaction mixture was incubated at 37 °C for 4 h. The reaction mixture was centrifuged and the supernatant subjected to gel filtration over Bio-gel P-2 (eluent H<sub>2</sub>O). Fractions containing product were combined and lyophilized for further preparative HPLC (HILIC column) using the standard protocol (**Table 3**) which then gave the respective products as amorphous white solids.

**HAI-3** (0.38 mg, 12 % yield): <sup>1</sup>H NMR (600 MHz, D<sub>2</sub>O):  $\delta$  8.10 (s, 1H, H-triazole), 8.20 – 6.72 (m, 30H, H-triazole, H-phenyl), 5.32 (s, 3H, H-1<sup>Glc</sup>), 4.42 – 4.36 (m, 9H), 4.14 – 3.41 (m, 99H), 2.65 – 2.32 (m, 9H), 1.98 – 1.94 (m, 24H), 1.66 (t,  $J$  = 12.3 Hz, 3H, H-3<sub>ax</sub><sup>Sia</sup>). HRMS:  $m/z$  calcd. for C<sub>177</sub>H<sub>237</sub>N<sub>27</sub>O<sub>87</sub> [M+3H]<sup>3+</sup> 1378.5056, found 1378.5057.

**HAI-4** (0.86 mg, 27 % yield): <sup>1</sup>H NMR (600 MHz, D<sub>2</sub>O):  $\delta$  4.37 (s, 6H), 4.15 – 3.24 (m, 92H), 2.64 – 2.56 (m, 2H, H-3<sub>eq</sub><sup>Sia</sup>), 2.07 – 1.84 (m, 27H), 1.70 – 1.60 (m, 2H, H-3<sub>ax</sub><sup>Sia</sup>). HRMS:  $m/z$  calcd. for C<sub>166</sub>H<sub>220</sub>N<sub>26</sub>O<sub>79</sub> [M+3H]<sup>3+</sup> 1281.4738, found 1281.4747.

### **Divalent-Lac-triazole-Glc-triazole-phenyl substrate 25**

Compound **24** (10 mg, 17  $\mu$ mol), propargyllactoside **10** (9.7 mg, 25.5  $\mu$ mol, 1.5 equiv), CuSO<sub>4</sub> 5H<sub>2</sub>O (0.4 mg, 1.7  $\mu$ mol, 0.1 equiv), sodium L-ascorbate (8.4 mg, 42.5  $\mu$ mol, 2.5 equiv) and THPTA (0.7 mg, 1.7  $\mu$ mol, 0.1 equiv) were dissolved in DMF/H<sub>2</sub>O (1:2, 0.5 mL). The reaction was performed under microwave irradiation at 80 °C for 1.5 h. The completion of the reaction was analyzed by TLC (DCM/MeOH 4:1 v/v). Then the mixture was concentrated *in vacuo*. The reaction mixture was dissolved in water (50  $\mu$ L) and centrifuged. Then the supernatant was subjected to gel filtration over Bio-gel P-2 (eluent H<sub>2</sub>O). Fractions containing

product were combined and lyophilized without further purification which gave the respective product as an amorphous white solid (18 mg, 79 % yield).

<sup>1</sup>H NMR (400 MHz, D<sub>2</sub>O): δ 8.38 (s, 2H, H-triazole), 8.24 (s, 2H, H-triazole), 7.74 (s, 4H, H-phenyl), 5.89 (d, *J* = 9.1 Hz, 2H, H-1<sup>Glc</sup>), 4.89 (d, *J* = 12.8 Hz, 2H, CCH<sub>2</sub>a), 4.83 – 4.74 (m, 4H, CCH<sub>2</sub>b, H-4<sup>Glc</sup>), 4.46 (d, *J* = 8.0 Hz, 2H, H-1<sup>Glc'</sup>), 4.35 (t, *J* = 9.8 Hz, 2H), 4.29 (d, *J* = 7.8 Hz, 2H, H-1<sup>Gal</sup>), 4.12 (t, *J* = 9.2 Hz, 2H, H-2<sup>Glc</sup>), 3.81 (d, *J* = 12.8 Hz, 2H), 3.76 (d, *J* = 3.4 Hz, 2H), 3.69 – 3.43 (m, 18H), 3.38 (dd, *J* = 10.0, 7.7 Hz, 2H, H-2<sup>Gal</sup>), 3.24 – 3.15 (m, 4H, H-2<sup>Glc'</sup>, H6); <sup>13</sup>C NMR (101 MHz, D<sub>2</sub>O, extracted from HSQC): δ 126.3, 124.7, 122.6, 102.8(C-1<sup>Gal</sup>), 101.3(C-1<sup>Glc'</sup>), 87.4 (C-1<sup>Glc</sup>), 78.2, 76.9, 76.9, 75.3, 74.6, 74.3, 73.5, 72.6, 72.5, 72.5, 70.9, 70.9, 68.5, 62.0, 61.9, 61.2, 60.9, 59.9, 59.6. HRMS: *m/z* calcd. for C<sub>52</sub>H<sub>74</sub>N<sub>12</sub>O<sub>30</sub> [M+H]<sup>+</sup> 1347.4707, found 1347.4707.

### Divalent-α2,6Sia-Lac-trizole-Glc-triazole-phenyl Ligand HAI-5

Compound **25** (3.5 mg, 2.6 μmol) and CMP-NANA (5 mg, 7.8 μmol, 3 equiv) were dissolved in Tris-HCl buffer (100 mM, pH 8.0, 500 μL) containing MgCl<sub>2</sub> (20 mM). To this, PmST1 mutant P34H/M144L (α2-6sialyltransferase, 2.3 mg/mL, 50 μL) was added. The resulting reaction mixture was incubated at 37 °C for 4 h. The reaction mixture was centrifuged and the supernatant subjected to gel filtration over Bio-gel P-2 (eluent H<sub>2</sub>O). Fractions containing product were combined and lyophilized for further preparative HPLC (HILIC column) using the standard protocol (**Table 3**) which then gave the respective product as an amorphous white solid (2.6 mg, 52 % yield).

<sup>1</sup>H NMR (600 MHz, D<sub>2</sub>O): δ 8.50 (s, 2H, H-triazole), 8.33 (s, 2H, H-triazole), 7.89 (s, 4H, H-phenyl), 5.97 (d, *J* = 9.2 Hz, 2H, H-1<sup>Glc</sup>), 4.97 (d, *J* = 12.9 Hz, 2H, CCH<sub>2</sub>a), 4.91 – 4.85 (m, 4H, CCH<sub>2</sub>b, H-4<sup>Glc</sup>), 4.54 (d, *J* = 8.0 Hz, 2H, H-1<sup>Glc'</sup>), 4.45 – 4.39 (m, 4H), 4.33 (d, *J* = 7.9 Hz, 2H, H-1<sup>Gal</sup>), 4.20 (t, *J* = 9.2 Hz, 2H, H-2<sup>Glc</sup>), 3.90 – 3.85 (m, 4H), 3.83 (d, *J* = 3.5 Hz, 2H), 3.80 – 3.70 (m, 10H), 3.62 (dd, *J* = 10.4, 1.9 Hz, 2H), 3.60 – 3.52 (m, 14H), 3.50 (dd, *J* = 10.7, 4.0 Hz, 2H), 3.46 (dd, *J* = 9.1, 1.9 Hz, 2H), 3.43 (dd, *J* = 10.1, 7.9 Hz, 2H), 3.33 – 3.26 (m, 4H, H-2<sup>Glc'</sup>, H6), 2.61 (dd, *J* = 12.4, 4.7 Hz, 2H, H-3<sub>eq</sub><sup>Sia</sup>), 1.92 (s, 6H, Ac<sup>Sia</sup>), 1.64 (t, *J* = 12.2 Hz, 2H, H-3<sub>ax</sub><sup>Sia</sup>); <sup>13</sup>C NMR (151 MHz, D<sub>2</sub>O, extracted from HSQC): δ 126.5, 124.7, 122.7, 103.2(C-1<sup>Gal</sup>), 101.3(C-1<sup>Glc'</sup>), 87.4(C-1<sup>Glc</sup>), 79.5, 77.0, 74.6, 73.7, 73.6, 72.7, 72.6, 72.5, 72.4, 71.8, 70.8, 70.0, 68.5, 68.4, 68.4, 67.0, 63.6, 63.5, 62.7, 62.0, 61.5, 60.2, 59.7, 59.7, 51.8, 51.7, 40.2, 40.1, 22.1(CH<sub>3</sub>CO). HRMS: *m/z* calcd. for C<sub>74</sub>H<sub>108</sub>N<sub>14</sub>O<sub>46</sub> [M+2H]<sup>2+</sup> 965.3344, found 965.3341.

## Divalent-LacNAc-Lac-triazole-Glc-triazole-phenyl substrate 26

Compound **24** (0.66 mg, 1.1  $\mu\text{mol}$ ), **12** (2.5 mg, 3.3  $\mu\text{mol}$ , 3 equiv),  $\text{CuSO}_4 \cdot 5\text{H}_2\text{O}$  (25  $\mu\text{g}$ , 0.1  $\mu\text{mol}$ , 0.1 equiv), sodium L-ascorbate (0.5 mg, 2.5  $\mu\text{mol}$ , 2.5 equiv) and THPTA (50  $\mu\text{g}$ , 0.1  $\mu\text{mol}$ , 0.1 equiv) were dissolved in DMF/ $\text{H}_2\text{O}$  (1:2, 300  $\mu\text{L}$ ). The reaction was performed under microwave irradiation at 80  $^\circ\text{C}$  for 1.5 h. The completion of the reaction was analyzed by TLC (DCM/methanol 4:1 v/v). Then the mixture was concentrated *in vacuo*. The reaction mixture was dissolved in water (50  $\mu\text{L}$ ) and centrifuged. Then the supernatant was subjected to gel filtration over Bio-gel P-2 (eluent  $\text{H}_2\text{O}$ ). Fractions containing product were combined and lyophilized for further preparative HPLC (HILIC column) using the standard protocol (**Table 3**) which gave the respective product as an amorphous white solid (2 mg, 87 % yield).

$^1\text{H}$  NMR (600 MHz,  $\text{D}_2\text{O}$ ):  $\delta$  8.50 (s, 2H, H-triazole), 8.32 (s, 2H, H-triazole), 7.90 (s, 4H, H-phenyl), 5.98 (d,  $J = 9.7$  Hz, 2H, H-1<sup>Glc</sup>), 4.97 (d,  $J = 12.6$  Hz, 2H, CCH<sub>2</sub>a), 4.89 – 4.84 (m, 4H, CCH<sub>2</sub>b, H-4<sup>Glc</sup>), 4.60 (d,  $J = 8.3$  Hz, 2H, H-1<sup>GlcNAc</sup>), 4.53 (d,  $J = 8.1$  Hz, 2H, H-1<sup>Glc'</sup>), 4.46 – 4.40 (m, 4H), 4.38 (d,  $J = 7.7$  Hz, 2H, H-1<sup>Gal'</sup>), 4.34 (d,  $J = 8.0$  Hz, 2H, H-1<sup>Gal</sup>), 4.20 (t,  $J = 9.2$  Hz, 2H, H-2<sup>Glc</sup>), 4.06 (d,  $J = 3.0$  Hz, 2H), 3.89 – 3.84 (m, 4H), 3.83 – 3.82 (d,  $J = 3.3$  Hz, 2H), 3.77 – 3.46 (m, 42H), 3.44 (dd,  $J = 8.0, 2.0$  Hz, 2H, H-2<sup>Gal'</sup>), 3.57 – 3.41 (m, 2H), 3.30 (dd,  $J = 13.3, 4.1$  Hz, 2H), 3.26 (t,  $J = 8.3$  Hz, 2H, H-2<sup>Glc'</sup>), 1.94 (s, 6H, Ac);  $^{13}\text{C}$  NMR (151 MHz,  $\text{D}_2\text{O}$ , extracted from HSQC):  $\delta$  126.6, 124.7, 122.7, 102.9(C-1<sup>Gal</sup>), 102.9(C-1<sup>Gal'</sup>), 102.8(C-1<sup>GlcNAc</sup>), 101.4(C-1<sup>Glc'</sup>), 87.4(C-1<sup>Glc</sup>), 82.1, 78.3, 78.2, 77.0, 75.2, 74.8, 74.6, 74.5, 73.6, 72.8, 72.6, 72.5, 72.2, 71.0, 70.0, 68.6, 68.4, 62.1, 62.1, 61.5, 61.0, 60.0, 59.9, 59.8, 59.7, 55.2, 22.2(CH<sub>3</sub>CO). HRMS:  $m/z$  calcd. for  $\text{C}_{80}\text{H}_{120}\text{N}_{14}\text{O}_{50}$  [M+2H]<sup>2+</sup> 1039.3712, found 1039.3714.

## Divalent- $\alpha$ 2,6Sia-LacNAc-Lac-triazole-Glc-triazole-phenyl Ligand HAI-6

Compound **26** (1 mg, 0.48  $\mu\text{mol}$ ) and CMP-NANA (1.2 mg, 1.9  $\mu\text{mol}$ , 4 equiv) were dissolved in Tris-HCl buffer (100 mM, pH 7.5, 500  $\mu\text{L}$ ) containing  $\text{MgCl}_2$  (20 mM). To this, PmST1 mutant P34H/M144L ( $\alpha$ 2-6sialyltransferase, 2.3 mg/mL, 50  $\mu\text{L}$ ) was added. The resulting reaction mixture was incubated at 37  $^\circ\text{C}$  for 4 h. The reaction mixture was centrifuged and the supernatant subjected to gel filtration over Bio-gel P-2 (eluent  $\text{H}_2\text{O}$ ). Fractions containing product were combined and lyophilized for further preparative HPLC (HILIC column) using the standard protocol (**Table 4**) which then gave the respective product as an amorphous white solid (0.7 mg, 55 % yield).

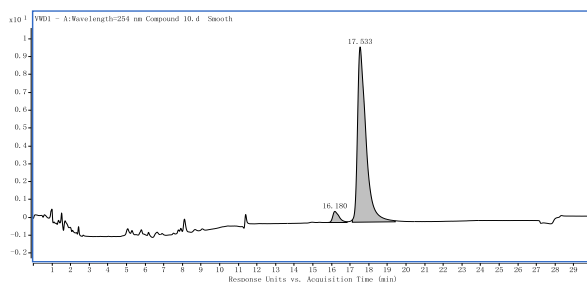
$^1\text{H}$  NMR (600 MHz,  $\text{D}_2\text{O}$ ):  $\delta$  8.50 (s, 2H, H-triazole), 8.32 (s, 2H, H-triazole), 7.91 (s, 4H, H-phenyl), 5.98 (d,  $J = 9.0$  Hz, 2H, H-1<sup>Glc</sup>), 4.97 (d,  $J = 12.8$  Hz, 2H), 4.87 (m, 4H), 4.63 (d,  $J = 7.2$  Hz, 2H, H-1<sup>GlcNAc</sup>), 4.54 (d,  $J = 8.2$  Hz, 2H, H-1<sup>Glc'</sup>), 4.47 – 4.39 (m, 4H), 4.38 – 4.31 (m, 4H, H-1<sup>Gal</sup>, H-1<sup>Gal'</sup>), 4.18 (t,  $J = 9.2$  Hz, 2H, H-2<sup>Glc</sup>), 4.06 – 4.02 (m, 4H), 3.92 – 3.40 (m, 72H), 3.31 – 3.24 (m, 6H), 2.57 (dd,  $J = 13.0, 3.7$  Hz, 2H, H-3<sub>eq</sub><sup>Sia</sup>), 1.96 (s, 6H, Ac), 1.93 (s, 6H, Ac<sup>Sia</sup>), 1.62 (t,  $J = 12.1$  Hz, 2H, H-3<sub>ax</sub><sup>Sia</sup>). HRMS:  $m/z$  calcd. for  $\text{C}_{102}\text{H}_{154}\text{N}_{16}\text{O}_{66}$   $[\text{M}+2\text{H}]^{2+}$  1330.4666, found 1330.4673.

### $\alpha$ 2,6Sia-LacNAc-dextran HAI-7

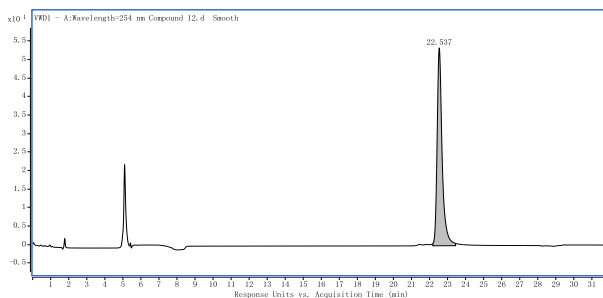
The azido polymer was dissolved in water followed by the addition of compound **8** (3 mg, 1.3 equiv).  $\text{CuSO}_4 \cdot 5\text{H}_2\text{O}$  (0.1 equiv) and sodium L-ascorbate (0.3 equiv) were dissolved in water separately and added to the reaction mixture. The reaction was carried out at 100 °C with microwave radiation for 60 min. The solvent was evaporated and the crude reaction mixture was purified by dialysis using a cellulose based dialysis cassette (MWCO: 2K) against deionized water for 3-4 days and freeze dried to give a white compound (3 mg, 24 %). The disappearance of the azide stretching peak in the IR spectra of the final compound confirmed that all of the azido groups had reacted.

### 3.4.3 Other HPLC spectra of the HA inhibitors

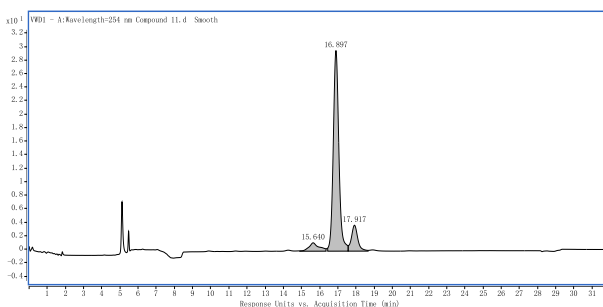
#### HAI-1 (95.8 %)



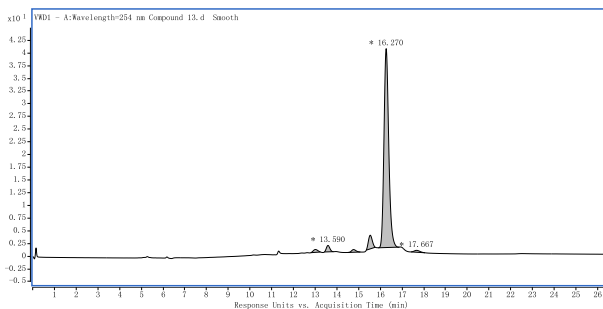
## HAI-2 (99.9 %)



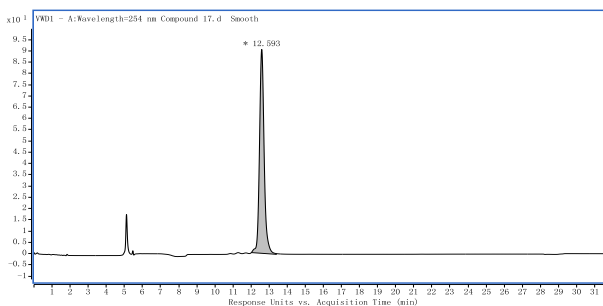
## Tri-LacNAc-Lac substrate 22 (86.5 %)



## Tri-LacNAc-Lac-triazole-phenyl substrate 23 (89.6 %)



## HAI-5 (99.9 %)



## References

- 1 C. Fasting, C. A. Schalley, M. Weber, O. Seitz, S. Hecht, B. Kokschi, J. Dervede, C. Graf, E. W. Knapp and R. Haag, Multivalency as a chemical organization and action principle, *Angew. Chemie - Int. Ed.*, 2012, **51**, 10472–10498.
- 2 S. Bhatia, L. C. Camacho and R. Haag, Pathogen inhibition by multivalent ligand architectures, *J. Am. Chem. Soc.*, 2016, **138**, 8654–8666.
- 3 M. Mammen, S. K. Choi and G. M. Whitesides, Polyvalent interactions in biological systems: Implications for design and use of multivalent ligands and inhibitors, *Angew. Chem. Int. Ed.*, 1998, **37**, 2754–2794.
- 4 S. Cecioni, A. Imberty and S. Vidal, Glycomimetics versus multivalent glycoconjugates for the design of high affinity lectin ligands, *Chem. Rev.*, 2015, **115**, 525–561.
- 5 V. Wittmann and R. J. Pieters, Bridging lectin binding sites by multivalent carbohydrates, *Chem. Soc. Rev.*, 2013, **42**, 4492–4503.
- 6 A. Bernardi, J. Jiménez-Barbero, A. Casnati, C. De Castro, T. Darbre, F. Fieschi, J. Finne, H. Funken, K.-E. Jaeger, M. Lahmann, T. K. Lindhorst, M. Marradi, P. Messner, A. Molinaro, P. V. Murphy, C. Nativi, S. Oscarson, S. Penadés, F. Peri, R. J. Pieters, O. Renaudet, J.-L. Reymond, B. Richichi, J. Rojo, F. Sansone, C. Schäffer, W. B. Turnbull, T. Velasco-Torrijos, S. Vidal, S. Vincent, T. Wennekes, H. Zuilhof and A. Imberty, Multivalent glycoconjugates as anti-pathogenic agents., *Chem. Soc. Rev.*, 2013, **42**, 4709–27.
- 7 L. L. Kiessling, J. E. Gestwicki and L. E. Strong, Synthetic multivalent ligands as probes of signal transduction, *Angew. Chem. Int. Ed. Engl.*, 2006, **45**, 2348–2368.
- 8 R. J. Pieters, Maximising multivalency effects in protein-carbohydrate interactions, *Org. Biomol. Chem.*, 2009, **7**, 2013–2025.
- 9 M. N. Matrosovich, L. V. Mochalova, V. P. Marinina, N. E. Byramova and N. V. Bovin, Synthetic polymeric inhibitors of influenza virus receptor-binding activity suppress virus replication, *FEBS Lett.*, 1990, **272**, 209–21.
- 10 W. J. Lees, A. Spaltenstein, J. E. Kingery-Wood and G. M. Whitesides, Polyacrylamides bearing pendant  $\alpha$ -sialoside groups strongly inhibit agglutination of erythrocytes by influenza A virus: Multivalency and steric stabilization of particulate biological systems, *J. Med. Chem.*, 1994, **37**, 3419–3433.
- 11 S. K. Choi, M. Mammen and G. M. Whitesides, Generation and in situ evaluation of libraries of poly(acrylic acid) presenting sialosides as side chains as polyvalent inhibitors of influenza-mediated hemagglutination, *J. Am. Chem. Soc.*, 1997, **119**, 4103–4111.
- 12 H. Kamitakahara, T. Suzuki, Y. Suzuki, O. Kanie and C. Wong, A Lysoganglioside / Poly- l -glutamic Acid, *Angew. Chemie Int. Ed.*, 1998, **37**, 1524–1528.
- 13 I. Papp, C. Sieben, A. L. Sisson, J. Kostka, C. Bötcher, K. Ludwig, A. Herrmann and R. Haag, Inhibition of influenza virus activity by multivalent glycoarchitectures with matched sizes, *ChemBioChem*, 2011, **12**, 887–895.

- 14 S. Bhatia, D. Lauster, M. Bardua, K. Ludwig, S. Angioletti-Uberti, N. Popp, U. Hoffmann, F. Paulus, M. Budt, M. Stadtmüller, T. Wolff, A. Hamann, C. Böttcher, A. Herrmann and R. Haag, Linear polysialoside outperforms dendritic analogs for inhibition of influenza virus infection *in vitro* and *in vivo*, *Biomaterials*, 2017, **138**, 22–34.
- 15 X. Li, P. Wu, G. F. Gao and S. Cheng, Carbohydrate-functionalized chitosan fiber for influenza virus capture, *Biomacromolecules*, 2011, **12**, 3962–3969.
- 16 H. W. Yeh, T. S. Lin, H. W. Wang, H. W. Cheng, D. Z. Liu and P. H. Liang, S-Linked sialyloligosaccharides bearing liposomes and micelles as influenza virus inhibitors, *Org. Biomol. Chem.*, 2015, **13**, 11518–11528.
- 17 G. D. Glick and J. R. Knowles, Molecular recognition of bivalent sialosides by influenza virus, *J. Am. Chem. Soc.*, 1991, **113**, 4701–4703.
- 18 S. Sabesan, J. O. Duss, P. Domaille, S. Kelm and J. C. Paulson, Synthesis of cluster sialoside inhibitors for influenza virus, *J. Am. Chem. Soc.*, 1991, **113**, 5865–5866.
- 19 R. Roy, D. Zanini, S. J. Meunier and A. Romanowska, Solid-phase synthesis of dendritic sialoside inhibitors of influenza A virus hemagglutinin, *Chem. Commun.*, 1993, 1869–1872.
- 20 T. Ohta, N. Miura, N. Fujitani, F. Nakajima, K. Niikura, R. Sadamoto, C. T. Guo, T. Suzuki, Y. Suzuki, K. Monde and S. I. Nishimura, Glycotentacles: Synthesis of cyclic glycopeptides, toward a tailored blocker of influenza virus hemagglutinin, *Angew. Chemie-Int. Ed.*, 2003, **42**, 5186–5189.
- 21 A. Marra, L. Moni, D. Pazzi, A. Corallini, D. Bridi and A. Dondoni, Synthesis of sialoclusters appended to calix[4]arene platforms via multiple azide-alkyne cycloaddition. New inhibitors of hemagglutination and cytopathic effect mediated by BK and influenza A viruses, *Org. Biomol. Chem.*, 2008, **6**, 1396–1409.
- 22 F. Feng, N. Miura, N. Isoda, Y. Sakoda, M. Okamoto, H. Kida and S.-I. Nishimura, Novel trivalent anti-influenza reagent, *Bioorg. Med. Chem. Lett.*
- 23 M. Waldmann, R. Jirmann, K. Hoelscher, M. Wienke, F. C. Niemeyer, D. Rehders and B. Meyer, A nanomolar multivalent ligand as entry inhibitor of the hemagglutinin of avian influenza, *J. Am. Chem. Soc.*, 2014, **136**, 783–788.
- 24 M. Yamabe, K. Kaihatsu and Y. Ebara, Sialyllactose-modified three-way junction DNA as binding inhibitor of influenza virus hemagglutinin, *Bioconjug. Chem.*, 2018, **29**, 1490–1494.
- 25 V. Bandlow, S. Liese, D. Lauster, K. Ludwig, R. R. Netz, A. Herrmann and O. Seitz, Spatial screening of hemagglutinin on Influenza A Virus particles: Sialyl-LacNAc displays on DNA and PEG scaffolds reveal the requirements for bivalency enhanced interactions with weak monovalent binders, *J. Am. Chem. Soc.*, 2017, **139**, 16389–16397.
- 26 W. Peng, R. P. de Vries, O. C. Grant, A. J. Thompson, R. McBride, B. Tsogtbaatar, P. S. Lee, N. Razi, I. A. Wilson, R. J. Woods and J. C. Paulson, Recent H3N2 viruses have evolved specificity for extended, branched human-type receptors, conferring potential for increased avidity, *Cell Host Microbe*, 2017, **21**, 23–34.



- 27 Y. Ji, Y. J. White, J. A. Hadden, O. C. Grant and R. J. Woods, New insights into influenza A specificity: an evolution of paradigms, *Curr. Opin. Struct. Biol.*, 2017, **44**, 219–231.
- 28 J. B. McArthur, H. Yu, J. Zeng and X. Chen, Converting *Pasteurella multocida*  $\alpha$ 2-3-sialyltransferase 1 (PmST1) to a regioselective  $\alpha$ 2-6-sialyltransferase by saturation mutagenesis and regioselective screening, *Org. Biomol. Chem.*, 2017, **15**, 1700–1709.
- 29 H. Yu, H. A. Chokhawala, S. Huang and X. Chen, One-pot three-enzyme chemoenzymatic approach to the synthesis of sialosides containing natural and non-natural functionalities, *Nat. Protoc.*, 2006, **1**, 2485–2492.
- 30 W. Peng, J. Pranskevich, C. Nycholat, M. Gilbert, W. Wakarchuk, J. C. Paulson and N. Razi, *Helicobacter pylori* 1,3-N-acetylglucosaminyltransferase for versatile synthesis of type 1 and type 2 poly-LacNAcs on N-linked, O-linked and I-antigen glycans, *Glycobiology*, 2012, **22**, 1453–1464.
- 31 O. Blixt, J. Brown, M. J. Schur, W. Wakarchuk and J. C. Paulson, Efficient preparation of natural and synthetic galactosides with a recombinant  $\beta$ -1,4-galactosyltransferase-/UDP-4'-gal epimerase fusion protein, *J. Org. Chem.*, 2001, **66**, 2442–2448.
- 32 V. Hong, S. I. Presolski, C. Ma and M. G. Finn, Analysis and optimization of copper-catalyzed azide-alkyne cycloaddition for bioconjugation, *Angew. Chemie - Int. Ed.*, 2009, **48**, 9879–9883.
- 33 S. I. Presolski, V. Hong, S. Cho and M. G. Finn, Tailored ligand acceleration of the Cu-catalyzed azide-alkyne cycloaddition reaction: Practical and mechanistic implications, *J. Am. Chem. Soc.*, 2010, **132**, 14570–14576.
- 34 F. Pertici, N. J. De Mol, J. Kemmink, R. J. Pieters and N. J. de Mol, Optimizing divalent inhibitors of *Pseudomonas aeruginosa* lectin leca by using a rigid spacer, *Chem. Eur. J.*, 2013, **19**, 16923–16927.
- 35 C. M. Nycholat, R. McBride, D. C. Ekiert, R. Xu, J. Rangarajan, W. Peng, N. Razi, M. Gilbert, W. Wakarchuk, I. A. Wilson and J. C. Paulson, Recognition of sialylated poly-N-acetylglucosamine chains on N- and O-linked glycans by human and avian influenza A virus hemagglutinins, *Angew. Chemie - Int. Ed.*, 2012, **51**, 4860–4863.
- 36 D. Haksar, E. de Poel, L. H. C. Quarles van Ufford, S. Bhatia, R. Haag, J. M. Beekman and R. J. Pieters, Strong inhibition of cholera toxin B subunit by affordable, polymer-based multivalent inhibitors, *Bioconjug. Chem.*, 2019, acs.bioconjchem.8b00902.



# *Chapter 4*

*Evaluation of the di- & trivalent hemagglutinin  
inhibitors of Influenza A virus*

## 4.1 Introduction

Influenza A virus (IAV) causes the flu and poses a serious threat in a variety of hosts, like humans, swine, wild water fowl and poultry. The interaction between IAV and infectious receptors is a crucial factor of host, tissue and cell specificity. IAV contains two major virulence factors on its surface, that both bind to sialylated glycans. The hemagglutinin (HA) is responsible for attachment of the virus to the tissue surface to be infected, and its specificity lies at the origin of the species specificity and tissue tropism of the virus and is also of importance for the viral fusion with the endosome.<sup>1</sup> The neuraminidase (NA) is a glycosidase enzyme that removes the sialic acid group from glycans which leads to a release of the HA-based attachment and allows the virus to burrow through the protective mucosa and enter the cell. A high HA-receptor density and high binding affinity are considered to be prime requirements for an efficient primary interaction leading to a productive infection. The binding between an HA binding site and a sialic acid molecules is usually weak ( $K_D \sim 0.3-3$  mM), while multivalent interactions between them at the contact surface ensures the viral adhesion to the host cell with high avidity.

Several examples of multivalent sialic acid containing glycans that have anti-HA effects have been reported. Relatively large molecular entities can take advantage of their size to bridge multiple HA trimers simultaneously. Some of these have yielded potency enhancements of 3-4 orders of magnitude. Small molecules that were designed based on the structure of a single HA trimer are also being investigated for potent inhibitory effects. Besides the development of optimal molecular designs to inhibit HA, effective methods to evaluate the inhibition activities are also crucial for the research. The study of molecular binding processes is a key aspect in many fields of chemical research. Determining which molecules interact, how they interact, and why they interact can ultimately lead to more effective drugs. There are a variety of different methods that have been developed to study HA protein specificity and activity independently, as well to a limited extent in the context of the virus particle.

The hemagglutination inhibition assay (HAI), developed in 1942,<sup>2</sup> measures the agglutination of red blood cells (RBC) by virus particles and allows to estimate the number of virus particles and enable the study of virus binding properties. Interaction between virus and carbohydrates on the surface of the erythrocytes in solution leads to the formation of an extended, cross-linked gel (hemagglutination). The HAI assay measures the ability of an inhibitor to prevent hemagglutination by

the inhibitor binding to the viral surface. This widely and most commonly used assay is fast and requires little instrumentation. Reproducibility depends on controlled experimental conditions, such as temperature, incubation time, and the type of RBC. Inhibitors like  $\alpha$ -sialoside linked biotin-labeled polyacrylamides,<sup>3</sup> C-3-modified sialoside Neu5Ac3 $\alpha$ F-DSPE (distearoyl phosphoethanolamine),<sup>4</sup> peptide derived from the fibroblast growth factor 4 (FGF-4) signal sequence,<sup>5</sup> multivalent S-sialoside Human Serum Albumin (HSA) and Bovine Serum Albumin (BSA) conjugates,<sup>6</sup> multivalent peptide-nanoparticle conjugates<sup>7</sup> were all evaluated by HAIs which showed promising results in these studies.

The enzyme-linked immunosorbent assay (ELISA) is a commonly used analytical biochemistry assay, which uses a solid-phase enzyme immuneassay (EIA) to detect the presence of a protein in a liquid sample using antibodies directed against the protein to be measured. This method has been developed to study the IAV-receptor interactions as well.<sup>8</sup> Viruses can be immobilized on microtiter plates and evaluated for their binding to sialylated glycans and also the other way around.<sup>9</sup> This ELISA-based assay is also well suited to study binding specificities towards  $\alpha$ -2,3- or  $\alpha$ -2,6-sialylated glycans.

More recently, in order to investigate glycan binding properties of cell surface lectins, glycan microarray technology has been developed and is now widely used.<sup>10</sup> Binding of lectins is monitored by using labelled versions of the lectins, or using fluorescently labeled antibodies that detect the lectins, followed by image acquisition on a confocal scanner. Similar to the ELISA assay, the glycan microarray is useful for the analysis of receptor binding for both whole viruses and recombinant HA proteins.<sup>10</sup> Paulson's group used this technology to investigate the binding properties of a series of sialylated poly-N-acetylglucosamine chains on N- and O-linked glycans<sup>11</sup> which provided inspiration for our own designs of HA inhibitors. However, the use of viruses in the assay has drawbacks such as the binding influence caused by the viral NA activity, although this can be blocked by a neuraminidase inhibitor. Furthermore, there is a difference in the density of glycans displayed on an array surface compared to on a tissue surface *in vivo*.

Despite these methods for HA binding specificity and activity, there are also methods developed for kinetic analysis of HA and NA activities. Surface plasmon resonance (SPR) enables highly sensitive, label-free detection and real-time monitoring in the determination of kinetic rate constants which was shown to be an effective assay for studying receptor-ligand interactions. Synthetic glycans or glycoproteins were immobilized on a surface in a flow-cell, after which IAV binding and release was studied in a real-time analysis.<sup>12</sup> Waldmann and coworkers

used SPR technology to determine the apparent dissociation constant  $K_D$  of their most potent HA inhibitor which was 450 nM.<sup>13</sup> Their research on trivalent glycopeptide is one of several aiming to reach the three binding sites of HA (see **chapter 1**).

Bio-layer interferometry (BLI) provides a recently developed alternative for real-time interaction studies.<sup>14</sup> Like SPR spectroscopy, BLI is also a label-free technology for measuring biomolecular interactions. It is an optical analytical technique that analyzes the interference pattern reflected from two surfaces: a layer of immobilized protein on the biosensor tip, and an internal reference layer. Any change in the number of molecules bound to the biosensor tip causes a shift in the interference pattern that can be measured in real-time. This technique provides the ability to monitor binding specificity, rates of association and dissociation, or concentration with precision and accuracy. Wright and coworkers used BLI to evaluate analogs of antiviral drug Arbidol<sup>®</sup> which has a  $K_D$  for HA of 0.08  $\mu$ M.<sup>15</sup>

In this chapter, we focused on the evaluation of the di- & trivalent hemagglutinin inhibitors that have been described in **Chapter 3**, with the technology of a BLI binding assay, an HAI assay and an infection-inhibition experiment. The results of the analysis are discussed with respect to the structural features of the inhibitors.

The evaluation of the potential HA inhibitors was performed at and by our collaborators from the Department of Infectious Diseases and Immunology of Faculty of Veterinary Medicine, Utrecht University. Experimental details are provided so the results can be evaluated and discussed within the right context.

## **4.2 Materials and Methods**

### **4.2.1 Recombinant viruses**

Influenza virus WU95 and VI75 contain the HA gene of A/Netherlands/178/95 H3N2 or A/Bilthoven/1761/76 H3N2, respectively, in the background of A/Puerto Rico/8/34/Mount Sinai H1N1 (Taxonomy ID: 183764). Generation of these viruses has been described previously<sup>16</sup>. Viruses were grown in MDCK-II cells (ATCC) as described previously<sup>17</sup> and stored aliquoted at -80 °C until use.

### **4.2.2 Chemicals**

All compounds for the assays were synthesized in house as described in **Chapter 2 & 3**, and purified by preparative HPLC using a HILIC column and obtained in

good purities. Oseltamivir carboxylate (OC) was obtained from Roche, dissolved in DMSO at 100 nM concentration, aliquoted and stored at -20 °C.

<sup>1</sup>H NMR for quantitative analysis was used to determine the exact amount of the inhibitors we obtained in chapter 3 to be used in the assays, which was used because the quantities of the inhibitors were small. An exact amount of 1-propanol was added to a solution of the respective ligand in D<sub>2</sub>O. Then a measurement was performed by <sup>1</sup>H NMR. By integrating the CH<sub>3</sub> signal of 1-propanol and the axial H-3 signal of the sialic acid part of the ligand (**Figure 1**), we could determine the concentration of the ligands.

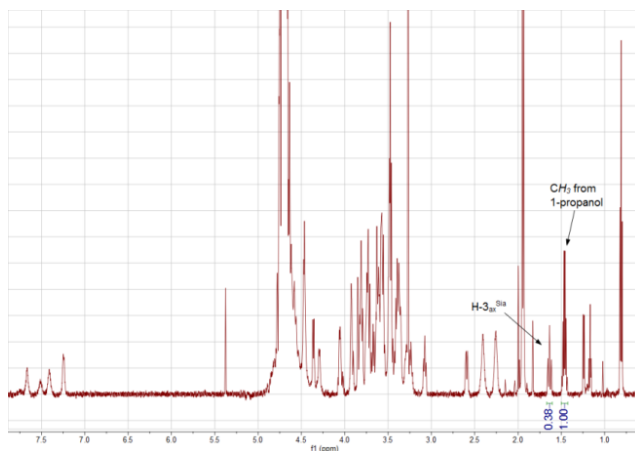


**Figure 1.** Quantitative analysis of multivalent inhibitor **HAI-2** by <sup>1</sup>H NMR.

#### 4.2.2 Bio-layer interferometry (BLI) binding assay

All BLI experiments were carried out using Octet Red384 (Fortebio) and initial binding rates were determined similarly as described previously.<sup>18</sup> In short, standard streptavidin sensors were loaded to saturation with biotinylated Lysosomal-associated membrane glycoprotein 1 (LAMP1) in phosphate buffered saline (PBS, 10 mM phosphate, 150 mM NaCl, pH 7.4). The biotinylation of this recombinant protein was performed similarly as described previously for fetuin.<sup>18</sup> After loading the sensors were washed in the PBS buffer until a stable baseline was obtained. Subsequently, sensors were moved to wells containing a mix of virus and different concentrations of the indicated compounds, which had been pre-incubated for 4 hours at room temperature, to analyze virus binding. 8 hemagglutinating units corresponding to  $2.5 \times 10^8$  virus particles as determined by nanoparticle tracking analysis (Nanosight NS300; Malvern) were used per well. When indicated Oseltamivir carboxylate (OC; 10 μM end concentration) was added to this mixture

to block NA activity. As a control, the initial binding rate was determined in the absence of inhibitory compounds. The instrument emits white light to the sensor surface and collects the reflected light. The reflection spectrum of different frequencies is affected by the thickness of the photosensor layer of the biosensor. These interferences of lights are detected by the spectrometer and form an interference spectrum, which is shown by the phase shift intensity (nm) of the interference spectrum. Therefore, once the number of molecules bound to the sensor surface increases or decreases, the spectrometer will detect the displacement of the interference spectrum in real time.

#### **4.2.3 Hemagglutination inhibition assay**

Four hemagglutination units of influenza virus were preincubated with limiting dilutions of the indicated compounds for 4 hours at room temperature in the presence of OC. Subsequently, 0.5 % (v/v) erythrocytes were added and incubated for 2 hours at 4 °C. The lowest concentration of compound that inhibited hemagglutination was determined. The hemagglutination inhibition assay was performed twice in duplicate. The mean values of these experiments are shown.

#### **4.2.4 Infection-inhibition experiments**

Prior to infection, viruses (IAV WU95) diluted in Opti-mem (Gibco) were incubated with **HAI-4** (15  $\mu$ M) for 4 h at room temperature in the presence of 1  $\mu$ M OC (Oseltamivir carboxylate). MDCK-II cells were inoculated for 2 h, after which cells were washed with PBS, and cells were incubated in Opti-mem with bafilomycin (10 nM) overnight at 37 °C, 5 % CO<sub>2</sub>. Cells were fixed in methanol at -20 °C for 5 min, after which infected cells were visualized by using antibody HB65<sup>17</sup> specific for the nucleoprotein and Alexa Fluor 488-labeled Donkey anti-Mouse IgG (H+L) antibodies (Thermo Fisher Scientific). Monolayers were inspected and pictures were taken using using EVOS FL (Thermo Fisher Scientific).

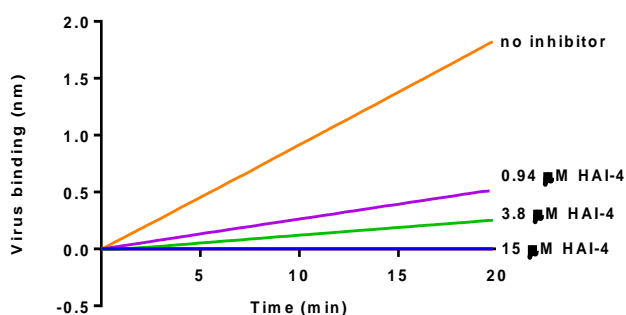
### **4.3 Results and discussion**

#### **4.3.1 Virus concentration-independent determination of relative receptor-specificity**

The inhibition study was started with a bio-layer interferometry (BLI) assay. In this assay, a streptavidin coated biosensor was loaded with a sialylated polymer. IAV



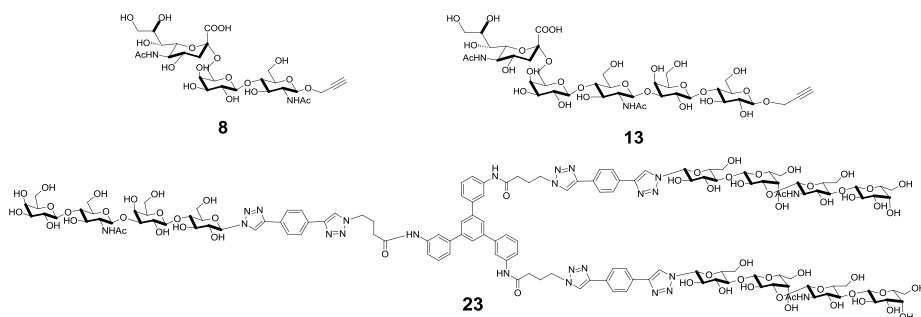
WU95 was chosen for the inhibition which has a preference of binding to  $\alpha$ -2,6-sialylated glycans and its binding to the sensor could readily be observed. Addition of the synthesized compounds led to a reduction in the IAV binding to the BLI sensor, in a concentration dependent manner. Furthermore, the degree of inhibition was dependent on the structure of the inhibitors. A representative experiment was performed to find out the concentration-dependent inhibition of virus binding with **HAI-4**, is shown in Figure 2. The absence of the inhibitor gave a strong signal of virus binding with the biosensor. When adding different amounts of **HAI-4** (concentrations ranging from 0.94  $\mu$ M to 15  $\mu$ M), concentration dependent inhibition effects were clearly observed.



**Figure 2.** A representative experiment of concentration-dependent inhibition of virus binding by compound **HAI-4** is shown as determined by the BLI wavelength shift.

#### 4.3.2 IAV inhibition by multivalent inhibitors using a BLI assay

After the concentration-dependent experiment, the BLI assay was applied to all synthesized  $\alpha$ -2,6-sialylated carbohydrates (Figure 3) with different valencies of chapter 3.



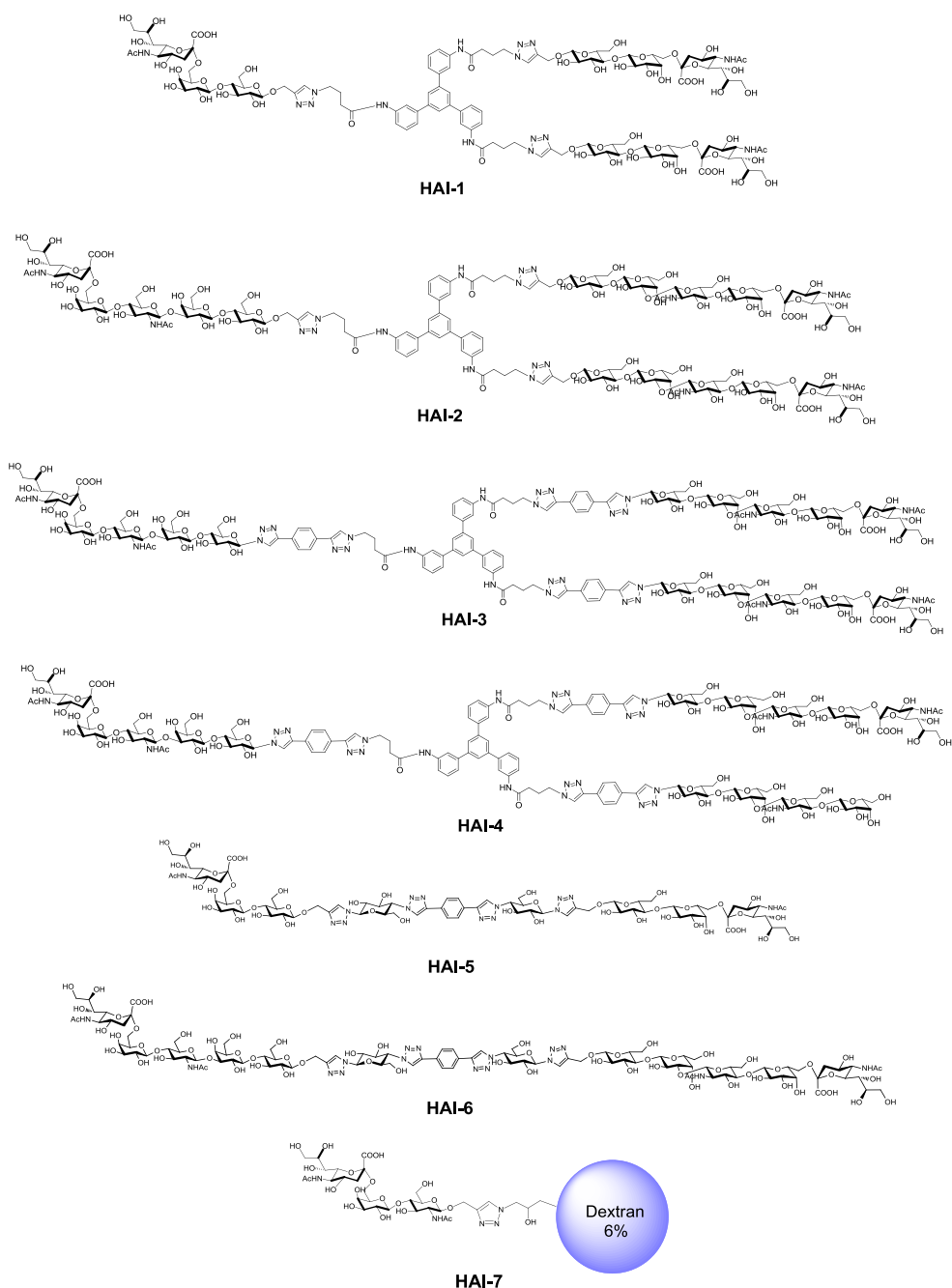


**Figure 3.** Synthesized  $\alpha$ -2,6-sialylated carbohydrates which were evaluated with the BLI assay.

By using a range of concentrations for each compound, inhibition curves of the real-time kinetic analysis of virus binding to LAMP1 were obtained and the results were determined by non-linear regression analysis of the normalized inhibition data using Graphpad Prism 7.04 software (see the curves in section 4.5) and shown in **Table 1**.

**Table 1.** Results of IAV inhibition by multivalent inhibitors using BLI assay.

Construct	Glycoligand	Valency	IC <sub>50</sub> BLI (μM) <sup>a</sup>	Relative potency (per sugar) <sup>b</sup>
<b>8</b>	SiaLacNAc	1	304 ±11	1 (1)
<b>13</b>	SiaLacNAcLac	1	396 ±3	1 (1)
<b>23</b>	LacNAcLac-triazole-Ph	3	No inhib. at 20 μM	-
<b>HAI-1</b>	SiaLac	3	15 ±0.3	20 (7)
<b>HAI-2</b>	SiaLacNAcLac	3	4.3 ±3.7	71(24)
<b>HAI-3</b>	SiaLacNAcLac-triazole-Ph	3	0.71 ±0.08	428(143)
<b>HAI-4</b>	SiaLacNAcLac-triazole-Ph	2	0.71 ±0.15	428(214)
<b>HAI-5</b>	SiaLac	2	13 ±1	23(12)
<b>HAI-6</b>	SiaLacNAcLac	2	9.4 ±0.46	32(16)
<b>HAI-7</b>	SiaLacNAc	55	1.51 ±0.16	201(4)

<sup>a</sup>in the presence of 10 μM oseltamivir, <sup>b</sup>relative to the potency of compound **8**.

The first thing to note is the inhibition with the two reference compounds **8** and **13**. These two compounds were monovalent sialylated lactoside moieties. Their inhibition results showed relatively low IC<sub>50</sub> values below the millimolar level as is commonly associated with the binding of sialic acid derivatives to either whole virus or HA. Another notable fact is that the virus inhibition of the two compounds is very similar, indicating that the added lactose moiety of **8** does not help the binding. Another reference compound was compound **23**. It contains the triphenyl

benzene core (a rigid spacer) linked to the LacNAcLac arms. The combined presence of the hydrophobic aromatic core, and the 12 sugar moieties of Lac and LacNAc did not yield any detectable inhibition in the assay up to the 20  $\mu\text{M}$  used in the assay. This result indicated the binding specificity of sialic acid moiety to the IAVs, other carbohydrates may just contribute binding preference after the first virus-receptor interaction.

For the results of the ‘larger’ molecules, **HAI-3** and **HAI-4** were the most potent inhibitors in the BLI assay, with  $\text{IC}_{50}$ ’s of 0.7  $\mu\text{M}$ , representing a 428-fold enhancement over reference compound **8**, the short version of monomer ligand. Although **HAI-4** contains one less sialic acid unit comparing to **HAI-3**, these two compounds performed strikingly similar in the assay, clearly indicating that two sialic acid groups might already be quiet sufficient for binding. Unfortunately, a simultaneous binding to all three HA sites with **HAI-3** was not achieved. The fact that both inhibition effects of the compounds were similar indicates that the expected statistical advantage of **HAI-3** is compensated by other factors. The distance between the ligands attached to two of the three arms of **HAI-3** seems long enough to bridge two sialic acid binding sites of HA, but the binding of the third arm may be more difficult to achieve according to the relatively rigid structure of this molecule. The trivalent compounds with a shorter ligand moiety (sialyl-Lac) **HAI-1** and with the shorter linker (sialyl-LacNAcLac) **HAI-2** were considerably weaker inhibitors with  $\text{IC}_{50}$ ’s of 15  $\mu\text{M}$  and 4.3  $\mu\text{M}$ , respectively. Comparing the three trivalent inhibitors, it is clear to see the importance of the length of the ligands. Although these two compounds may be too short to bind two binding pocket of a single HA, they still showed better binding affinity compared to monovalent reference compounds **8** and **13**, with similar carbohydrate ligand moieties in their structure. These inhibition results also confirmed the interesting multivalency effects of these molecules. Besides the results with the trivalent ligands, ligands based on the linear divalent scaffold were also instructive. The divalent scaffold **24** contains a similar number of atoms separating the azido groups as trivalent scaffold **4** that was the basis of **HAI-1-4**. Notably, compounds based on **24**, i.e. **HAI-5** and **HAI-6** had very similar potency when compared to those derived from **4**, i.e. **HAI-1** and **HAI-2**, which contained the same glycan ligands. This result again indicates that divalent binding mode is likely the case for all of these inhibitors, since otherwise a higher inhibitory potency was expected for the trivalent inhibitors. Nevertheless, also here, the results indicate the importance of the length of the arm, as a longer arms leads to enhanced inhibition with stronger binding interactions. Interestingly, the polymeric glycoconjugate **HAI-7**, while a potent inhibitor with an  $\text{IC}_{50}$  of 1.5  $\mu\text{M}$ , was even weaker than the tri- and di-valent

inhibitors **HAI-3** and **HAI-4**, and much more so when corrected for valency, as the relative potency per sugar is only 3.75. This result clearly shows that the divalent ligand designs provide a useful benefit, besides other advantages of a relatively small homogeneous molecule over a heterogeneous polymer with possibly a risk of immunogenicity.

The above experiments were run in the presence of 10  $\mu\text{M}$  of neuraminidase (NA) inhibitor Oseltamivir carboxylate (OC), to inhibit NA that could potentially cleave off the sialic acid moieties from the inhibitors. In order to find out the influence of OC, a direct comparison was made between experiments involving inhibitory concentrations (3  $\mu\text{M}$ ) of compounds **HAI-2**, **HAI-3** and **HAI-4** in the presence of oseltamivir, with the same experiments without this NA inhibitor (Figure 4).

Inhibition on WU95R after 4h treatment with and without OC

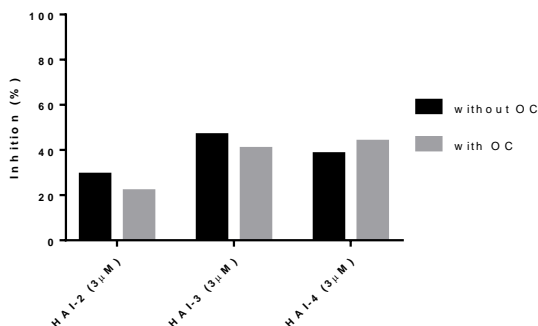


**Figure 4.** Analysis of compound **HAI-2**, **HAI-3** and **HAI-4** inhibition targeting IAV WU95 by BLI assay performed with/without oseltamivir.

As we can see from the figure, these experiments showed similar degrees of inhibition whether OC was present or not. Repeating these experiments with a different IAV, i.e. VI75, showed, first of all, similar degrees of inhibition, and secondly, only a small effect of oseltamivir (Figure 5).

#### Inhibition on VI75 after 4h treatment with and without OC

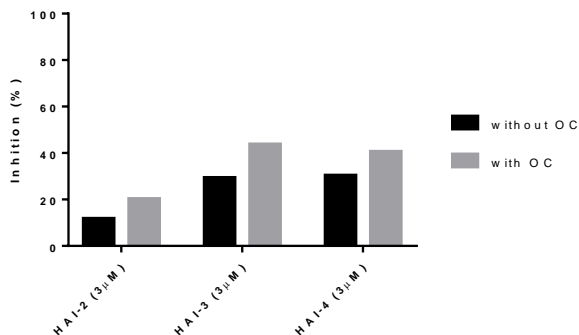


**Figure 5.** Analysis of compound **HAI-2**, **HAI-3** and **HAI-4** inhibition targeting IAV VI75 by BLI assay performed with/without oseltamivir.

It was interesting that no major effect of the oseltamivir was observed both for IAV WU95 and VI75. Perhaps the reason lies in the fact that neuraminidases typically perform better inhibition on  $\alpha$ -2,3-isomers and are less proficient in cleaving the  $\alpha$ -2,6-sialylglycans as present in our inhibitors. Furthermore, in these BLI assays, the di- and trivalent glycans may be tightly bound with a long residence times due to the multivalency effect of chelation, making it more difficult for NA to do its job, which confirmed the potency of these glycans.

#### 4.3.3 IAV inhibition by multivalent inhibitors using HAI assay

Besides the BLI assay, also a hemagglutination inhibition assay was performed for a number of compounds. Four hemagglutination units of IAV WU95 were preincubated with limiting dilutions of the targeting carbohydrates for 4 hours at room temperature in the presence of OC. Then erythrocytes were added and incubated for 2 hours at 4 °C. The inhibition results are shown in Table 2.

**Table 2.** Results of IAV inhibition by multivalent inhibitors using HAI assay.

Construct	Glycoligand	Valency	K <sub>i</sub> HAI (μM)	Relative potency (per sugar) <sup>a</sup>
<b>13</b>	SiaLacNAcLac	1	360 ±139	1(1)
<b>HAI-1</b>	SiaLac	3	53 ±15	7(2)
<b>HAI-3</b>	SiaLacNAcLac -triazole-Ph	3	9.4 ±3.8	38(13)
<b>HAI-4</b>	SiaLacNAcLac -triazole-Ph	2	10.3 ±5.6	35(17)
<b>HAI-7</b>	SiaLacNAc	55	3.75 ±1.4	96(2)

<sup>a</sup>relative to the potency of compound **13**.

Comparing the data to the results of the BLI assay, it is clear that the same trends can be seen as in the HAI assay. The reference compound  $\alpha$ -2,6-sialylLacNAcLac **13** showed relatively low K<sub>i</sub> values as well considering the monovalent binding mode. The divalent sialyl glycans and the long armed trivalent compound without triazole-phenyl unit were not determined in this assay. The K<sub>i</sub>'s for the most potent compounds **HAI-3** and **HAI-4** in 4.3.2 were not as low, but still in the low micromolar range. Although the results of the HAI assay were not as intriguing as the BLI assay, it still should be noted that the conditions are different in both assays, and especially multivalency effects can vary due to the *in vitro* assay conditions.

#### 4.3.4 Infection inhibition test of multivalent inhibitors

To further evaluate the potential of the compounds as IAV inhibitors, an infection inhibition test was performed. Here we chose one of our most potent trivalent compound **HAI-4** for evaluation. As such MDCK-II cells were exposed to a dose of IAV in the presence and absence of compound **HAI-4** at 15 μM. The results of the experiment are shown in Figure 6, which shows images of cell culture but stained with a fluorescent marker that indicates viral infection.

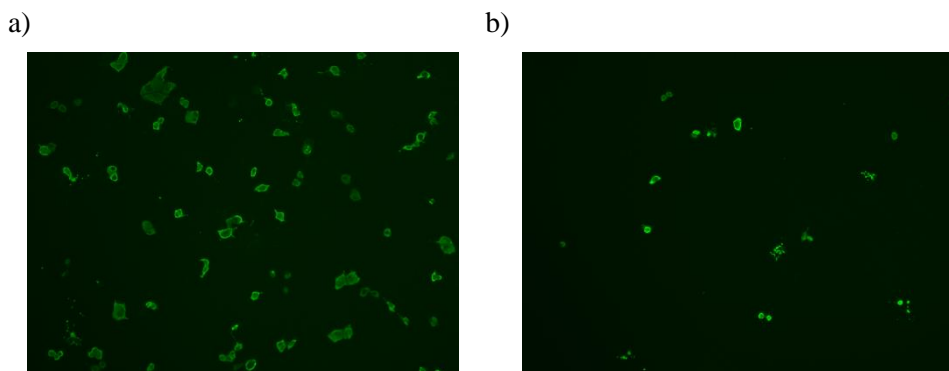


**Figure 6.** Monolayers of MDCK-II cells were inoculated with IAV in the presence of oseltamivir and in the absence (a) or presence (b) of **HAI-4**. Infected cells were visualized using a nucleoprotein-specific antibody.

The experiment was run in the presence of 1  $\mu$ M of oseltamivir and Figure 6a) shows the situation without **HAI-4** present, and a widespread infection is seen. In Figure 6b), it can clearly be seen that far fewer cells were actually infected with the 4 h preincubation treatment of **HAI-4**. This result now indicates that **HAI-4** is able to inhibit the binding of IAV in two assays and was tested with two different IAV types, and also the subsequent infection as shown here with a cell line. Notably in this case, the inhibitory effect of **HAI-4** dropped to a large extent when oseltamivir was not present, which was not the case in the BLI assay. The reason for the difference is unclear, but the used glycosylated surfaces in the two assays differ greatly and therefore also possibly the interaction mode of the virus. It seems clear that the trivalent inhibitor **HAI-4** shows much more potency in this inhibition experiment when using a combination treatment of HA and NA inhibitors.

#### 4.4 Conclusion and outlook

We here showed the multiple assays to evaluate the properties of multivalent sialic acid containing glycoconjugates. These well-defined carbohydrate systems were found to inhibit the binding of IAV in a dose dependent manner in the bio-layer interferometry (BLI) assay. Obviously, a combination of structural features is needed for inhibition as a single sugar arm is only weakly active and the non-sialyl system is not active. Enhancements of 428-fold were achieved with the long-armed systems containing either two or three sialic acid units. Furthermore, the use of

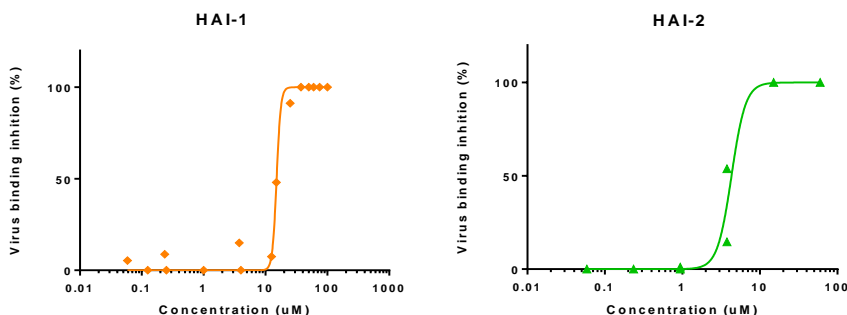


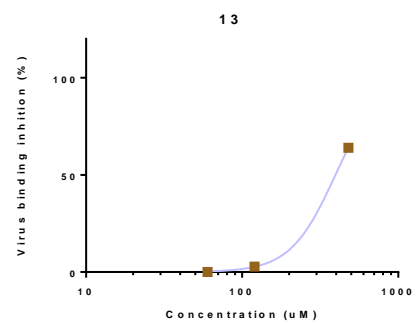
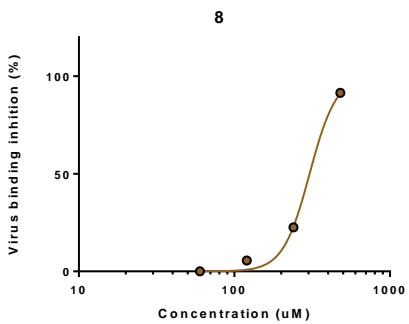
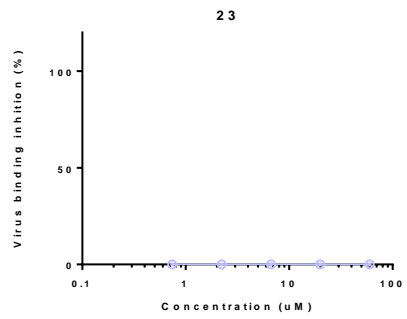
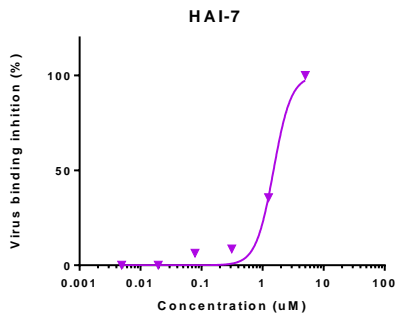
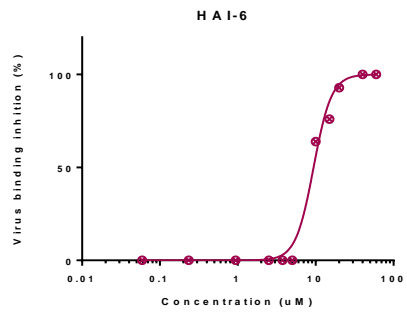
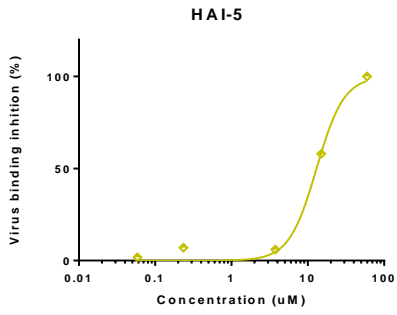
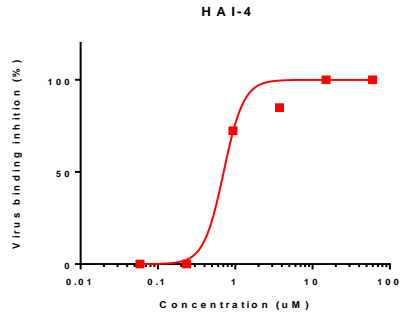
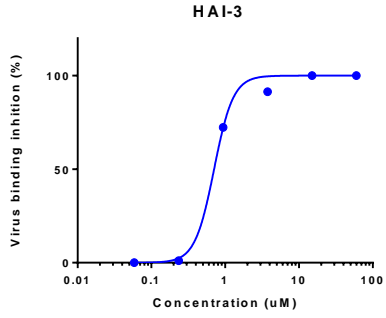
divalent systems were also investigated which showed similar results when compared to experiments performed with trivalent systems. Clearly, not all three binding sites can be occupied simultaneously by our system, but two seems possible, as previously indicated for large bi-antennary glycans<sup>19</sup> and DNA bridged divalent ligands.<sup>20</sup> The length of the glycan arms is an important factor to achieve higher potency in designing IAV inhibitors. On the other hand, the hemagglutination inhibition experiments gave the same trends as the BLI assay but the effects were considerably smaller. A difference was seen in the degree of inhibition and multivalency effects. Overall the data are consistent with a bivalent chelating binding mode but some degree of statistical rebinding may also occur.

As such this is the first example of a non-macromolecular compound to successfully demonstrate this binding strategy, indicating that a therapeutic avenue with some additional optimization is within reach. In the BLI assay it was remarkable that no significant effect of the oseltamivir was observed, and it should be note that neuraminidases are typically relatively slow acting on the  $\alpha$ -2,6-isomers. In addition to the BLI-based adhesion assay and hemagglutination inhibition, compound **HAI-4** was also shown to largely inhibit the infection of MDCK-II cells by IAV. In this virus inhibition assay, a neuraminidase inhibitor effect was observed. In order to lower the effect caused by NA cleaving, it would be a preferred strategy to introduce S-linked sialic acid moieties, as previously reported,<sup>21</sup> as a prerequisite for our type of compounds. Furthermore, the multivalent approach may not be limited to IAV inhibitor discovery, but can likely be extended to other biological systems as previously shown for adenovirus, bacteria lectins and toxins as well.<sup>22-24</sup>

## 4.5 Supplementary figures

Real-time kinetic analysis of virus binding to LAMP1 performed by BLI.





## References

- 1 B. S. Hamilton, G. R. Whittaker and S. Daniel, Influenza virus-mediated membrane fusion: Determinants of hemagglutinin fusogenic activity and experimental approaches for assessing virus fusion, *Viruses*, 2012, **4**, 1144–1168.
- 2 M. D. George, K. Hirst, The quantitative determination of Influenza virus and antibodies by means of red cell agglutination, *J. Exp. Med.*, 1942, **75**, 49–64.
- 3 G. B. Sigal, M. Mammen, G. Dahmann and G. M. Whitesides, Polyacrylamides bearing pendant  $\alpha$ -sialoside groups strongly inhibit agglutination of erythrocytes by influenza virus: The strong inhibition reflects enhanced binding through cooperative polyvalent interactions, *J. Am. Chem. Soc.*, 1996, **118**, 3789–3800.
- 4 C. T. Guo, X. L. Sun, O. Kanie, K. F. Shortridge, T. Suzuki, D. Miyamoto, K. I. P. J. Hidari, C. H. Wong and Y. Suzuki, An O-glycoside of sialic acid derivative that inhibits both hemagglutinin and sialidase activities of influenza viruses, *Glycobiology*, 2002, **12**, 183–190.
- 5 J. C. Jones, E. A. Turpin, H. Bultmann, C. R. Brandt and S. Schultz-Cherry, Inhibition of influenza virus infection by a novel antiviral peptide that targets viral attachment to cells, *J. Virol.*, 2006, **80**, 11960–11967.
- 6 Y. Yang, H. P. Liu, Q. Yu, M. B. Yang, D. M. Wang, T. W. Jia, H. J. He, Y. He, H. X. Xiao, S. S. Iyer, Z. C. Fan, X. Meng and P. Yu, Multivalent S-sialoside protein conjugates block influenza hemagglutinin and neuraminidase, *Carbohydr. Res.*, 2016, **435**, 68–75.
- 7 D. Lauster, M. Glanz, M. Bardua, K. Ludwig, M. Hellmund, U. Hoffmann, A. Hamann, C. Bötcher, R. Haag, C. P. R. Hackenberger and A. Herrmann, Multivalent peptide–nanoparticle conjugates for influenza-virus inhibition, *Angew. Chemie - Int. Ed.*, 2017, **56**, 5931–5936.
- 8 A. S. Gambaryan and M. N. Matrosovich, A solid-phase enzyme-linked assay for influenza virus receptor-binding activity, *J. Virol. Methods*, 1992, **39**, 111–123.
- 9 H. Kamitakahara, T. Suzuki, Y. Suzuki, O. Kanie and C. Wong, A Lysoganglioside/Poly-L-glutamic acid conjugate as a picomolar inhibitor of influenza hemagglutinin, *Angew. Chemie - Int. Ed.*, 1998, **37**, 1524–1528.
- 10 O. Blixt, S. Head, T. Mondala, C. Scanlan, M. E. Huflejt, R. Alvarez, M. C. Bryan, F. Fazio, D. Calarese, J. Stevens, N. Razi, D. J. Stevens, J. J. Skehel, I. van Die, D. R. Burton, I. A. Wilson, Printed covalent glycan array for ligand profiling of diverse glycan binding proteins, *Proc. Natl. Acad. Sci.*, 2004, **101**, 17033–17038.
- 11 C. M. Nycholat, R. McBride, D. C. Ekiert, R. Xu, J. Rangarajan, W. Peng, N. Razi, M. Gilbert, W. Wakarchuk, I. A. Wilson and J. C. Paulson, Recognition of sialylated poly-N-acetyllactosamine chains on N- and O-linked glycans by human and avian influenza A virus hemagglutinins, *Angew. Chemie - Int. Ed.*, 2012, **51**, 4860–4863.
- 12 W. Wang, M. W. Wolff, U. Reichl and K. Sundmacher, Avidity of influenza virus : Model-based identification of adsorption kinetics from surface plasmon resonance experiments, *J. Chromatogr. A*, 2014, **1326**, 125–129.

- 13 M. Waldmann, K. Hoelscher, M. Wienke, F. C. Niemeyer, D. Rehders and B. Meyer, A nanomolar multivalent ligand as entry inhibitor of the hemagglutinin of avian influenza, *J. Am. Chem. Soc.*, 2014, **136**, 783–788.
- 14 D. C. Ekiert, A. K. Kashyap, J. Steel, A. Rubrum, G. Bhabha, R. Khayat, J. Hyun Lee, M. A. Dillon, R. E. O’Neil, A. M. Faynboym, M. Horowitz, L. Horowitz, A. B. Ward, P. Palese, R. Webby, R. A. L., Neutralization of influenza A viruses by insertion of a single antibody loop into the receptor binding site, *Nature*, 2012, **27**, 526–532.
- 15 Z. V. F. Wright, N. C. Wu, R. U. Kadam, I. A. Wilson and D. W. Wolan, Structure-based optimization and synthesis of antiviral drug Arbidol analogues with significantly improved affinity to influenza hemagglutinin, *Bioorganic Med. Chem. Lett.*, 2017, **27**, 3744–3748.
- 16 B. F. Koel, D. F. Burke, T. M. Bestebroer, S. Van Der Vliet, G. C. M. Zondag, G. Vervaeke, E. Skepner, N. S. Lewis, M. I. J. Spronken, C. A. Russell, M. Y. Eropkin, A. C. Hurt, I. G. Barr, J. C. De Jong, G. F. Rimmelzwaan, A. D. M. E. Osterhaus, R. A. M. Fouchier and D. J. Smith, Substitutions near the receptor binding site determine major antigenic change during influenza virus evolution, *Science*, 2013, **342**, 976–979.
- 17 E. de Vries, D. M. Tscherne, M. J. Wienholts, V. Cobos-Jiménez, F. Scholte, A. Garc á-Sastre, P. J. M. Rottier and C. A. M. de Haan, Dissection of the influenza A virus endocytic routes reveals macropinocytosis as an alternative entry pathway, *PLoS Pathog.*, DOI:10.1371/journal.ppat.1001329.
- 18 Guo, H.; Rabouw, H.; Slomp, A.; Dai, M.; van der Vegt, F.; van Lent, J. W. M.; McBride and C. A. M. de H. Paulson, J. C.; de Groot, R. J.; van Kuppeveld, Frank, J. M.; E. de Vries, Kinetic analysis of the influenza A virus HA/NA balance reveals contribution of NA to virus-receptor binding and NA-dependent rolling on receptor-containing surfaces, 2018, vol. 14.
- 19 M. Yamabe, K. Kaihatsu and Y. Ebara, Sialyllactose-modified three-way junction DNA as binding inhibitor of influenza virus hemagglutinin, *Bioconjug. Chem.*, 2018, **29**, 1490–1494.
- 20 V. Bandlow, S. Liese, D. Lauster, K. Ludwig, R. R. Netz, A. Herrmann and O. Seitz, Spatial screening of hemagglutinin on influenza A virus particles: Sialyl-LacNAc displays on DNA and PEG scaffolds reveal the requirements for bivalency enhanced interactions with weak monovalent binders, *J. Am. Chem. Soc.*, 2017, **139**, 16389–16397.
- 21 R. R. Kale, H. Mukundan, D. N. Price, J. F. Harris, D. M. Lewallen, B. I. Swanson, J. G. Schmidt and S. S. Iyer, Detection of intact influenza viruses using biotinylated biantennary S-sialosides, *J. Am. Chem. Soc.*, 2008, **130**, 8169–8171.
- 22 S. Spjut, W. Qian, J. Bauer, R. Storm, L. Frängsmyr, T. Stehle, N. Arnberg and M. Elofsson, A potent trivalent sialic acid inhibitor of adenovirus type 37 infection of human corneal cells, *Angew. Chemie - Int. Ed.*, 2011, **50**, 6519–6521.
- 23 A. Bernardi, J. Jiménez-Barbero, A. Casnati, C. De Castro, T. Darbre, F. Fieschi, J. Finne, H. Funken, K. E. Jaeger, M. Lahmann, T. K. Lindhorst, M. Marradi, P. Messner, A. Molinaro, P. V. Murphy, C. Nativi, S. Oscarson, S. Penadés, F. Peri, R.

- J. Pieters, O. Renaudet, J. L. Reymond, B. Richichi, J. Rojo, F. Sansone, C. Sch äffer, W. B. Turnbull, T. Velasco-Torrijos, S. Vidal, S. Vincent, T. Wennekes, H. Zuilhof and A. Imberty, Multivalent glycoconjugates as anti-pathogenic agents, *Chem. Soc. Rev.*, 2013, **42**, 4709–4727.
- 24 D. Haksar, E. de Poel, L. H. C. Quarles van Ufford, S. Bhatia, R. Haag, J. M. Beekman and R. J. Pieters, Strong inhibition of cholera toxin B subunit by affordable, polymer-based multivalent inhibitors, *Bioconjug. Chem.*, 2019, acs.bioconjchem.8b00902.



# *Chapter 5*

*Summary and future perspective*

The aim of this thesis is to develop multivalent carbohydrate-based ligands (Figure 1) as inhibitors of the adhesion of the Influenza A virus (IAV). The adhesion protein hemagglutinin (HA) plays a central role in the infection process, and has potential as a drug target besides the neuraminidase. HA is a challenging target, since it binds only weakly to its target ligands: sialylated LacNAc derivatives, relying on multivalency for strong viral adhesion. While viral adhesion inhibition by large polymeric molecules has proven viable, limited success was reached for a design based approach to reach the three binding pockets of HA by smaller molecules. By linking sialylated LacNAc units to di- and trivalent scaffolds, inhibitors were obtained with a potent inhibition effect in several assays.

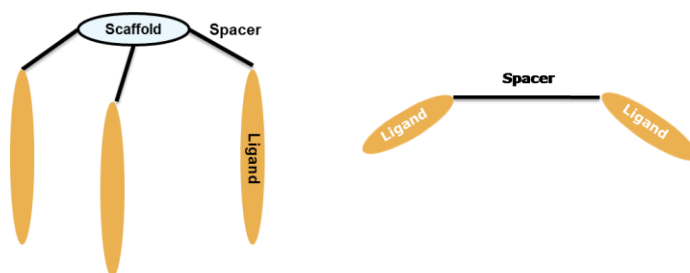


**Figure 1.** Proposed generic structures of the multivalent inhibitors synthesized and evaluated in this thesis.

## 5.1 Summary

Protein-carbohydrate interactions play a very important role in many biological processes. A single interaction between a protein and a carbohydrate is usually weak, but multivalent ligands can compensate for this deficiency by binding to multiple binding sites of one biological entity simultaneously. Over the past few years, numerous efforts have been made for the design and synthesis of carbohydrate-based multivalent ligands thereby serving as potent inhibitors for pathogens such as the influenza A virus.

In **Chapter 1**, we described a variety of multivalent carbohydrate-based systems from small to large molecules which showed potent inhibitory effect against several pathogens, such as *Pseudomonas aeruginosa*, cholera toxin, ebola virus and influenza A virus (IAV). Firstly, we discussed the different effects of multivalent



binding: the chelate effect, subsite binding, statistical rebinding and also aggregation. By understanding these mechanisms of multivalent interactions, we discussed glycopolymers, nanoparticles, dendrimers, calixarenes, liposomes, DNA derivatives etc. as multivalent inhibitors. These ligands could potentially be used as new anti-pathogenic agents or could be used complementary to the current drugs and improve therapy. Secondly, we focused on the past and current research on IAV inhibition. Large molecular entities, e.g. functionalized polymers,<sup>1-7</sup> chitosan,<sup>8</sup> liposomes,<sup>9,10</sup> nanostructures,<sup>6</sup> and dendrimers,<sup>11</sup> showed their inhibitory advantages by interacting with multiple HA trimers simultaneously and/or binding to more than one binding site within an HA trimer. Smaller molecules containing proper carbohydrate units can in some cases be effective IAV inhibitors depending on whether their topological design allows them to bind simultaneously to several binding sites of a single HA trimer,<sup>12,13</sup> or even to binding sites on nearby trimers. Such efforts and promising results might lead to the next generation of multivalent glycoconjugates for therapeutic applications for IAV and also other pathogens.

Based on the nature of HA binding properties, we designed two kinds of inhibitors which were described in **Chapter 2**. The first design strategy is based on the trimeric structure of the “head” of the hemagglutinin protein which contains three binding sites. The inhibitor design consisted of three different parts: a ligand that contains an  $\alpha$ -2,6-sialylated glycan (3 copies), a propeller shaped scaffold, and a short rigid spacer that links the ligands to the scaffold. The synthetic strategy to combine these three parts is based on the efficient copper catalyzed azide-alkyne cycloaddition (CuAAC, ‘click’) reaction under microwave assistance. Another strategy is based on similar research within our group in which we have designed a series of divalent ligands presenting galactose residues with variations in the length of the spacer to fit a divalent binding mode.<sup>14-16</sup> In this chapter, reliable pathways for the synthesis of the building blocks (Figure 2) to build up hemagglutinin inhibitors were found.

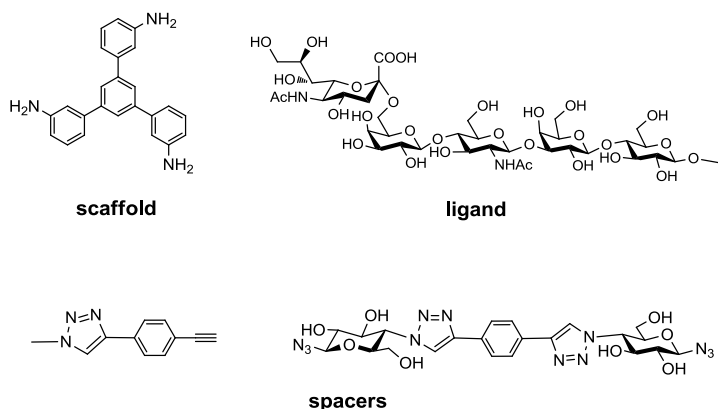


**Figure 2.** Building blocks that were synthesized for the HA inhibitors.

Different strategies were investigated. The amino functionalized 1,3,5-triphenyl benzene scaffold<sup>17</sup> is ideal for the available area on the top area of the HA protein, taking advantage of the groove areas for the spacer arms. For the first time, a rigid spacer attachment was introduced in the design of a HA inhibitor to hopefully enhance the binding affinity between the sugar moiety and the virus surface protein. Different lengths of spacers were synthesized for building a series of di- and trivalent HA inhibitors. Rigid spacers attachments and lactose or LacNAc-Lac moieties were used, of these the carbohydrate units were incorporated using enzymes like *H. Pylori*β3GlcNAcT, *LgtB* and PmST1 mutant P34H/M144L. The non-conjugated building blocks are also important reference compounds for the subsequent biological activity analysis.

In **Chapter 3**, we showed the successful synthesis and characterization of multivalent sialic acid containing glycoconjugates based on the structure of the HA protein. Their synthesis was performed by a combination of chemical scaffold synthesis, enzymatic carbohydrate synthesis and CuAAC conjugation. We started from the shortest version of trivalent α-2,6-sialyl-Lac ligand to investigate the proper ‘click’ reaction conditions. After that, longer chains were attached to the propeller shaped scaffold and also the divalent spacer core using similar methods with good yields. The largest of the compounds were even larger than a biantennary Sia (LacNAc)<sub>3</sub> linked to a tri-mannose core. For comparison with the ‘small’ molecule scaffolds, the α-2,6-Sia-LacNAc was coupled to a modified dextran polymer<sup>18</sup> with a degree of substitution of 6 %. Although the characteri-

zation of some of the HA inhibitors was difficult, we managed by combining multiple analysis technologies such as  $^1\text{H}$  NMR, HSQC, LC-MS, HRMS and IR. The syntheses were performed on a low milligram scale, and future attempts on a larger scale should also be investigated. Variations of the conjugate structures should also be performed to find the optimal designs for IAV inhibitors.

Multiple assays to evaluate the properties of our multivalent sialic acid containing glycoconjugates were described in **Chapter 4**. Firstly, the well-defined carbohydrate systems were evaluated in a bio-layer interferometry (BLI) assay. The monovalent compounds showed relatively low  $\text{IC}_{50}$  values below the millimolar level as is commonly associated with the binding of sialic acid derivatives to either whole virus or HA. For the best multivalent systems, a 428-fold enhancement was achieved with the long-armed inhibitors containing either two or three sialyl-LacNAc-Lac units. Furthermore, the use of divalent systems with a rigid spacer were also investigated which showed similar results as their trivalent counterparts, indicating that a divalent binding mode is likely the case for both our trivalent and divalent systems. Secondly, the hemagglutination inhibition experiments gave the same trends as the BLI assay with somewhat reduced enhancements, but still in the low micromolar range. In addition to the BLI and hemagglutination inhibition, compound **HAI-4** was also shown to largely inhibit the infection of MDCK-II cells. All data are consistent with a bivalent chelating binding mode, but statistical rebinding may also be involved to some extent, like previously discussed for large bi-antennary glycans<sup>19</sup> and DNA bridged divalent ligands.<sup>20</sup> In our virus inhibition assays, an NA inhibitor effect was observed. In order to lower the effect caused by NA cleaving, it would be a proper strategy to introduce S-linked sialic acid moieties into the system that should be stable to NA, as previously reported.<sup>21</sup> Furthermore, the multivalency approach may not be limited to IAV inhibitor discovery, but can likely be extended to other biological systems as previously shown for adenovirus, bacteria lectins and toxins as well.<sup>18,22,23</sup>

## 5.2 Future perspective

Proteins that bind to carbohydrate structures based on a multivalency effect represent a vast potential for the development of clinical therapeutics. In order to design a successful multivalent carbohydrate-based inhibitor, we need to have a

detailed understanding of the biological process of pathogen infection. It is difficult to make compounds with an exact size and multivalency to match natural systems such as viruses, which is one of the challenges. Scaffold structure, molecule size, linker between scaffold and ligand, ligand density, and also mechanical properties are important parameters that need to be optimized for the design of multivalent inhibitors. Besides high binding affinities, other mechanisms such as steric shielding and clustering effects are also important for successful pathogen inhibition.

A reasonable scaffold size, spacer length and shape are important factors for the design of an HA inhibitor which should match the geometry of the trimeric HA and try to connect multiple binding sites simultaneously. Different kinds of building blocks have been investigated in our and other groups using trimeric scaffolds, rigid spacers, elongated glycans, peptides, etc. with interesting results of HA inhibition. Optimizing the current components might help us find more potent ligands. In the future investigation of HA inhibitors, scaffolds with a larger size, containing either more rigid spacers or longer flexible arms, e.g. containing glycans with two or three LacNAc repeats or even suitable peptide chains should also be considered into the structure design. Furthermore, the O-linked sialic acid could be replaced by S-linked moieties, which would be more stable to NA, and may be more potent not only for HA inhibition, but also for the prevention of viral infection. As IAV is a kind of virus that mutates and travels fast across the world, looking for a broad-spectrum anti-viral drug would be an effective way of treatment. In this thesis, we mainly focused on the ligands containing  $\alpha$ -2,6-sialic acids while  $\alpha$ -2,3-sialic acid moieties should be introduced into the structure design in the future as well, as the infections in avian is also a serious issue nowadays. Evaluations of the anti-viral activity that were used in the thesis already gave us some convincing results of these inhibitors, while there are still evaluations that could be done. More virus strains should be tested with these synthetic compounds, molecular modeling should also be done in the future to investigate the ligand-protein interactions and correlate the experimental results with modeling. After successful inhibition of HA and also IAV *in vitro*, *in vivo* tests should also be done in the future after successful further optimization of the ligand.

Even though the small molecules seem to be more promising for drug design purposes, larger sized systems still have their own advantages that could be applied in the future. Glycopolymers, nanoparticles, dendrimers, liposomal systems already

provided highly potent inhibitors in a lot of research reports, however in our own research the polymer was not better than the well-defined ‘small’ molecule. These larger polyvalent based systems may engage more sialic acid binding proteins, which would also block the viral infection more effectively. While for the evaluation of these large molecules, challenges of pharmacokinetics and immunogenicity should be taken into consideration. Suitable pharmaceutical delivery systems to carry and release the drug *in vivo* should be investigated to find a proper way of treatment.

As IAV infection is a severe disease occurred worldwide, the urgency of preparation for large IAV pandemics make this the right time to keep the investigation of multivalent inhibitor design going towards the clinics. The research on HA inhibitors could be applied to either stand-alone anti-flu drugs but more likely in combination with other options such as vaccines and NA inhibitors.<sup>24,25</sup> The multivalent strategy of inhibitor design would also be interesting for other biological systems which could be developed with more applications for therapeutic and diagnostic purposes.

## References

- 1 M. N. Matrosovich, L. V. Mochalova, V. P. Marinina, N. E. Byramova and N. V. Bovin, Synthetic polymeric inhibitors of influenza virus receptor-binding activity suppress virus replication, *FEBS Lett.*, 1990, **272**, 209–21.
- 2 W. J. Lees, A. Spaltenstein, J. E. Kingery-Wood and G. M. Whitesides, Polyacrylamides bearing pendant  $\alpha$ -sialoside groups strongly inhibit agglutination of erythrocytes by influenza A virus: Multivalency and steric stabilization of particulate biological systems, *J. Med. Chem.*, 1994, **37**, 3419–3433.
- 3 S. K. Choi, M. Mammen and G. M. Whitesides, Generation and *in situ* evaluation of libraries of poly(acrylic acid) presenting sialosides as side chains as polyvalent inhibitors of influenza-mediated hemagglutination, *J. Am. Chem. Soc.*, 1997, **119**, 4103–4111.
- 4 G. B. Sigal, M. Mammen, G. Dahmann and G. M. Whitesides, Polyacrylamides bearing pendant  $\alpha$ -sialoside groups strongly inhibit agglutination of erythrocytes by

- influenza virus: The strong inhibition reflects enhanced binding through cooperative polyvalent interactions, *J. Am. Chem. Soc.*, 1996, **118**, 3789–3800.
- 5 H. Kamitakahara, T. Suzuki, Y. Suzuki, O. Kanie and C. Wong, A Lysoganglioside / Poly-1-glutamic Acid, *Angew. Chemie Int. Ed.*, 1998, **37**, 1524–1528.
- 6 I. Papp, C. Sieben, A. L. Sisson, J. Kostka, C. Bötcher, K. Ludwig, A. Herrmann and R. Haag, Inhibition of influenza virus activity by multivalent glycoarchitectures with matched sizes, *ChemBioChem*, 2011, **12**, 887–895.
- 7 S. Bhatia, D. Lauster, M. Bardua, K. Ludwig, S. Angioletti-Uberti, N. Popp, U. Hoffmann, F. Paulus, M. Budt, M. Stadtmüller, T. Wolff, A. Hamann, C. Bötcher, A. Herrmann and R. Haag, Linear polysialoside outperforms dendritic analogs for inhibition of influenza virus infection *in vitro* and *in vivo*, *Biomaterials*, 2017, **138**, 22–34.
- 8 X. Li, P. Wu, G. F. Gao and S. Cheng, Carbohydrate-functionalized chitosan fiber for influenza virus capture, *Biomacromolecules*, 2011, **12**, 3962–3969.
- 9 H. W. Yeh, T. S. Lin, H. W. Wang, H. W. Cheng, D. Z. Liu and P. H. Liang, S-Linked sialyloligosaccharides bearing liposomes and micelles as influenza virus inhibitors, *Org. Biomol. Chem.*, 2015, **13**, 11518–11528.
- 10 X.-L. Sun, Y. Kanie, C.-T. Guo, O. Kanie, Y. Suzuki and C.-H. Wong, Syntheses of C-3-modified sialylglycosides as selective inhibitors of influenza hemagglutinin and neuraminidase, *European J. Org. Chem.*, **2000**, 2643–2653.
- 11 R. Roy, D. Zanini, S. J. Meunier and A. Romanowska, Solid-phase synthesis of dendritic sialoside inhibitors of influenza A virus hemagglutinin, *Chem. Commun.*, 1993, 1869–1872.
- 12 P. I. Kitov, J. M. Sadowska, G. Mulvey, G. D. Armstrong, H. Ling, N. S. Pannu, R. J. Read and D. R. Bundle, Shiga-like toxins are neutralized by tailored multivalent carbohydrate ligands, *Nature*, 2000, **403**, 669–672.
- 13 J. E. Gestwicki, C. W. Cairo, L. E. Strong, K. A. Oetjen and L. L. Kiessling, Influencing receptor-ligand binding mechanisms with multivalent ligand architecture, *J. Am. Chem. Soc.*, 2002, **124**, 14922–14933.
- 14 F. Pertici and R. J. Pieters, Potent divalent inhibitors with rigid glucose click spacers for *Pseudomonas aeruginosa* lectin LecA, *Chem. Commun.*, 2012, **48**, 4008–4010.
- 15 F. Pertici, N. J. De Mol, J. Kemmink and R. J. Pieters, Optimizing divalent inhibitors of *Pseudomonas aeruginosa* lectin LecA by using a rigid spacer, *Chem. - A Eur. J.*, 2013, **19**, 16923–16927.

- 16 R. Visini, X. Jin, M. Bergmann, G. Michaud, F. Pertici, O. Fu, A. Pukin, T. R. Branson, D. M. E. Thies-Weesie, J. Kemmink, E. Gillon, A. Imberty, A. Stocker, T. Darbre, R. J. Pieters and J. L. Reymond, Structural insight into multivalent galactoside binding to *Pseudomonas aeruginosa* Lectin LecA, *ACS Chem. Biol.*, 2015, **10**, 2455–2462.
- 17 R. J. Pieters, J. Cuntze, M. Bonnet and F. Diederich, Enantioselective recognition with C3-symmetric cage-like receptors in solution and on a stationary phase, *J. Chem. Soc. Perkin Trans.*, 1997, 1891–1900.
- 18 D. Haksar, E. de Poel, L. H. C. Quarles van Ufford, S. Bhatia, R. Haag, J. M. Beekman and R. J. Pieters, Strong inhibition of cholera toxin B subunit by affordable, polymer-based multivalent inhibitors, *Bioconjug. Chem.*, 2019, acs.bioconjchem.8b00902.
- 19 M. Yamabe, K. Kaihatsu and Y. Ebara, Sialyllactose-modified three-way junction DNA as binding inhibitor of influenza virus hemagglutinin, *Bioconjug. Chem.*, 2018, **29**, 1490–1494.
- 20 V. Bandlow, S. Liese, D. Lauster, K. Ludwig, R. R. Netz, A. Herrmann and O. Seitz, Spatial screening of hemagglutinin on Influenza A Virus particles: Sialyl-LacNAc displays on DNA and PEG scaffolds reveal the requirements for bivalency enhanced interactions with weak monovalent binders, *J. Am. Chem. Soc.*, 2017, **139**, 16389–16397.
- 21 R. R. Kale, H. Mukundan, D. N. Price, J. F. Harris, D. M. Lewallen, B. I. Swanson, J. G. Schmidt and S. S. Iyer, Detection of intact influenza viruses using biotinylated biantennary S-sialosides, *J. Am. Chem. Soc.*, 2008, **130**, 8169–8171.
- 22 S. Spjut, W. Qian, J. Bauer, R. Storm, L. Frängsmyr, T. Stehle, N. Arnberg and M. Elofsson, A potent trivalent sialic acid inhibitor of adenovirus type 37 infection of human corneal cells, *Angew. Chemie - Int. Ed.*, 2011, **50**, 6519–6521.
- 23 A. Bernardi, J. Jiménez-Barbero, A. Casnati, C. De Castro, T. Darbre, F. Fieschi, J. Finne, H. Funken, K. E. Jaeger, M. Lahmann, T. K. Lindhorst, M. Marradi, P. Messner, A. Molinaro, P. V. Murphy, C. Nativi, S. Oscarson, S. Penadés, F. Peri, R. J. Pieters, O. Renaudet, J. L. Reymond, B. Richichi, J. Rojo, F. Sansone, C. Schäffer, W. B. Turnbull, T. Velasco-Torrijos, S. Vidal, S. Vincent, T. Wennekes, H. Zuilhof and A. Imberty, Multivalent glycoconjugates as anti-pathogenic agents, *Chem. Soc. Rev.*, 2013, **42**, 4709–4727.
- 24 L. Y. Zeng, J. Yang and S. Liu, Investigational hemagglutinin-targeted influenza virus inhibitors, *Expert Opin. Investig. Drugs*, 2017, **26**, 63–73.

- 25 M. Kiso, T. J. S. Lopes, S. Yamayoshi, M. Ito, M. Yamashita, N. Nakajima, H. Hasegawa, G. Neumann and Y. Kawaoka, Combination therapy with neuraminidase and polymerase inhibitors in nude mice infected with influenza virus, *J. Infect. Dis.*, 2018, **217**, 887–896.



# *Appendices*

*Nederlandse Samenvatting*

*List of Abbreviations*

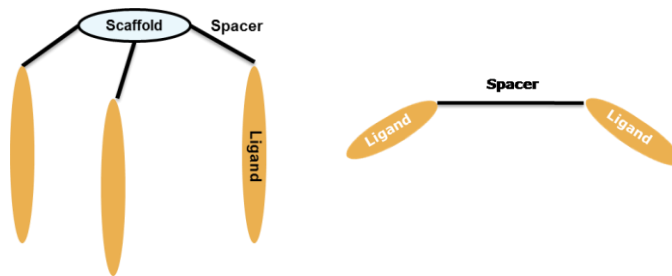
*List of Publications and Presentations*

*Acknowledgements*

*Curriculum Vitae*

## Nederlandse Samenvatting

Het doel van dit proefschrift is het ontwikkelen van inhibitoren of remmers van de adhesie van Influenza A virus (IAV), die gebaseerd zijn op koolhydraten. Het adhesie-eiwit hemagglutinine (HA) is hierin van cruciaal belang en kan worden beschouwd als een doeleiwit voor geneesmiddelontwikkeling naast het welbekende neuraminidase (NA). HA is geen gemakkelijk doeleiwit aangezien het slechts zwak bindt aan z'n natuurlijke liganden: gesialyleerde LAcNAc derivaten. Het virus en HA maken gebruik van multivalentie voor sterke adhesie aan celoppervlakken. Hoewel inhibitie hiervan door grote polymere moleculen mogelijk is gebleken, is er slechts beperkt succes geboekt met kleine moleculen die ontworpen zijn om de drie bindingsplaatsen van HA tegelijkertijd te binden. Door het verbinden van gesialyleerde LacNAc eenheden aan di- of trivalente moleculen, zijn krachtige inhibitoren verkregen die dit in meerderde assays hebben laten zien.



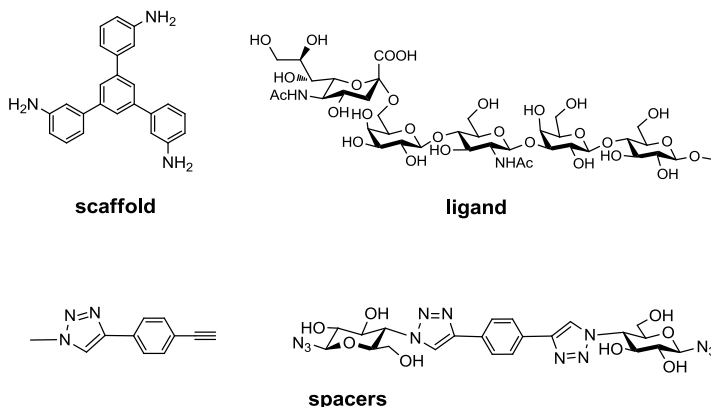
**Figuur 1.** Voorgestelde generieke structuren van multivalente inhibitoren die gesynthetiseerd zijn en beschreven in dit proefschrift.

Eiwit-koolhydraat interacties spelen een zeer belangrijke rol in veel biologische processen. Een enkelvoudige interactie tussen een eiwit en een koolhydraat is normaal gesproken zwak, maar multivalente liganden kunnen hiervoor compenseren door tegelijkertijd aan meerdere bindingsplaatsen van een eiwit te binden. De laatste jaren zijn er in toenemende mate multivalente koolhydraat liganden ontworpen en gesynthetiseerd als potentiële inhibitoren voor pathogenen zoals het influenza A virus.

In **Hoofdstuk 1** worden multivalente koolhydraten beschreven variërend van klein tot groot, die inhibitie van een aantal pathogenen lieten zien waaronder

*Pseudomonas aeruginosa*, cholera toxine, ebola virussen het influenza A virus (IAV). Eerst worden de verschillende mechanismen van multivalente binding besproken zoals: het chelaat effect, ‘subsite’ binding, statistische herbinding en aggregatie. Met deze mechanismen in ons achterhoofd worden vervolgens glycopolymeren, nanodeeltjes, dendrimeren, calixarenen, liposomen en DNA derivaten besproken als multivalente inhibitoren. Liganden zoals deze kunnen mogelijk worden gebruikt als nieuwe anti-pathogene stoffen als ‘stand alone’ therapie of samen met huidige geneesmiddelen om de therapie te verbeteren. Hierna ligt de focus in dit hoofdstuk op onderzoek naar IAV inhibitie. Grote moleculaire constructen zoals gefunctionaliseerde polymeren,<sup>1-7</sup> chitosan,<sup>8</sup> liposomen,<sup>9,10</sup> nanostructuren,<sup>6</sup> en dendrimeren,<sup>11</sup> hebben hun voordeel laten zien door meerdere HA trimeren tegelijk te binden en/of meerdere bindingsplaatsen binnen één HA trimeer. Kleine multivalentemoleculen met de juiste koolhydraat structuren kunnen in sommige gevallen goede IAV inhibitoren zijn, afhankelijk van het feit of hun topologisch ontwerp ze in staat stelt om tegelijkertijd meerdere bindingsplaatsen binnen een HA trimeer te binden of te binden aan meerdere nabijgelegen HA trimeren.<sup>12,13</sup> Dit type onderzoek en de veelbelovende resultaten ervan kunnen wellicht leiden tot een nieuwe generatie therapeutica tegen IAV of andere pathogenen.

Gebaseerd op de HA-bindingseigenschappen zijn twee types inhibitoren ontworpen die beschreven zijn in **Hoofdstuk 2**. De eerste strategie is geïnspireerd op de trimere structuur van het bovenste gedeelte van het HA-eiwit dat drie bindingsplaatsen bevat. Het ontwerp bestaat uit drie delen: een ligand dat een  $\alpha$ -2,6-siaalzuur bevat, een propeller-achtig basis molecuul en een starre ‘spacer’ die zorgt voor de verbinding van de twee. De synthetische strategie hiervoor is gebaseerd op de efficiënte CuAAC reactie ofwel ‘click’ chemie doorgaans uitgevoerd in de magnetron. Een andere strategie is gebaseerd op verwant werk binnen onze groep waarin we een serie divalente galactose liganden hebben ontworpen van verschillende lengtes, om het zo goed mogelijk divalent te laten binden.<sup>14-16</sup> In dit hoofdstuk worden betrouwbare synthesroutes beschreven voor de bouwstenen van de HA inhibitoren (Figuur 2).



**Figuur 2.** Gesynthetiseerde bouwstenen voor de HA inhibitoren.

Verschillende strategieën zijn onderzocht. Het amine-gefunctionaliseerde 1,3,5-trifenylnitrobenzeen kernmolecuul<sup>17</sup> lijkt de ideale kandidaat om het bovenste HA deel te bezetten en gebruik te maken van groeves voor de verbonden ‘spacer’ armen. Voor het eerst werd ook een star element ingebouwd in een HA-inhibitor om hopelijk de binding tussen suikerligand en viruseiwit te versterken. Meerdere ‘spacer’ lengtes zijn gesynthetiseerd voor de opbouw van de serie di- en trivalente HA-inhibitoren. Hiervoor werden onder meer starre fenyl-triazool eenheden gebruikt en ook lactose en LacNAc-Lac. Aan de lactose werden enzymatisch koolhydraten gekoppeld met enzymen zoals *H. Pylori*β3GlcNAcT, *LgtB* en PmST1 mutant P34H/M144L. De niet-geconjugeerde suiker bouwstenen zijn ook gebruikt als belangrijke referentieverbindingen bij de biologische activiteitsbepalingen.

In **Hoofdstuk 3**, wordt de succesvolle synthese en karakterisatie beschreven van de multivalente siaalzuurbevattende glycoconjugaten gebaseerd op de structuur van het HA eiwit. De synthese was uitgevoerd door een combinatie van chemische bouwsteensynthese, enzymatische synthese en CuAAC conjugatie. We begonnen met de kortste versie van het trivalente α-2,6-sialyl-Lac ligand om de reactie condities voor de ‘click’ reacties te optimaliseren. Hierna werden langere ketens aan het propellervormige trivalente kernmolecuul gezet, en ook aan de divalente ‘spacer’ met vergelijkbare methodes en goed opbrengsten. De grootste moleculen waren nog langer dan de natuurlijke biantennaire Sia(LacNAc)<sub>3</sub> verbonden aan een trimannose kern. Voor vergelijking met de ‘kleine’ moleculen werd ook α-2,6-Sia-LacNAc gekoppeld aan een gemodificeerd dextraan polymeer waarvan 6 % van de

monomeren was gefunctionaliseerd.<sup>18</sup> Hoewel de karakterisatie van enkele HA inhibitoren moeilijk was, was het mogelijk dit te doen door methodes te combineren zoals <sup>1</sup>H NMR, HSQC, LC-MS, HRMS en IR. De syntheses werden uitgevoerd op een beperkt aantal milligrammen en in de toekomst zouden de syntheses ook op een grotere schaal moeten worden uitgevoerd met daarin verdere variaties voor de optimalisatie van de HA-inhibitoren.

Meerdere analyses om de inhibitie-eigenschappen van de gemaakte multivalente sialaazuur bevattende glycoconjugaten te onderzoeken zijn beschreven in **Hoofdstuk 4**. Ten eerste werden de goed gedefinieerde koolhydraat systemen onderzocht met behulp van een ‘bio-layerinterferometry’ (BLI) analyse. De monovalente verbindingen lieten IC<sub>50</sub> waarden zien van onder de milimolair, wat laag te noemen is voor de binding van sialaazuur derivaten aan IAV-virussen of HA eiwitten. De beste multivalente moleculen lieten een 428-voudige versteking van de inhibitie zien. Het ging hier om de liganden met de langste sialyl-LacNAc-Lac bevattende armen waarvan er twee of drie aanwezig waren. Verder zijn ook de divalente moleculen onderzocht die vergelijkbare resultaten te zien gaven met de corresponderende trivalente stoffen. Dit geeft aan dat onze systemen maximaal divalente binding te zien gaven, ook al waren drie armen beschikbaar. Als tweede analysemethode werd ‘hemaglutination’ inhibitie gebruikt en de resultaten ervan lieten dezelfde trends zien als de BLI analyse. De versterkingen door multivalentie waren wel iets kleiner, maar de beste verbindingen waren nog steeds actief met lage milimolair activiteit. Naast de BLI en ‘hemaglutination’ inhibitie methodes werd voor verbinding **HAI-4** ook aangetoond dat deze stof in staat is de IAV infectie van MDCK-II cellen grotendeels te voorkomen. Alle data wijzen op een divalente binding modus, met wellicht een zekere mate van statistische herbinding zoals eerder ook is geconcludeerd voor grote bi-antennaire glycanen<sup>19</sup> en DNA-gebrugde divalente liganden.<sup>20</sup> In onze virus infectie analyses is aangetoond dat een NA inhibitor noodzakelijk is voor optimale activiteit. Het is daarom aan te raden de sialaazurmoleculen te verbinden aan de LacNAc via een zwavel in plaats van een zuurstof, zoals eerder is gedaan,<sup>21</sup> zodat deze niet door NA van de inhibitor kan worden verwijderd hetgeen de inhibitor zou inactiveren. Verder is het aannemelijk dat de effectiviteit van de multivalente aanpak zoals hier beschreven niet beperkt zal zijn tot het blokkeren van IAV maar dat dat ook voor andere pathogenen het geval zou zijn zoals adenovirus, bacteriële lectines en toxines.<sup>18,22,23</sup>

## List of Abbreviations

Ac	acetyl
Ac <sub>2</sub> O	acetic anhydride
BF <sub>3</sub> Et <sub>2</sub> O	boron trifluoride diethyl etherate
BLI	bio-layer interferometry
BSA	bovine Serum Albumin
CH <sub>3</sub> CN	acetonitrile
CIAP	calf intestine alkaline phosphatase
CMP-NANA	CMP- <i>N</i> -acetylneuraminic acid
COSY	correlation spectroscopy
CTB	Cholera toxin B-subunit
CuAAC	Cu (I)-catalyzed alkyne-azide cycloaddition
DCM	dichloromethane
DIPEA	<i>N,N</i> -diisopropylethylamine
DMAP	4-dimethylaminopyridine
DMF	<i>N,N</i> -dimethylformamide
DMSO	dimethyl sulfoxide
DNA	deoxyribonucleic acid
dPGSA	dendritic polyglycerol sialoside
EDC	1-ethyl-3-(3-dimethylaminopropyl)carbodiimide
EIA	enzyme immunoassay
ELISA	enzyme linked immunosorbent assay
ESI-MS	electrospray ionization mass spectrometry
Q-TOF-MS	quadrupole time-of-flight mass spectrometry
Et <sub>3</sub> N	triethylamine
EtOAc	ethyl acetate
EtOH	ethanol
FGF-4	fibroblast growth factor 4
Gal	galactose
Gb <sub>3</sub>	Gal $\alpha$ (1-4)-Gal $\beta$ (1-4)-Glc $\beta$ 1-ceramide
Glc	glucose
GlcNAc	<i>N</i> -acetyl-D-glucosamine
GM1	monosialotetrahexosylganglioside

GM1os	GM1 oligosaccharide
<i>H. Pylori</i> β3GlcNAcT	<i>Helicobacter pylori</i> β-1,3- <i>N</i> -acetylglucosaminyltransferase
H <sub>2</sub> SO <sub>4</sub>	sulfuric acid
HA	hemagglutinin
HAI	hemagglutinin inhibition assay
HEPES	4-(2-hydroxyethyl)-1-piperazineethanesulfonic acid
HILIC	hydrophilic interaction chromatography
HMDS	hexamethyldisilane
HPLC	high-performance liquid chromatography
HRMS	high-resolution mass spectrometry
HSQC	heteronuclear single quantum coherence
Hz	Hertz
IAV	Influenza A virus
IC50	half maximal inhibitory concentration
IgG	immunoglobulin G
IR	infrared spectroscopy
<i>J</i>	coupling constant
K <sub>2</sub> S <sub>2</sub> O <sub>7</sub>	potassium pyrosulfate
KCl	potassium chloride
K <sub>d</sub>	dissociation constant
K <sub>i</sub>	inhibition constant
Lac	lactose
LacNAc	<i>N</i> -acetyl- D-lactosamine
LAMP1	lysosomal-associated membrane glycoprotein 1
LC-MS	liquid chromatography-mass spectrometry
LecA	<i>Pseudomonas aeruginosa</i> Lectin PA-IL
<i>LgtB</i>	<i>Neisseria meningitides</i> β-1,4-galactosyltransferase
LPGSA	linear polyglycerol sialoside
lyso-GM3	lysoganglioside GM3
M2 ion channel	Matrix-2 ion channel
MDCK	Madin-Darby canine kidney
MeOH	methanol
MES	2-( <i>N</i> -morpholino)ethanesulfonic acid
MgCl <sub>2</sub>	magnesium chloride
MnCl <sub>2</sub>	manganese(II) chloride
NA	neuraminidase

Na <sub>2</sub> S <sub>2</sub> O <sub>3</sub>	sodium thiosulfate
Na <sub>2</sub> SO <sub>4</sub>	sodium sulfate
NaHCO <sub>3</sub>	sodium bicarbonate
NaN <sub>3</sub>	sodium azide
NaOH	sodium hydroxide
NaOMe	sodium methoxide
Neu5Ac	<i>N</i> -acetylneuraminic acid
NMR	nuclear magnetic resonance
OC	Oseltamivir carboxylate
PAMAM	polyamidoamine
PBS	phosphate buffered saline
Pd/C	palladium on activated carbon
PDB	protein data bank
Ph	phenyl
PmST1	<i>Pasteurella multocida</i> sialyltransferase
PNA	peptide nucleic acid
RBC	red blood cell
RNP	ribonucleoprotein
SA	sialic acid
SL	sialyllactose
SPR	surface plasmon resonance
TBAF	tetrabutylammonium fluoride
TFA	trifluoroacetic acid
THF	tetrahydrofuran
THPTA	tris(3-hydroxypropyltriazolylmethyl) amine
TLC	thin layer chromatography
Tris-HCl	tris(hydroxymethyl)aminomethane hydrochloride
UDP	uridine 5'-(trihydrogen diphosphate)
UV	ultraviolet
δ	chemical shift



## List of publications and presentations

### *Publications*

1. Wenjing Lu\*, Roland J. Pieters. Carbohydrate–protein interactions and multi-valency: implications for the inhibition of influenza A virus infections. *Expert Opinion on Drug Discovery*, 2019, 14: 387-395.
2. Wenjing Lu\*, Wenjuan Du\*, Victor J. Somovilla Busto, Guangyun Yu, Diksha Haksar, Erik J. de Vries, Geert-Jan Boons, Robert P. de Vries, Cornelis A. M. de Haan, Roland J. Pieters. Enhanced Inhibition of Influenza A virus adhesion by Di- and Trivalent Hemagglutinin Inhibitors. Submitted.
3. Wenjing Lu\*, Mi Zhou, Zongsuo Liang. Quality evaluation standards and factors affecting quality of *Polyporus umbellatus*. *Chinese Journal of Experimental Traditional Medical Formulae*, 2013, 17: 366-370.
4. Wenjing Lu\*, Zongsuo Liang. Study on the quality standard of *Polyporus umbellatus*(Pers.)Fries. *Northern Horticulture*, 2013, 16: 189-192.
5. Wenjing Lu\*, Zongsuo Liang, Yuanting Wu, Wenrui Li, Ruifang Liu. The effects on *Polyporus* polysaccharide and ergosterol contents by using different dehydrating methods. *Journal of Northwest Forestry University*, 2013, 4: 144-148.
6. Wenjing Lu\*, Shiheng Luo, Shizhong Chen. Simultaneous determination of several alkaloids in *Chelidonium majus* L. by HPLC. *Lishizhen Medicine and Materia Medica Research*, 2013, 3: 601-603.

### *Poster presentations*

CHAINS, 2015, Veldhoven, the Netherlands:

**Wenjing Lu**, Robert P. de Vries, Roland J. Pieters. Blocking the Hemagglutinin of Influenza A Virus.

CHAINS, 2017, Veldhoven, the Netherlands:

**Wenjing Lu**, Roland J. Pieters. Blocking the Hemagglutinin of Influenza A Virus by using multivalent rigid inhibitors.

## Acknowledgement

Over the five-year research journey as a PhD candidate in the department of Chemical Biology and Drug Discovery, it has now finally culminated in the completion of this thesis. Along the way, so many people have helped me and therefore it is the time to express my most sincere gratitude to all of them.

First and foremost, my deep gratitude goes first to my supervisor Prof. Roland J Pieters, who gave me the opportunity to conduct my PhD research in Utrecht. I still remembered the first day when I landed in Schiphol airport at 5 a.m., you were there waiting for me and drove me back to the campus, showing me the brand new view of the Netherlands. Also, you lead me to the world of carbohydrate chemistry and multivalency effects which broaden my horizons in the drug discovery studies. I am very grateful for your inspiring guidance on how to perform a synthesis experiment, how to analyze the results, how to present my own work to others, how to do the scientific writing and so on. Thank you for your constant support and supervision during my PhD research and study in the Netherlands.

I would like to thank Prof. Geert-Jan Boons for the collaboration of providing enzymes used in my research, and thank you for your insightful comments to my thesis. Victor, you're just like my daily supervisor during the last year of my research who helped me solve enzyme problems, showed me how to use the Agilent instrument, and also how to analyze complicated data. Thank you so much for your support and encouragement, all my best wishes to you and Nuria for your life in Spain.

Dr. Cornelis A. M. de Haan, thanks for your great effort in our collaboration of the biological evaluation experiments as described in Chapter 4 of this thesis. Thanks very much for your suggestions in this part of my thesis. Wenjuan, thank you very much for your contribution to our collaboration. Every time I sent you the samples for an activity test, you were always available and willing to help me finish the evaluation work. I wish you can get your PhD with a big success.

Rob, thank you for providing enzymes during these years of my research and giving me suggestions on enzymatic reactions. Javier, you are always polite and patient helping me with all the LC-MS problems, also thank you for the HRMS measurements. To other dedicated members of CBDD: Nathaniel, Dirk, Tom,

Arwin, John, Johan, Seino, Margreet, Ed, Linda, I highly appreciate all the guidance and support you have given me which are very important in my academic period.

Thanks to all the members of 'sugar' group, who had directly or indirectly helped me in the development of my work. Ou, thank you for sharing your fume hood and help me start the chemical synthesis at the beginning of my work. Special thanks also go to Hao, Jie and Xin. We were supposed to enroll together, but I was 'late' for five months. Thank you for all your support and help during my life in the Netherlands. Guangyun, thanks for providing the long spacer as one of the building blocks of my work and helping me during the days I stayed in China. Diksha, thanks for the polymer you synthesized and discussions we had in the lab. Xuan, thank you for your companionship when I was so frustrated with the experiments in my last year of work. Suhela, thank you for always encouraging me. I still remember the song you mentioned: 'Don't worry, be happy'. Reshmi, thanks for your inspirations about science, career and life in the future. Barbara, Torben, Aliaksei, Alen, Marjon, Pouya, Margherita and Cyril, thank you all for helping me at every stage of my work, it was really nice to have you around in the lab.

I would like to extend my gratitude to all the CBDD colleagues: Jack, Frederik, Apoorva, Ivan, Mehman, Rosanne, Gerlof, Dushen, Ingrid, Hanna, Tim, Minglong, Yanyan, Xiufen, Liangwei, Yvette, Xianke, Pieter, Lifeng, Gađ, Matthijs, Laurens, Timo, Kamal, Tom, Charlotte, Yongzhi and Yurui, thank you all for helping me at every stage of my work and I enjoyed a lot with all of you during my PhD life.

I would like to gratefully acknowledge the China Scholarship Council (CSC) for providing the scholarship which supported me to study and undertake my PhD in the Netherlands.

Here I would also like to thank my Chinese friends I met in the Netherlands. 子丹, 我很幸运能与你一起做三年半的室友, 一起分享喜怒哀乐。刘芳, 非常感谢你在科研和生活中给我的建议和帮助, 在我最迷茫的时候替我出主意想办法, 希望你在 Total 的工作一切顺利。张浩、杨欣、施杰, 很高兴能与你们三个同在一个组, 每次跟你们相处都是欢乐无穷, 感谢你们在实验过程中对我的帮助, 我也会很怀念在荷兰那些一起聚餐的日子。光允, 谢谢你在我回国期间帮我处理答辩的各种琐事, 也恭喜你即将拿到 PhD, 步入人生的新阶段。韦萱, 谢谢你在这最后一年相处中的帮助与包容, 还记得多少次你陪我一起加班到深夜, 还有我们一起逛吃逛吃的日子。小岛, 谢谢你每次耐心地帮我解决实验中的难

题，相信你在科研这条路上一定会越走越好。玉珑，谢谢你在我刚到荷兰时对我的帮助，让我能够很快适应了那里的生活。增慧，我们在 Laan van Vollenhove 聚餐、谈心的日子总是让人难忘，希望你在云大一切顺利。晓琳，我在荷兰的第一个邻居，很怀念我们去 open market 采购食材的那一个个周末。郭勇、海丽、晏娜、富强，下班后五公里的跑步计划希望我们在各奔东西之后还能继续坚持。DDW 的陈婧、娄博、孙飞龙、张育茂、陈建明、高永志、李婧、刘明龙、孙丽凤、孟宪珂、陈度伸、张良伟、刘秀芬、张宇睿、付东龙、叶馨蔚、朝乐梦，很高兴能认识你们，感谢我们一起度过的那些美好时光。还有 Utrecht 的其他朋友，刘敬洋、林俐、魏一璞、符仲芳、刘梅、孙晓婧、王玉茹、黄璐欢、郭宏波、李文涛、郎一飞、杜文娟，祝愿大家一切顺利，心想事成。

My deepest appreciation goes to my parents, husband and other family members for always being supportive for my study. 感谢爸妈一直以来对我无私的支持和关心，是你们给了我努力追求梦想的勇气和信心，让我能够永不言弃，坚持一路走下来。张先生，经历八年异地异国之后的我们终于拥有了属于自己的家，希望将来的生活会越来越幸福，谢谢你的一路陪伴，愿岁月静美，花自盛开。

Wenjing Lu

2019 March, Xi'an

## Curriculum Vitae

Wenjing Lu was born on June 16<sup>th</sup>, 1988, in Baoji, Shaanxi Province, China. She grew up and attended primary, middle and high school in her hometown. In the fall of 2006, she was enrolled in the bachelor program of traditional Chinese pharmacology at Tianjin University of Traditional Chinese Medicine, China. During that time, she also applied for an internship working at the College of Pharmaceutical Sciences, Peking University under the supervision of Prof. Shizhong Chen, studying the analysis of active compounds of traditional Chinese medicine. In the summer of 2010, she finished her bachelor thesis and then entered a master program of Medicinal Botany at the College of Life Science, Northwest Agriculture & Forestry University, China, under the supervision of Prof. Zongsuo Liang. During her three years of study, she focused on the optimization of quality standards of *Polyporus umbellatus* (Pers.) Fries. In the spring of 2014, she started working as a PhD candidate in the department of Chemical biology and Drug discovery at Utrecht University in the Netherlands, under the supervision of Prof. Roland J. Pieters with funding provided by the China Scholarship Council. Her PhD research was mainly focused on designing and synthesizing multivalent inhibitors of the Influenza A virus. The results of her doctoral work are published in this thesis and have been presented in several national conferences. She now is employed as an assistant researcher by Shaanxi Academy of Traditional Chinese Medicine, China.